

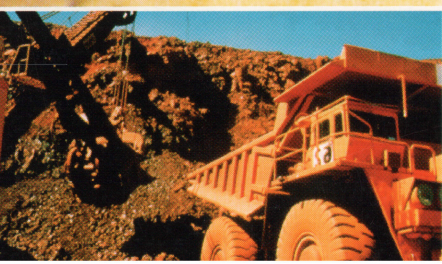
RESEARCH *newsletter*

MAY 2001 • Number 34



In this ISSUE:

- Gold mineral systems in the Tanami region: New insights from NTGS-AGSO research **2**
- A mineral systems approach to mapping Australia's endowment **10**
- Sources of organic matter in Wallis Lake **15**
- North Pilbara National Geoscience Mapping Accord project (1995-2000): Scientific highlights **25**
- Metallogenic potential of mafic-ultramafic intrusions in the Arunta Province, central Australia: Some new insights **29**
- Rapid mapping of soils and salt stores: Using airborne radiometrics and digital elevation models **33**



ALSO INCLUDED

- List of recent publications involving AGSO authors **20**

Editor: Julie Wissmann

Graphic Designer: Karin Weiss

Cover photo: Matt Peljo,
Lynton Jaques & Dean Hoatson

This publication is issued free of charge. It is published twice a year by the Australian Geological Survey Organisation. Apart from any use permitted under the *Copyright Act 1968*, no part of this newsletter is to be reproduced by any process without written permission. Requests and enquiries can be directed to AGSO's Chief Executive Officer at the address shown below.

Every care is taken to reproduce articles as accurately as possible, but AGSO accepts no responsibility for errors, omissions or inaccuracies. Readers are advised not to rely solely on this information when making a commercial decision.

© Commonwealth of Australia 2000

ISSN 1039-091X

Printed in Canberra
by National Capital Printing

**Australian Geological
Survey Organisation**

GPO Box 378, Canberra ACT 2601
cnr Jerrabomberra Ave &
Hindmarsh Dr
Symonston ACT 2609 AUSTRALIA

Internet: www.agso.gov.au

Chief Executive Officer
Dr Neil Williams

Editorial enquiries

Julie Wissmann

Phone +61 2 6249 9249

Fax +61 2 6249 9977

E-mail julie.wissmann@agso.gov.au

**AGSO Research Newsletter is
available on the web at
[www.agso.gov.au/information/
publications/resnews/](http://www.agso.gov.au/information/publications/resnews/)**

Readers please note: AGSO Research Newsletter ceases publication with issue number 34 (May 2001). AGSO is no longer publishing research papers under its own imprint. Papers that would normally appear in the Research Newsletter will be sent to other journals.

Gold mineral systems in the Tanami region

New insights from NTGS-AGSO research

AS Wygralak, TP Mernagh, G Fraser, DL Huston, G Denton, B McInnes,
A Crispe & L Vandenberg

Preliminary results of a joint NTGS-AGSO research program to document gold deposits of the Tanami region in the Northern Territory raise important new questions regarding ore genesis. Deposits in the Dead Bullock Soak and The Granites goldfields are related to regional D₃ or D₆ structural events. The ore fluids were low to moderate salinity (4–10 eq wt % NaCl), moderate to high temperature (260–460°C) and gas-rich. Ore deposition occurred at depths of three to eight kilometres. In contrast, ore fluids in the Tanami goldfield (also related to D₃ structures) were low temperature (120–220°C) with minor CO₂, and ore deposition occurred at depths of less than 1.5 kilometres. Preliminary ⁴⁰Ar/³⁹Ar studies of biotite tentatively suggest that mineralisation at Callie occurred at 1720–1700 Ma. Lead isotope data indicate that the Pb in the deposits was not derived solely from nearby granites. In the Dead Bullock Soak and The Granites goldfields, O and H isotopic data are consistent with either a metamorphic or magmatic origin for the ore fluids; in the Tanami district these data require an additional meteoric fluid input. These results illustrate the complexity of gold mineralisation in the Tanami region, and raise important questions about the origin and timing of these deposits.

The Tanami region, located 600 kilometres north-west of Alice Springs, is one of the most important new gold provinces in Australia. It straddles the Northern Territory–Western Australian border along the southern margin of the Palaeoproterozoic North Australian Craton. The Tanami region contains more than 50 gold occurrences including three established goldfields (Dead Bullock Soak, The Granites and Tanami), as well as several significant gold prospects (Groundrush, Titania, Crusade, Coyote and Kookaburra). The region has produced 4.5 Moz Au. The remaining resource is 8.4 Moz (260 t) Au, but this figure is steadily growing because of extensive exploration.

Outcrop in the area is sparse (5%), requiring the development and fine-tuning of new geophysical and geochemical techniques to allow the detection of 'blind' gold mineralisation under the regolith cover. Understandably, successful explorers safeguard their methodology and data to maintain their perceived competitive advantage. This has resulted in a lack of a regional understanding of geological factors controlling mineralisation.

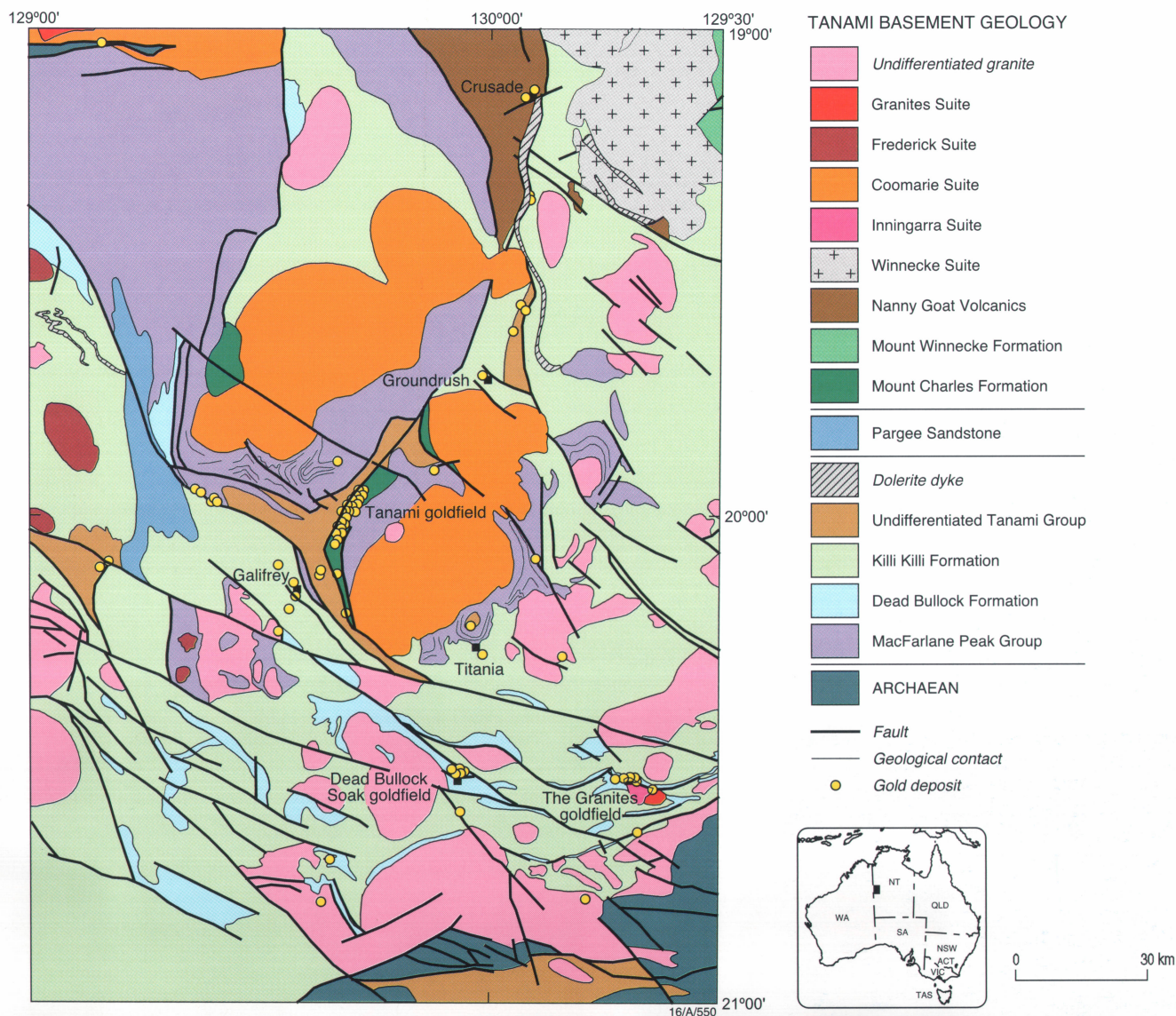
Being aware of this problem and recognising the economic importance of the Tanami region, the Northern Territory Geological Survey invited the Australian Geological Survey Organisation to commence a joint National Geoscience Agreement project in 1999. The purpose was to study hydrothermal systems and develop models that facilitate mineral exploration.

Regional geology

Recent stratigraphic¹, structural² and igneous³ studies indicate that the Tanami region has a similar geological history to the Pine Creek Orogen, Tennant Creek Province and eastern Halls Creek Orogen of Western Australia (Eastern Lamboo Complex).

The oldest Tanami rocks are isolated inliers of Archaean gneiss and schist such as the Billabong complex (60 km east of The Granites mine; figure 1), and the Browns Range Metamorphics (southern flank of Browns Range Dome³). SHRIMP based U-Pb zircon geochronology indicates protolith ages around 2510 Ma and high-grade metamorphism at 1882 Ma.⁴ The 1882 Ma event is assigned to the Barramundi Orogeny in the Pine Creek Orogen. It is the maximum age for rift initiation, basin formation and deposition of the overlying orogenic sequences.

Figure 1. Geology of the Tanami region with the location of gold occurrences



These orogenic sequences comprise the multiply deformed volcanics and sediments of MacFarlane Peak and Tanami Groups. The MacFarlane Peak Group consists of mafic volcanics, turbiditic sandstone, siltstone and minor calc-silicate. The Tanami Group comprises basal quartzite, the Dead Bullock Formation—which consists of carbonaceous siltstone, graphitic shale, minor iron-rich BIF and chert—and the turbiditic Killi Killi Formation. Dolerite sills intrude both MacFarlane Peak and Tanami Groups and predate deformation. The Tanami Group signifies rapid marine transgression, then deep marine starved sedimentation, followed by rapid prograding wedge sedimentation.

Tanami Group sedimentation is terminated by the onset of the Tanami Orogenic Event (TOE) between 1848 and 1825 Ma.² Recent geochronological evidence (detrital zircons as young as 1815 Ma in the Killi Killi Formation) suggests that this event is younger than the previously accepted age of the Barramundi Orogeny. The TOE involved multiple deformation (D_{1-3}) and syn to post D_1 greenschist to amphibolite facies metamorphism (M_1). The TOE is probably equivalent to the Eastern Halls Creek Orogeny, which was related to the collision of the North Australian and Kimberley Cratons at around 1835 Ma.^{5,6} The Pargée Sandstone, a coarse siliciclastic molasse, unconformably overlies the Killi Killi Formation and represents a sub-basin formed during the TOE.

The period immediately after the TOE is characterised by D_4 extensional rifting, sedimentation, felsic volcanism and granite intrusion. Aeromagnetics indicate that intercalated basalt and turbidite of the Mount Charles Formation lie above deformed MacFarlane Peak and Tanami Groups.^{7,8} Geochemistry indicates a continental rift setting for Mount Charles basalt.⁹ The age of Mount Charles Formation is poorly constrained, but it is intruded by Coomarie Suite aplite dykes dated at 1824 ± 12 Ma (AGSO OZCHRON). Extrusion of the Mount Winnecke Group felsic volcanics during D_4 rifting (1825–1815 Ma) is also coincident with widespread granite

intrusion. Five granite suites have been identified: Winnecke Suite, Frederick Suite, Inningarra Suite, Coomarie Suite, and The Granites Suite.³ Most granites are I-type with similar characteristics to those in the Halls Creek Orogen. D₅ faults formed after emplacement of the Winnecke, Fredrick, Inningarra and Coomarie granite suites.

Peneplanation of the Tanami basement and deposition of the Birrindudu Group siliciclastic platform cover sequence occurred sometime after intrusion of the Granites Suite (post 1800 Ma). Regional correlation with the Tomkinson Creek Group and Upper Wauchope subgroup in the Davenport Province and Tennant Inlier suggests a 1790–1760 Ma age.

Younger Proterozoic sequences include the Redcliff Pound Group, Antrim Plateau Volcanics, and siliciclastics of the overlying Lucas Formation, Pedestal Beds and Larranganni Beds. Redcliff Pound Group quartz arenite loosely correlates with the Amadeus Basin Heavitree Quartzite.¹⁰

D₆ faults cut all earlier generations of structures and are mainly defined from aeromagnetics.

Deposit geology

The Dead Bullock Soak (DBS) goldfield is the largest goldfield in the Tanami region, with a total resource of 6.3 Moz Au. Stratabound mineralisation is hosted in carbonaceous siltstone, iron-rich rocks and chert of the Dead Bullock Formation, which have been metamorphosed to greenschist facies. Although most deposits are hosted by BIF (e.g., Villa, Dead Bullock Ridge and Triumph Hill), by far the largest deposit, Callie (3.9 Moz), is hosted by carbon-rich siltstone at a stratigraphically lower position. All deposits occur in an east plunging anticlinorium (figure 2a). Unlike other goldfields in the Tanami region, there is not a close spatial association between gold mineralisation and granitoids.

The BIF-hosted deposits are localised in iron-rich parts of the Orac and Schist Hill formations (local mine terms) in the upper part of the local stratigraphy (part of Dead Bullock Formation). The iron-rich units have an amphibolite-chlorite±sulfide±magnetite assemblage. Although the distribution of the iron-rich units is a first-order control on mineralisation, high grade shoots are localised in zones of parasitic folds or structural thickening.¹¹

Mineralisation in the Callie deposit is localised in F₁ fold closures and is controlled by the intersection of a corridor of D₆ veining and carbonaceous rocks (figure 2b). Hydrothermal alteration varies with depth in the mine;

biotite assemblages at depth give way to chlorite at shallower levels. However, the ore is uniformly associated with decarbonised zones within the originally carbonaceous siltstone. Callie mineralisation consists largely (70%) of free gold and minor auriferous arsenopyrite.

The Granites goldfield (figure 3), which has a total resource of 1.6 Moz Au, comprises stratabound mineralisation within intensely folded, amphibolite facies iron-rich rocks of the Dead Bullock Formation. The host unit to the ore is amphibole-garnet-magnetite schist with up to 15 per cent sulfides (pyrrhotite, pyrite, arsenopyrite and chalcopyrite).

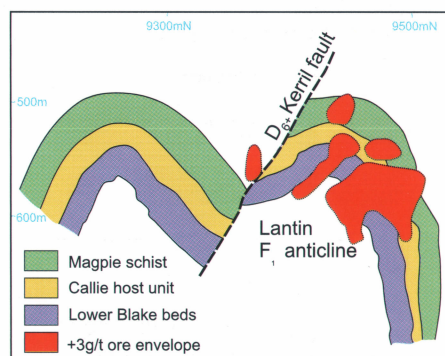


Figure 2b. A cross-section of Callie in Dead Bullock Soak

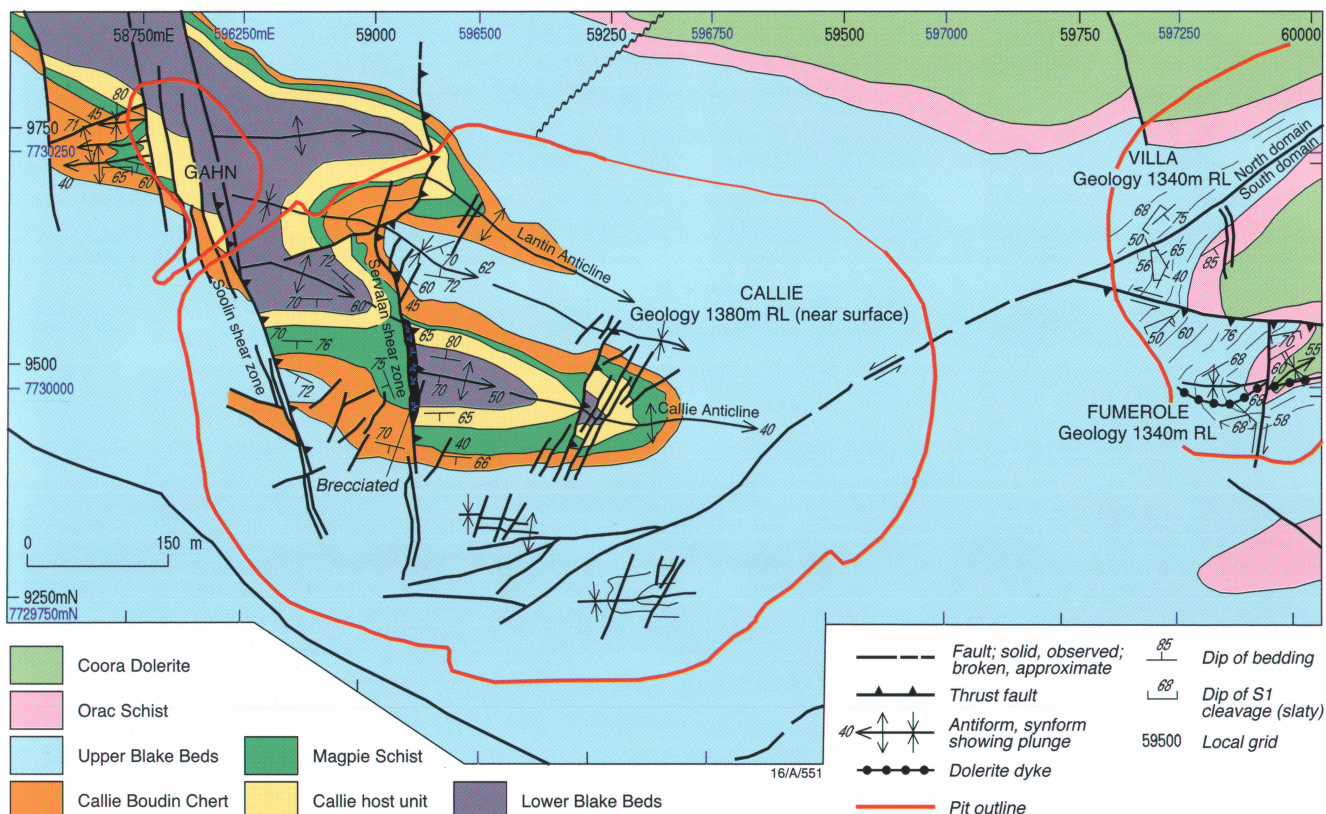
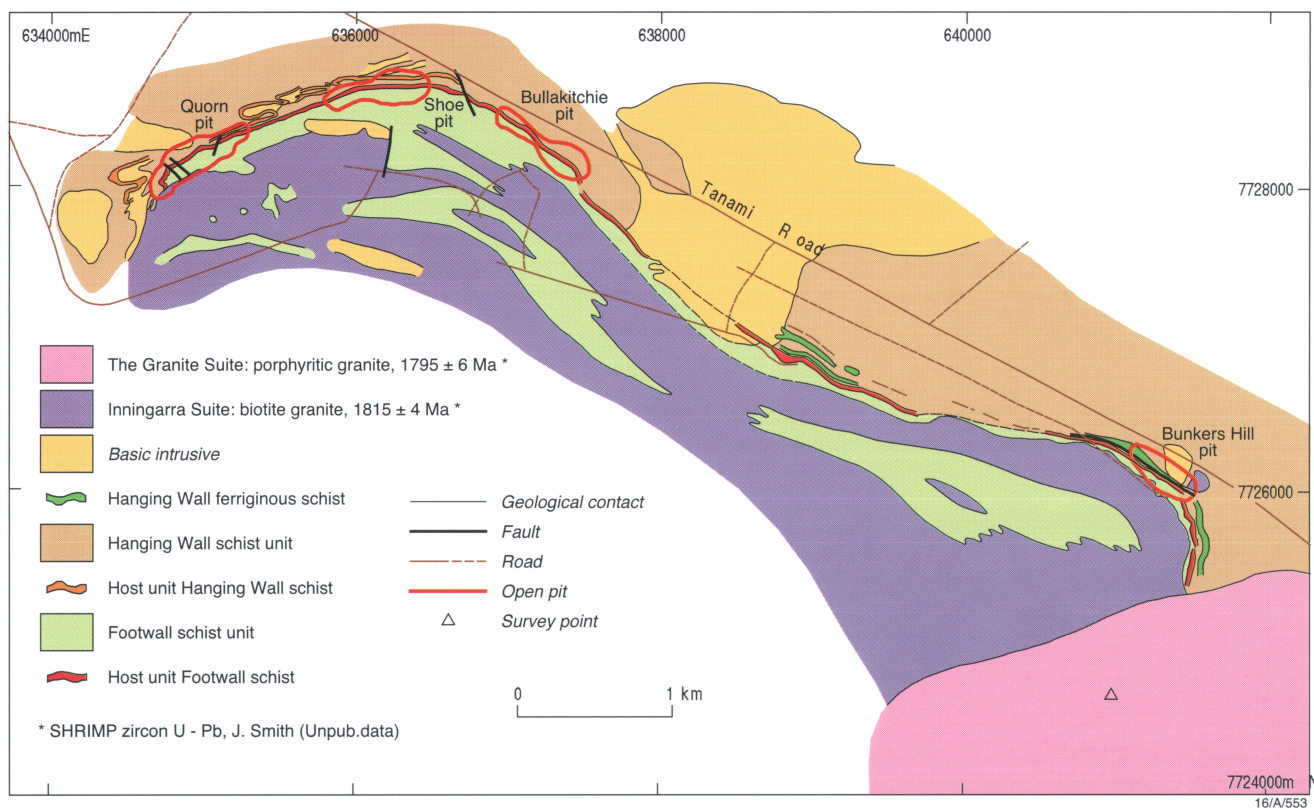


Figure 2a. Geology of Dead Bullock Soak (DBS) goldfield

Figure 3. Geology of The Granites goldfield



Although the orebodies are broadly tabular and steeply pitching, lenticular ore shoots are also present. At East Bullakitchie deposit, these ore shoots follow a prominent fold plunge.¹² Gold occurs in disseminated sulfides (arsenopyrite, pyrrhotite, pyrite), and is also associated with quartz-carbonate veining. Unlike the DBS goldfield, there is a close spatial association of mineralisation and granites. Inningarra and The Granites granite suites (1815±4 and 1795±5 Ma respectively) lie in close proximity to mineralisation. The geometry of the host sequence is related to D₅ deformation, which occurred in the interval between the Inningarra and The Granites granite intrusions.

The Tanami goldfield (figure 4), which has a total resource of 2.1 Moz Au, consists of quartz veins hosted by weakly deformed basalt and medium- to coarse-grained clastic sediments of the Mount Charles Formation. These units exhibit little metamorphism (sub-greenschist facies).

Mineralisation is controlled by three sets of D₅ faults striking 350–010°, 020–040° and 060–080°, and dipping east and south-east. The quartz veins are associated with an inner sericite-quartz-carbonate-pyrite alteration zone (within one meter of lodes) and an outer chlorite-carbonate zone (to 20 m).¹³ Feldspar is locally a gangue mineral in the auriferous veins. Gold occurs in

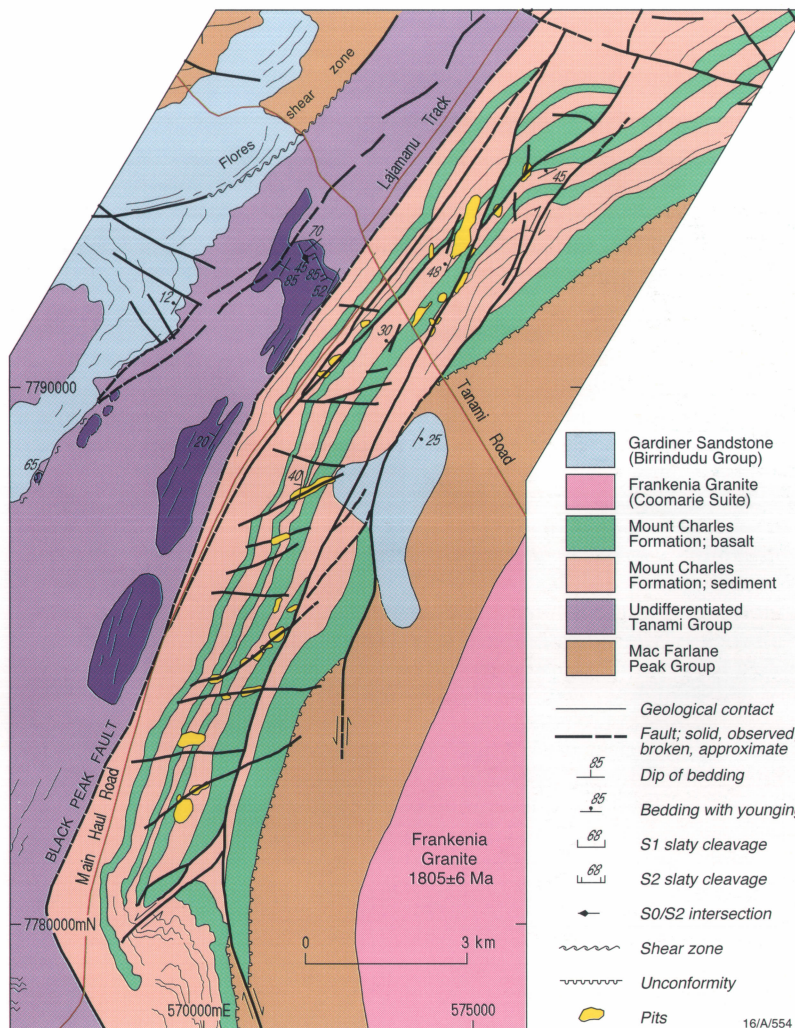


Figure 4. Geology of Tanami goldfield

sulfides (pyrite, arsenopyrite and pyrrhotite). Vein textures such as colloform banding indicate high-level mineralisation. Like The Granites goldfield, there is a spatial relationship with the Coomarie and Frankenia granites (1815 ± 4 Ma and 1805 ± 6 Ma respectively). This association has been used to infer a genetic link with the granites, either directly through a magmatic-hydrothermal origin of the fluids, or indirectly through contact metamorphic fluids.¹³

The Groundrush prospect (resource 0.7 Moz Au) is characterised by dolerite-hosted quartz vein mineralisation adjacent to a chilled margin of the Groundrush (Talbot South) granite dated at 1812 ± 5 Ma. The majority of the ore is free gold, but some auriferous arsenopyrite is also present. The orebody is open at depth. Mineralisation and deformation relationships remain to be determined.

The Titania (Oberon) prospect (resource 0.48 Moz Au) is hosted by turbidites in extensively folded, lower greenschist facies Killi Killi Formation. The ore bodies are structurally controlled by D₅ structures and are localised in anticlinal closures. Like Callie, mineralisation appears to be controlled by the amount of carbon in the host rock. Ore minerals include arsenopyrite, pyrite and free gold.

The Crusade prospect (resource 0.1 Moz Au) contains quartz vein mineralisation associated with a faulted rhyolite-basalt contact within the Nanny Goat Volcanics. The location of auriferous quartz veins is controlled by reverse thrusting related to D₅ deformation. A significant part of the ore comprises free gold.

Little public information is available on the Coyote and Kookaburra prospects that lie on the Western Australian side of the border, although they are currently being evaluated.

Age of mineralisation

Considerable uncertainty surrounds the age of gold mineralisation. The spatial relationship between mineralisation and granitoids (many of which are now dated) has led to proposed genetic links between granitoid intrusion and mineralisation; a postulation that remains to be further tested. In contrast, Callie is not obviously spatially related to granitoid, raising questions about any genetic role of granitoid in gold mineralising events.

A pilot $^{40}\text{Ar}/^{39}\text{Ar}$ study has been conducted to assess the potential of this method for improving age constraints on mineralisation. Samples for $^{40}\text{Ar}/^{39}\text{Ar}$ analysis were selected after petrographic examination that showed a variety of mineral phases and textures, including multiple vein generations. Interpretation of geochronological results is critical to understanding these geological relationships.

Wall-rock biotite of an ore-stage vein from Callie (sample 11666) yields a discordant spectrum with ages of less than 1000 Ma from the first two steps, giving way to ages between 1680 and 1950 Ma for the final 70 per cent of the gas release (figure 5a). The older part of the age spectrum exhibits an age peak at around 1850 Ma. Subsequent steps yield progressively younger ages leading to a relatively flat portion of the age spectrum at 1700 ± 20 Ma between 47 and 67 per cent of the gas release. The spectrum then rises to a maximum age of 1950 Ma before progressively 'younging' to around 1700 Ma. Coarse, unfoliated biotite from the vein margins in the same sample yields a relatively flat age spectrum in which all but two steps over approximately 80 per cent of the gas release, give ages between 1690 and 1730

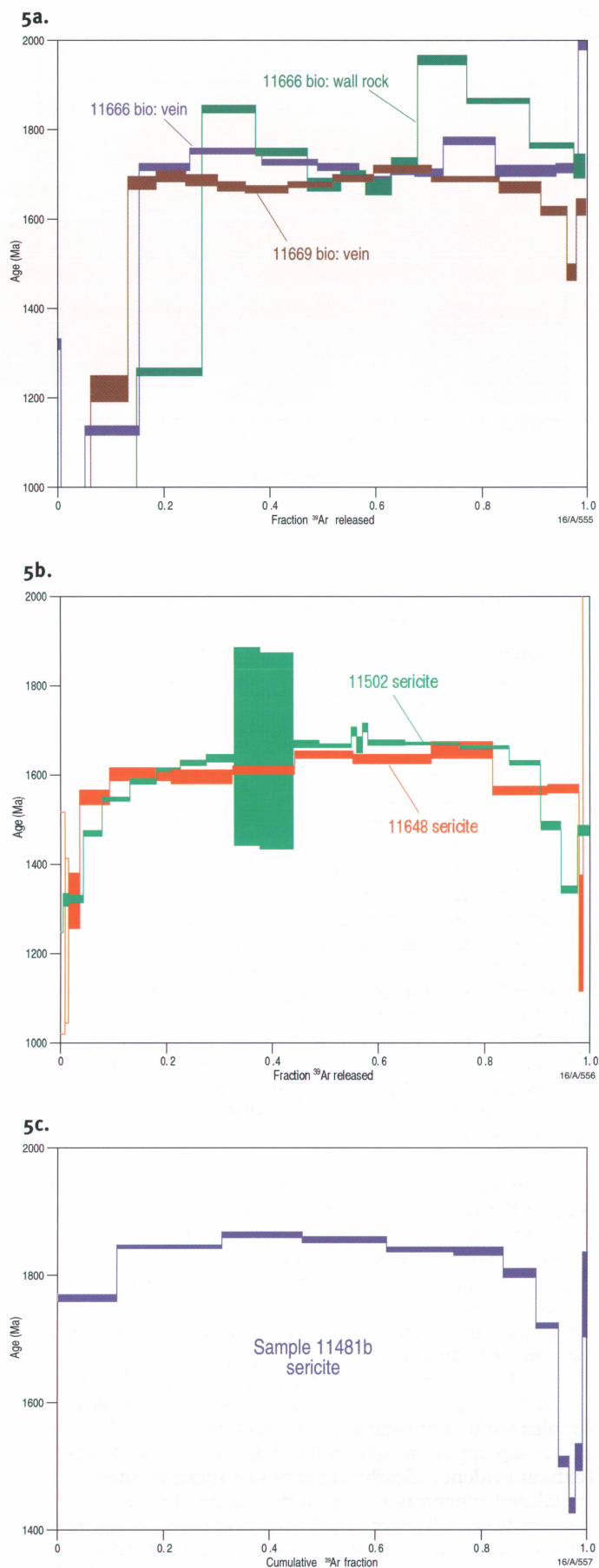
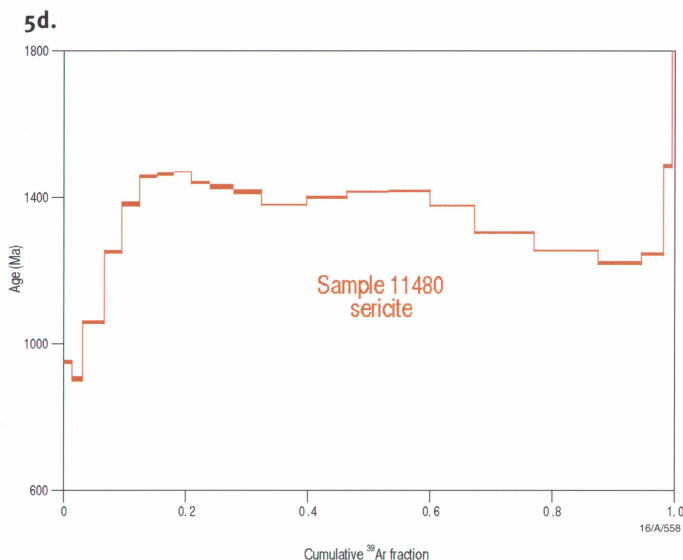


Figure 5. $^{40}\text{Ar}/^{39}\text{Ar}$ age spectra from gold deposits in the Tanami region: **a.** biotite age spectra from Callie deposit; **b.** sericite age spectra from the Galifrey (11648) and Titania (11502) deposits; **c.** sericite age spectrum from the Carbine deposit; **d.** sericite age spectra from the Callie deposit



Ma. The exceptions are two steps with slightly older apparent ages of 1752 and 1774 Ma (figure 5a).

Another biotite sample (11669) from ore-stage quartz vein at Callie returned relatively flat spectrum, with 70 per cent of the gas release yielding ages in the range 1666 to 1711 Ma (figure 5a). A sample of mixed, fine sericite and coarser muscovite associated with an auriferous vein from Callie (sample 11480) returned a discordant age spectrum. It rose from initial ages of 900 Ma to a maximum age of 1450 Ma at about 20 per cent of the gas release, followed by progressively younger ages spanning a range to around 1200 Ma (figure 5d). The non-ideal behaviour of this age spectrum is suggestive of ^{39}Ar recoil during irradiation, making interpretation problematic.

Hydrothermal sericite from the Carbine deposit (Tanami goldfield, sample 11481) yields an age spectrum in which 75 per cent of the gas yields ages between 1840 and 1865 Ma, before exhibiting considerably younger ages of 1500 Ma in the final few per cent of gas release (figure 5c). The convex upwards shape of this spectrum may also be indicative of ^{39}Ar recoil—a possibility supported by the total gas age of 1810 Ma, which is slightly older than the conventional K/Ar age of 1772 ± 20 Ma.

Sericite sample (11502) from Titania yields an age spectrum that rises gradually from initial ages around 1200 Ma to a flat section in which 60 per cent of the gas gives ages between 1660 and 1710 Ma (figure 5b).

Hydrothermal sericite from the ore zone at the Galifrey prospect (Tanami goldfield, sample 11648) yields an age spectrum which rises initially from 1200 Ma to a flat section, in which 60 per cent of the gas release yields ages between 1600 and 1660 Ma (figure 5b).

The three biotite-age spectra from the Callie deposit are plotted together in figure 5a. The two vein-biotite samples yield very similar age spectra with most of the gas having apparent ages in the range 1670 to 1720 Ma. Textural evidence clearly suggests that these biotites crystallised synchronously with the quartz veins in which they are hosted. This in turn is interpreted as synchronous with ore mineralisation. With typical values for argon closure in biotite around 300°C , and evidence from fluid inclusions that suggests temperatures in the quartz veins exceeded 300°C (see below), the biotite ages presented here should be regarded as minimum ages for the timing of ore mineralisation. However, ambient country-rock temperature before vein formation and mineralisation, at the estimated depth of between three and six kilometres, is likely to have been considerably less than the biotite

closure temperature (assuming near-surface geothermal gradients of less than $50^\circ\text{C}/\text{km}$). If mineralisation was relatively localised, the thermal effects could have been relatively short-lived—especially as maximum vein-formation temperatures were probably in the range $310\text{--}330^\circ\text{C}$. Given these considerations, the argon ages preserved in biotite give a close estimate of the timing of vein crystallisation and associated gold mineralisation.

The age spectra from Titania and Galifrey (two deposits 50 km apart) are remarkably similar in form and age, but their ages are 50 to 100 Ma younger than those derived from Callie biotites. These younger ages could represent cooling and isotopic closure ages of sericite significantly later than ore mineralisation.

In summary, the limited amount of $^{40}\text{Ar}/^{39}\text{Ar}$ data currently available is consistent with at least some of the Tanami gold mineralisation significantly post-dating the TOE in the region. In the case of the Callie deposit, the data may suggest a link with the Strangways Event ($1720\text{--}1730 \text{ Ma}^{14}$) that was responsible for widespread deformation and metamorphism in the Arunta Province to the south-east of the Tanami region.

Fluid inclusions studies

The physico-chemical character of the ore-bearing fluids has been investigated by microthermometric and laser Raman microprobe analysis of fluid inclusions.

At Callie the ore-stage, gas-rich, fluid inclusions homogenise over a temperature range of $310\text{--}330^\circ\text{C}$ and have salinities of 7–9 wt % NaCl eq. The laser Raman microprobe did not detect any CH_4 in these inclusions, but both CO_2 -rich and N_2 -rich inclusions are present. Two-phase aqueous inclusions also coexist with the gas-rich fluid inclusions and homogenise over the range $220\text{--}360^\circ\text{C}$. Their salinities range from 8–22 wt % NaCl eq. The estimated depth of formation of the gas-rich inclusions is 3.2–5.8 kilometres.

The Granites goldfield contains abundant CO_2 -bearing, primary fluid inclusions with salinities ranging from 4–8 wt % NaCl eq. Although most inclusions are CO_2 -rich, laser Raman microprobe analysis has shown that the vapour phase of some inclusions contains CO_2 and up to 73 mole % N_2 , while others contained CO_2 , small quantities of N_2 , and up to 50 mole % CH_4 . This indicates significant local variations in fluid composition. Some inclusions homogenised to the vapour phase. The majority, however, homogenised to a liquid over the range of $260\text{--}300^\circ\text{C}$. Two-phase aqueous inclusions are also present in lesser amounts and they coexist with the CO_2 -bearing inclusions. The aqueous inclusions have salinities ranging between 18 and 20 wt % NaCl eq and homogenise to the liquid phase over the range $240\text{--}260^\circ\text{C}$. The estimated depth of formation for the above inclusions range from 3.8–7.5 kilometres.

Rare, primary, CO_2 -rich fluid inclusions are found in a few deposits in the Tanami goldfield, but two-phase aqueous inclusions are the dominant type. No gases have been detected in the vapour phase of these inclusions. They can be grouped into three populations: (i) relatively saline inclusions with 18–23 wt % NaCl eq; (ii) moderately saline inclusions with 11–17 wt % NaCl eq; and (iii) low-salinity inclusions with 0–10 wt % NaCl eq.

Only type iii, low-salinity inclusions are associated with mineralisation. Necking down of inclusions has caused a wide spread in homogenisation temperatures, but there is a distinct mode at 160°C . Depth estimations for the aqueous inclusions range between 0.4 and 0.8 kilometres. It is estimated that the CO_2 -rich inclusions

formed between 1.3 and 1.5 kilometres. These shallow depths are consistent with a number of high-level features (comb quartz and chalcedonic textures).

Ore-stage fluid inclusions from the Groundrush deposit have a distinctly different character. The inclusion population is dominated by high-temperature, gas-rich inclusions. These inclusions homogenised over a temperature range of 220–460°C with a mode at 420°C. Their salinity ranged between 4–10 wt % NaCl eq. Laser Raman microprobe analysis indicates that the vapour phase is typically dominated by methane with lesser amounts of CO₂. The estimated depth of formation of these inclusions ranges between 5.5 and 8.3 kilometres.

Figure 6 summarises physico-chemical properties of fluid inclusions from the above deposits. Groundrush appears to have formed at the greatest depths and has the most reduced (CH₄-rich) fluids. The Granites goldfield and the Callie deposit formed at shallower depths. The Granites fluids were CO₂ rich, but variable in N₂ and CH₄. The Callie fluids show only small variations in temperature and salinity and are more oxidised with only CO₂ and N₂ being detected. The Tanami deposits appear to have formed at the shallowest levels and are dominated by low-salinity aqueous fluids, although some CO₂-bearing fluids have also been detected.

Source of metals

δ¹⁸O values calculated for ore fluids using mean temperatures obtained from fluid inclusions and δ¹⁸O values of quartz are 5.9±2.0 ‰ at Callie, 4.6±2.0 ‰ at The Granites, and range from 1.0 to 5.0 ‰ at the Tanami goldfield. The relevant fluid inclusion δD values are -85‰ to -58‰ (median -72‰) at Callie, -71‰ at The Granites and -69‰ to -37‰ (median -52‰) at the Tanami goldfield. The corresponding mean fluid inclusion δ¹³C values are -6.2‰ at Callie and -8.1‰ at The Granites. There was insufficient CO₂ to measure δ¹³C values at the Tanami goldfield.

The above data indicate involvement, at the ore stage, of metamorphic or magmatic fluid at Callie and The Granites, and a notably different exchanged meteoric fluid at the Tanami goldfield.

Further information on the provenance of metal-bearing fluids was obtained by comparing lead isotope ratios of hydrothermal K-spar and auriferous sulfides with lead isotope ratios of K-spar from granites spatially associated with mineralisation. The results obtained to date (figure 7) indicate that the initial lead isotopic ratios of sulfides from The Granites goldfield, Tanami goldfield and Groundrush deposit probably were similar to each other. They are significantly different, however, to the initial ratios of the granites as determined from K-feldspar separates. The initial ratio of the Groundrush granite is unique compared with the other granites. It may be indicative of derivation by partial melting of Archaean basement. Dolerite hosting the Groundrush deposit has lead isotopic values similar to the sulfides. However it is unclear whether this feature is primary, or if the isotopic ratios were re-equilibrated by subsequent hydrothermal activity.

A combination of stable isotope data and lead isotopic ratios—as well as significantly younger Ar-Ar ages of ore-related minerals, when compared with the age of granitic intrusions—suggest that these intrusions were not the source of ore-bearing fluids.

Tanami region gold mineral system

Results of this study indicate that gold deposits of the Tanami region are surprisingly diverse, with some being basalt and dolerite hosted, some in BIF, and some being sediment hosted. Moreover, fluid inclusion data suggest that the four main deposits all formed at different depths with Groundrush being the deepest and the Tanami deposits being the shallowest (figure 8, page 14). Hydrogen and oxygen isotope data are consistent with either a magmatic or metamorphic origin for the ore fluids, but the Pb isotope data show that the Pb in these deposits was not derived from a magmatic source.

Despite the evident differences these deposits have similarities, particularly Callie, Groundrush and The Granites. Most importantly, ore fluids have salinities less than or equal to 10 wt.% NaCl eq, and are CO₂-rich. The Tanami fluids differ in that they are not as CO₂-rich, consisting mostly of aqueous inclusions indicative of high-level fluid mixing. The composition of these fluids bears some similarities to the fluid chemistry of Archaean lode gold deposits¹⁵ that have mainly mixed aqueous-carbonic fluids with some moderate- to low-salinity aqueous inclusions. Fluid salinities in the Tanami deposits, however, lie in the upper range of those reported from Archaean gold deposits. Groundrush and Callie have greater levels of CH₄ and N₂, respectively, than that commonly observed in Archaean gold deposits. In this

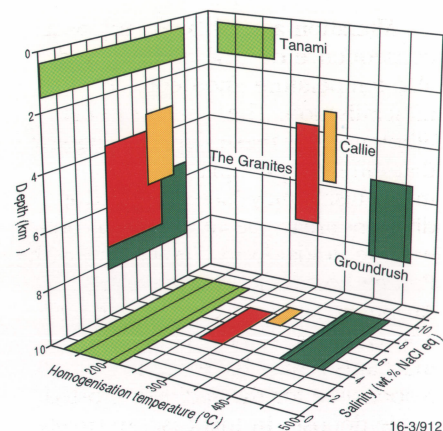


Figure 6. Summary of physico-chemical properties of ore-stage fluids at Callie, The Granites, Groundrush and Tanami corridor deposits

respect the fluid chemistry of these deposits appears to be more closely related to that reported for turbidite-hosted gold deposits.¹⁶

Figure 8 presents a preliminary gold system model based on these and other data for the entire Tanami region. The project's data conflicts in terms of the role of granites in the mineral system. Although there is a strong spatial association among deposits in the Tanami and The Granites goldfields and at Groundrush, Pb-isotope and ⁴⁰Ar/³⁹Ar data presented herein are not consistent with a direct genetic link between granite intrusion and mineralisation.

The Tanami goldfield has the most suggestive evidence for a role for granites. These deposits are located within a corridor between two granite domes, and the ⁴⁰Ar/³⁹Ar data overlap the age of intrusion of one of these granites. These granites may have acted as either a heat engine or focused fluid flow within the Tanami corridor. Other deposits such as Callie do not have a close spatial association with granites, and the ⁴⁰Ar/³⁹Ar age data do not accord with the time of granite intrusion. Given these uncertainties, the role of granites in the mineralising event is an open question.

Structural evidence² shows that D₅ or D₆ shear zones are important controls on gold mineralisation within the region. These structures facilitated regional fluid flow into deposition sites. Fluid flow was assisted by brittle failure and brecciation of competent rocks (e.g., Tanami), the formation of dilatant zones (e.g., The Granites) and the existence of structural corridors (e.g., Callie).

Alteration assemblages vary as a consequence of host lithology and also temperature and depth of mineralisation. The variety of host lithologies for these deposits suggests that different precipitation mechanisms may have operated in different areas. Desulfidation of ore-bearing fluids during interaction with Fe-rich host rocks may have led to Au precipitation at Groundrush and The Granites. A more complex mechanism may have been responsible for the sediment-hosted Callie deposit. In this case, relatively oxidising fluids reacted with graphitic sediments, reducing the fluid, decarbonising the rock, and producing CO₂ gas. H₂S was also partitioned into the gas phase, destabilising the gold bisulphide complexes and precipitating gold. Finally, gold was remobilised by later fluids that concentrated it near the top of decarbonised zones in a process analogous to 'zone refining' in volcanic-hosted massive sulfide deposits. Structural thickening during F₁ folding at Callie may have enhanced this process by preparing a thicker zone of reactive rock. Fluid-inclusion data from the Tanami goldfield suggest that the ore-bearing fluids mixed with a localised brine, and Au precipitation resulted from mixing and cooling processes.

The data suggest that a number of processes formed gold deposits in the Tanami region. This directly has resulted in a diversity of ore deposit characteristics. Consideration of this diversity, from a mineral systems perspective, highlights the likelihood that undiscovered gold deposits in the Tanami region will have a large range of characteristics and that mineral deposition can occur in a number of different host lithologies. Current evidence indicates that D₅ and D₆ structures should be the favoured targets for future exploration.

Future research

Results of this joint NTGS-AGSO research program raise more questions than they answer. To address these questions, the following research programs will be undertaken over the next year:

- further direct dating of mineralisation (including possibly dating zircon in late ore-stage veins);
- further lead isotope work;
- a more extensive program by AGSO on Western Australian prospects (e.g., Coyote) to detect any regional changes in the age and character of mineralisation;

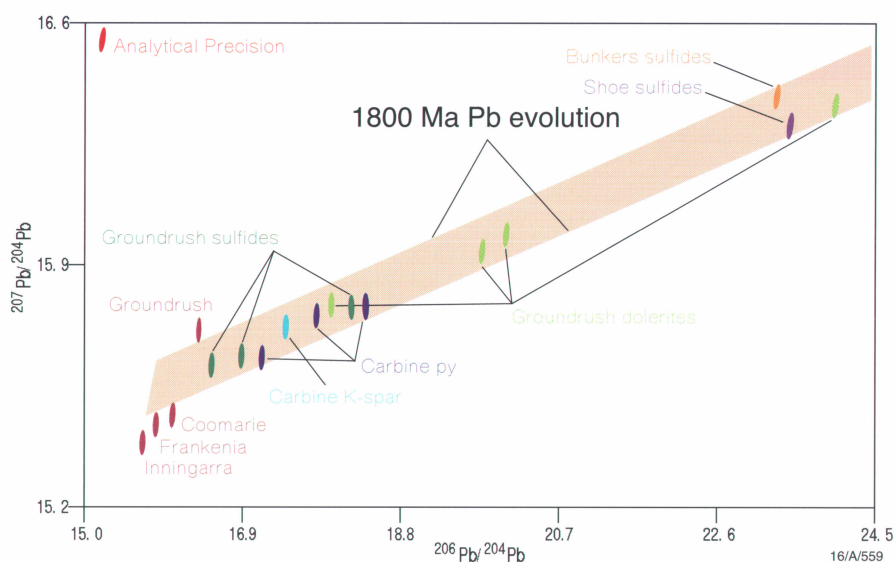


Figure 7. ²⁰⁶Pb/²⁰⁴Pb versus ²⁰⁷Pb/²⁰⁴Pb ratios of hydrothermal ore-related minerals, granites (Coomarie, Frankenia, Inningarra, Groundrush) and Groundrush dolerite

and

- extension of work to the Birrindudu area (quartz-Au veins in the Winnecke Granophyre).

References

1. Hendrickx MA, Slater KR, Crispe AJ, Dean AA, Vandenberg LC & Smith JB. 2000. Palaeoproterozoic stratigraphy of the Tanami region: Regional correlations and relation to mineralisation—preliminary results. Darwin: Northern Territory Geological Survey, record 2000\13.
2. Vandenberg LC, Hendrickx MA, Crispe AJ, Slater KR & Dean AA. 2001. Structural geology of the Tanami region. Darwin: Northern Territory Geological Survey, record 2001/04.
3. Dean AA. 2001. Igneous rocks of the Tanami region. Darwin: Northern Territory Geological Survey, record 2001/03.
4. Page RW. 1995. Geochronology of an exposed late Archaean basement terrane in The Granites–Tanami region. AGSO Research Newsletter; 22:19–20.
5. Tyler IM, Griffin TJ, Page RW & Shaw RD. 1995. Are there terranes within the Lamboo Complex of the Halls Creek Orogen? Perth: Geological Survey of Western Australia, Annual Review 1993–94; 37–46.
6. Sheppard S, Tyler IM, Griffin TJ & Taylor WR, 1999. Paleoproterozoic subduction-related and passive margin basalts in the Hall Creek Orogen, north-west Australia. Australian Journal of Earth Sciences; 46:679–690.
7. Slater KR. 2000. Tanami SE 52-15, 1:250 000 integrated interpretation of geophysics and geology. Edn 1. Darwin: Northern Territory Geological Survey; 15.
8. Slater KR. 2000. The Granites SF 52-3, 1:250 000 integrated interpretation of geophysics and geology. Edn 1. Darwin: Northern Territory Geological Survey; 16.
9. Tunks AJ. 1996. Structure and origin of gold mineralisation, Tanami mine, Northern Territory. Hobart: University of Tasmania, PhD thesis.
10. Blake DH, Hodgson IM & Muhling PC. 1979. Geology of The Granites–Tanami region, northern Territory and Western Australia. Canberra: Bureau of Mineral Resources, bulletin 197.
11. Smith MEH, Lovett DR, Pring PI & Sando BG. 1998. Dead Bullock Soak gold deposits. The Australasian Institute of Mining and Metallurgy, monograph 22; 449–460.
12. Mayer TE. 1990. The Granites goldfield. Melbourne: Australasian Institute of Mining and Metallurgy, monograph 14; 719–724.
13. Tunks A & Marsh S. 1998. Gold deposits of the Tanami Corridor. Melbourne: Australasian Institute of Mining and Metallurgy, monograph 22; 443–448.
14. Collins WJ & Shaw RD. 1995. Geochronological constraints on orogenic events in the Arunta Inlier, a review. Precambrian Research; 71:315–346.
15. Ridley JR & Diamond LW. 2000. Fluid chemistry of orogenic lode gold deposits and implications for genetic models. Reviews in Economic Geology; 13:141–162.

➡ Continued page 14

A minerals systems approach to mapping Australia's endowment

AL Jaques, N Evans & S Jaireth

Mineral endowment is a key element in determining prospectivity. As part of an ongoing assessment of Australia's prospectivity, AGSO has compiled density plots of recorded mineral occurrences, which not only map Australia's historic mineral provinces but also highlight regions with anomalously high metal contents.

Most regions with a high abundance of recorded mineral occurrences contain one or more world-class deposits—although there are notable exceptions in the case of buried deposits. An abundance of occurrences can be due to the compounded effects of sequential or overlapping mineralising systems. It may also reflect an inefficient mineralising process or processes that resulted in dispersed low-grade mineralisation. Nevertheless, most of the known world-class deposits are in regions with a high density of mineral occurrences—suggesting surface prospecting probably played a key role in the discovery of many such deposits. Early results of AGSO's ongoing assessment of Australia's mineral potential indicate that substantial areas of potential remain (especially under cover).

The bulk of the world's metal resources are contained in larger than the median-size deposits, and most is concentrated in giant or world-class ones (namely the top 10% of deposits on a contained metal basis).¹ Moreover, most of the world's base and precious metal resources are contained in deposits of higher grade, occur in relatively few ore deposit types, and are concentrated in particular regions of the world. These observations lead to the conclusion that some parts of the Earth's crust are unusually endowed in certain metals and therefore more prospective than other areas.

World-class or giant deposits can profoundly affect metal supply and have a huge influence on net present value and cash flow (mine

profitability). Such deposits therefore are a focus of global exploration today.

The minerals industry is undergoing radical change because of the combined influences of globalisation, low metal prices, investor demands for greater return on capital, competition for risk capital, the declining position of mining in equity markets, and the increased demands for community and environmental accountability (the 'triple bottom line'). In this environment, the industry will depend heavily on the discovery of major deposits with large, high-grade reserves to ensure low operating costs and long mine life. Other desired characteristics include a low environmental footprint and favourable ore mineralogy that allow ready extraction without environmental penalties.

The growth of the Australian minerals industry to its present position as a leading producer is built on a relatively small number of major (world-class) mines. These include historic giant deposits such as Kalgoorlie and Broken Hill that were found more than 100 years ago. Also included in Australia's list of major deposits and mineral districts—most of which were found in the last 40 years—are:

- Mount Isa copper and lead-zinc-silver deposits;
- bauxite deposits of Gove, Weipa, and the Darling Ranges;
- Bowen Basin coal seams;
- Hamersley iron province;
- Olympic Dam copper-uranium-gold deposit; and
- Yilgarn gold deposits.

This raises the question: 'What is Australia's mineral endowment and potential for further discoveries, especially for world-class resources?'

Australia's mineral endowment

The distribution of known deposits and occurrences provides an insight into known mineralising systems. Figures 1 a–f are density maps of the distribution of significant mines and deposits (including both historic and undeveloped deposits). These figures show recorded occurrences of gold, copper, lead/zinc, iron, nickel and uranium mineralisation from AGSO's MINLOC database, which contains more than 74 000 mineral locations. The recorded mineral occurrences are presented as kernel density plots using a 100-kilometre radius and shown simply as low, medium and high concentrations.

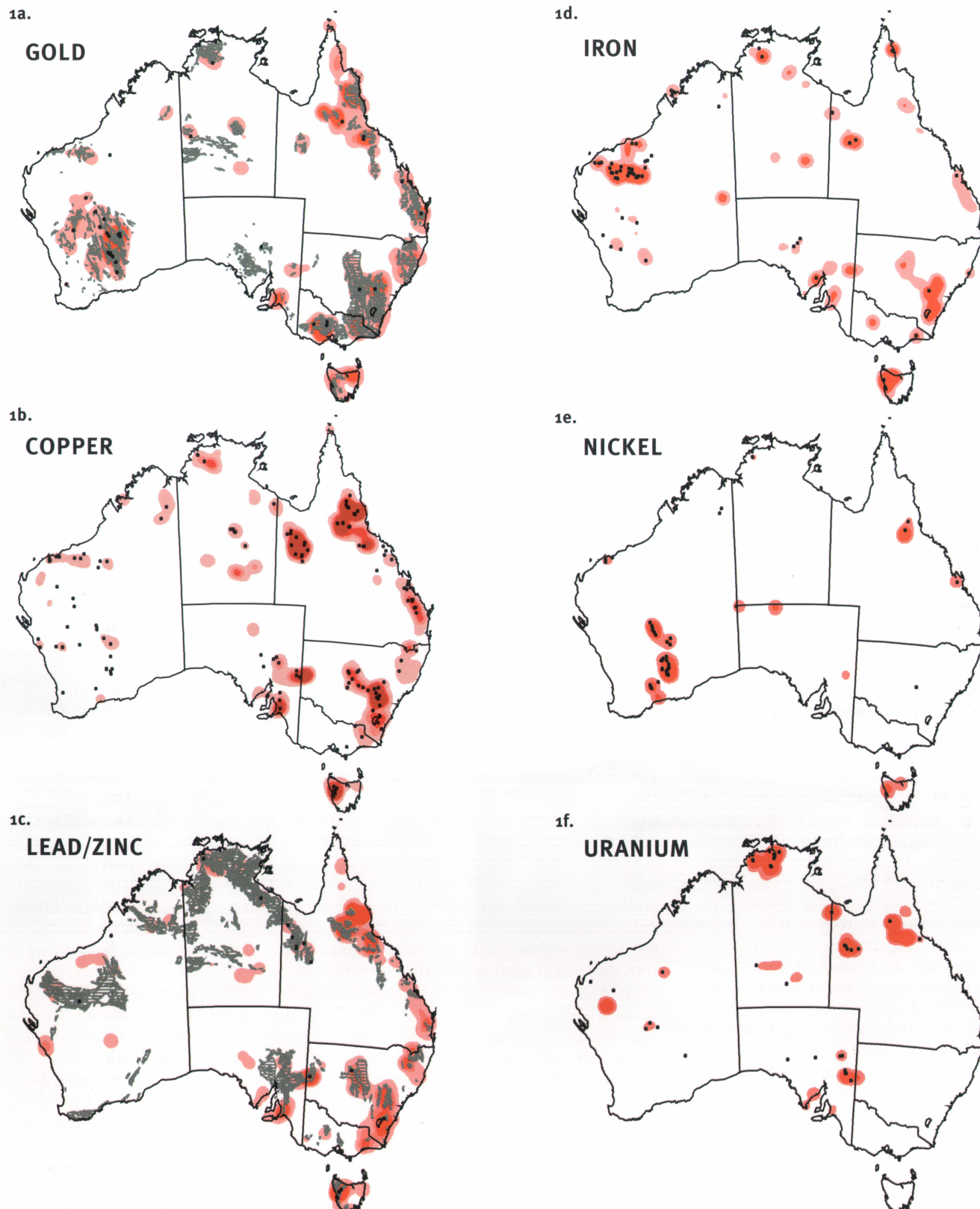
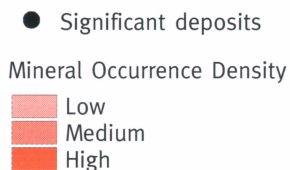
The plots show that gold and copper are the most widely recorded metals in Australia. Recorded gold occurrences (figure 1a) are concentrated in the Archaean Yilgarn craton and in the various elements of the Tasman Fold Belt. This includes northern Tasmania, the historic major lode gold deposits of the Ballarat–Bendigo field of Victoria, the porphyry-epithermal and lode gold of Lachlan Orogen in New South Wales, and the breccia-hosted, lode gold and epithermal deposits of central Queensland.

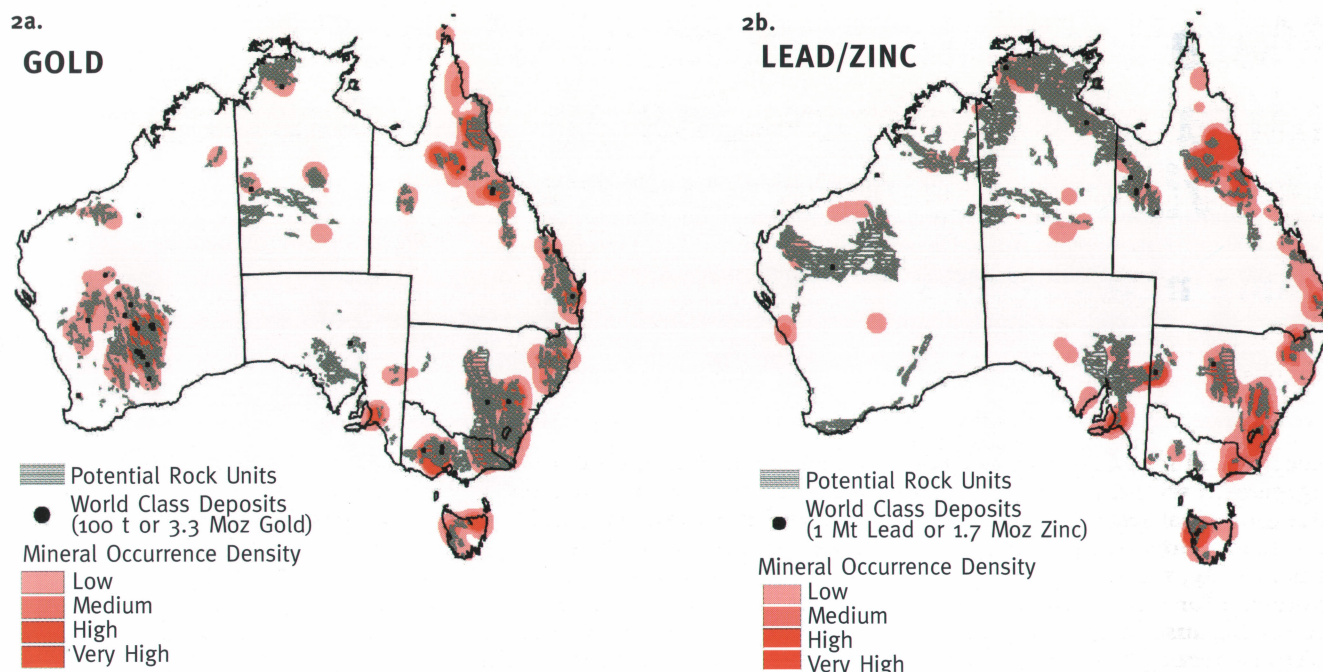
Copper deposits and recorded occurrences (figure 1b) are concentrated in the Mt Isa province, the Kanmantoo province, the western Curnamona craton, and widely distributed in the Tasman Fold Belt. These occurrences highlight the volcanic associated massive sulphide (VAMS) district of western Tasmania, the VAMS and porphyry deposits of the Lachlan Orogen, and the base metal provinces of central and north Queensland.

Figure 1c broadly maps Australia's lead-zinc provinces, especially the major VAMS districts of Tasmania and New South Wales, the Elura and Broken Hill deposits, as well as occurrence-rich regions of North Queensland (mostly in the Kennedy province). Other lead-zinc mineralised districts, such as the Lennard Shelf (the 7th largest zinc producing province in the world) and the Pine Creek province, are also identified. The world-class Carpentaria–Mt Isa zinc belt in northern Australia, however, is not especially prominent. This belt hosts more zinc than any other comparable province in the world with seven world-class, Proterozoic sediment-hosted base-metals deposits: McArthur River, Century, Dugald River, Hilton, Mt Isa, Lady Loretta (all with 2 Mt or more contained zinc), and Cannington (5 Mt contained lead, 1.9 Mt contained zinc).

Australia's iron ore provinces and occurrences of banded iron formations, iron-rich skarns and gossans are shown in figure 1d. In the case of nickel (figure 1e), the density occurrence map marks out the nickel districts of the Eastern Goldfields (Kambalda, Mount Keith–Agnew), the Forrestania belt, the west Pilbara, and the lateritic deposits in eastern Australia, notably the Greenvale area. The uranium density map (figure 1f) clearly marks out the Rum Jungle and Alligator River uranium districts in the Northern Territory, Mary Kathleen and Westmoreland uranium districts in Queensland, the Kintyre deposit in Western Australia, and the Beverley and Honeymoon uranium districts in South Australia. No significant deposits are known from the area of anomalously high, recorded uranium occurrences in the Ashburton province in Western Australia.

Figures 1 a–f. Kernel density plots of recorded mineral occurrences and major deposits (from AGSO's database) for gold, copper, lead/zinc iron, nickel, and uranium.





Figures 2a–b. Maps showing the distribution of world-class gold and lead/zinc deposits in relation to kernel density plots of recorded mineral occurrences and prospective rock sequences from AGSO's national GIS.

World-class deposits and mineral potential

Most regions with an anomalously high distribution of recorded mineral occurrences contain one or more world-class deposits of that metal(s) as shown, for example, in figure 2a: gold and figure 2b: lead/zinc. Clearly the most endowed region in terms of gold is the Yilgarn craton—notably the Eastern Goldfields, which hosts some 16 world-class deposits. World-class gold deposits are associated with many other concentrations of recorded gold occurrences, including Ballarat, Bendigo, Cadia, Cowal, Gympie, Kidston, Mt Leyshon and Charters Towers. A number of major deposits—such as Telfer, Boddington and Olympic Dam—however are not associated with a high density of recorded occurrences.

World-class deposits are not always found in regions with the highest density of recorded mineral occurrences. For example: no world-class lead or zinc deposits are currently associated with the high density of recorded occurrences in the Georgetown–Mt Garnet region (although a number of small deposits are known). Australia's major lead-zinc province is not highlighted as a province, even though there are concentrations centred about the McArthur River, Century, and Mt Isa–Hilton deposits, and a region north of the Roper River. Cannington is a blind deposit under 10–60 metres of cover.

A lack of major deposits associated with high-density occurrences in some districts, and a paucity of occurrences associated with world-class deposits in other mineral districts, may be due to several factors. Firstly, there are inherent weaknesses in the database, which is influenced by such factors as the nature of the outcrop, amount of cover, and exploration accessibility including that of early prospectors. Secondly, in some provinces high-density occurrences may reflect the influence of multiple, overlapping or sequential weak mineralising events, none of which may have resulted in major deposits. A third possibility is that high-density occurrences may indicate dispersion of mineralising fluids through 'leaky' or inefficient mineralising systems (source, transport and trap). The more focused or efficient mineralising events, therefore, may have resulted in less minor mineralisation (fewer occurrences), but significant deposits.

In a number of mineral districts² and petroleum basins³ there is a parabolic fractal relationship between size and rank of deposits when plotted on a log-log basis. This relationship is widely used to predict the ultimate size of oil and gas fields in a basin. The relationship is less certain in the case of mineral deposits. For example: a log-normal distribution has been demonstrated in some gold provinces but, taken as a group, giant gold deposits (>100 tonnes)

do not form part of a single population.² Rather, the well-endowed belts contain anomalously large gold deposits.² This is examined further in figure 3, which shows a cumulative frequency plot of gold deposits in the Eastern Goldfields, Murchison and Southern Cross terranes of the Yilgarn craton. Gold deposits from the Murchison and Eastern Goldfields terranes show a similar distribution, except for the super-giant Kalgoorlie deposit. Deposits in the Southern Cross terranes, in contrast, define a different curve (figure 3). This implies differences in the scale or efficiency (e.g., focusing or timing of fluid flow and fluid trap) of the gold mineralising systems. The Murchison terranes are more like those of the Eastern Goldfields than the Southern Cross terranes. Broken Hill is a mineral province that shows an even greater 'gap' between a giant and minor deposits. The giant Broken Hill silver-lead-zinc deposit (>150 Mt, pre-erosion possibly ~300 Mt) is distinct from a 'tail' of small deposits, suggesting that the mineralising system was highly efficient in focusing and concentrating the mineralisation.

The relationship of mineral occurrence, mineral resource and mineral potential is being further explored by using a mineral systems approach and resource data such as grade and tonnage curves. AGSO is undertaking an assessment of

Australia's mineral potential to support resource exploration and as an important input to land-use planning and infrastructure development.⁴ The assessment is using a GIS-based mineral systems approach, which attempts to identify all geological processes that control the generation and preservation of mineral deposits.⁵ Emphasis is placed on *source(s)* of heat (energy), metals and fluids, *transport* mechanisms for the migration of fluids, and *trap*—including the mechanical and physico-chemical conditions that result in precipitation of metals from fluids, as well as post-depositional modification and preservation of the mineralisation. The approach is based on determining the likely presence or absence of elements critical to formation of some 21 different ore deposit types known to host world-class deposits in Australia or in similar rocks elsewhere in the world, based on widely adopted models.⁶ Assessment of potential is based on examination of the time–event plots for each province. This includes basement geology, magmatic history, and basin evolution including sediment type, orogenic/metamorphic events, and metallogenic events.

The rock sequences prospective for gold and lead-zinc deposits based on this approach are shown in figures 2a and 2b. These figures show that the areas prospective for these metals extend beyond the known mineralised districts defined by the distribution of occurrences and deposits. Many of these areas are buried or poorly exposed, suggesting that considerable potential lies under cover.

Mineral occurrences, deposits and potential

From a preliminary examination of mineral occurrences, deposits and potential, the authors conclude that:

1. The density maps of recorded mineral occurrences highlight regions of crust with anomalously high metal contents and outline most of Australia's historic mineral provinces.
2. Most of the known world-class deposits, with important exceptions, occur in regions with a high density of recorded mineral occurrences. This suggests that most past discoveries, with the exception of blind deposits like Olympic Dam and Cannington, were strongly driven by surface prospecting.

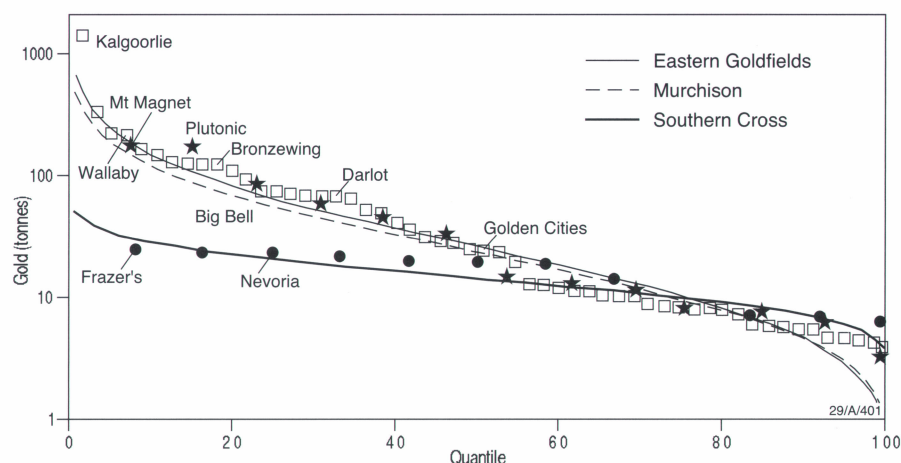


Figure 3. Cumulative frequency plots of gold deposit size (tonnes of contained gold) for the Eastern Goldfields, Murchison and Southern Cross terranes.

3. Most regions with a high density of recorded mineral occurrences contain one or more world-class deposits, but some have no known major deposit(s). It is not clear whether major deposits remain to be found in these areas. Some high concentrations appear to result primarily from the cumulative effects of low levels of occurrences associated with overlapping but distinct mineralising systems. These may also represent systems where the mineralised fluids were widely dispersed rather than focused to form economic deposits.
4. Early results of an assessment of mineral potential indicate that substantial areas of potential remain. The areas are likely to be in extensions of known provinces under cover, in poorly outcropping provinces, and especially in under-explored greenfields provinces under cover. Successful exploration of many of these areas will require a new approach that integrates new geophysical imaging tools (such as gravity gradiometry or seismic) with new conceptual approaches based on a better knowledge of the controls on mineralising processes.

References

1. Singer DA. 1995. World-class base and precious metal deposits—a quantitative analysis. *Economic Geology*; 90:88–104.
2. Hodgson CJ, Love DA & Hamilton JV. 1995. Giant ore deposits: Giant mesothermal gold deposits—descriptive characteristics, genetic model and area selection criteria. Society of Economic Geologists, special publication 2; 157–211.
3. Bradshaw MT, Bradshaw J, Weeden RJ, Carter P & de Vries DF. 1998. Assessment—translating the future into numbers. *APPEA Journal*; 38:528–550.
4. Jaireth S, Lambert I, Mieizitis Y & Jaques L. 2000. Mineral potential of Australia. Geological Society of Australia, abstracts 59; 251.
5. Wyborn LA, Heinrich CA & Jaques AL. 1984. Australian Proterozoic mineral systems: Essential ingredients and mappable criteria. AUSIMM annual conference, technical program proceedings; 109–115.
6. Cox DP & Singer DA, eds. 1986. Mineral deposit models. Reston (Va): United States Geological Survey, bulletin 1693.

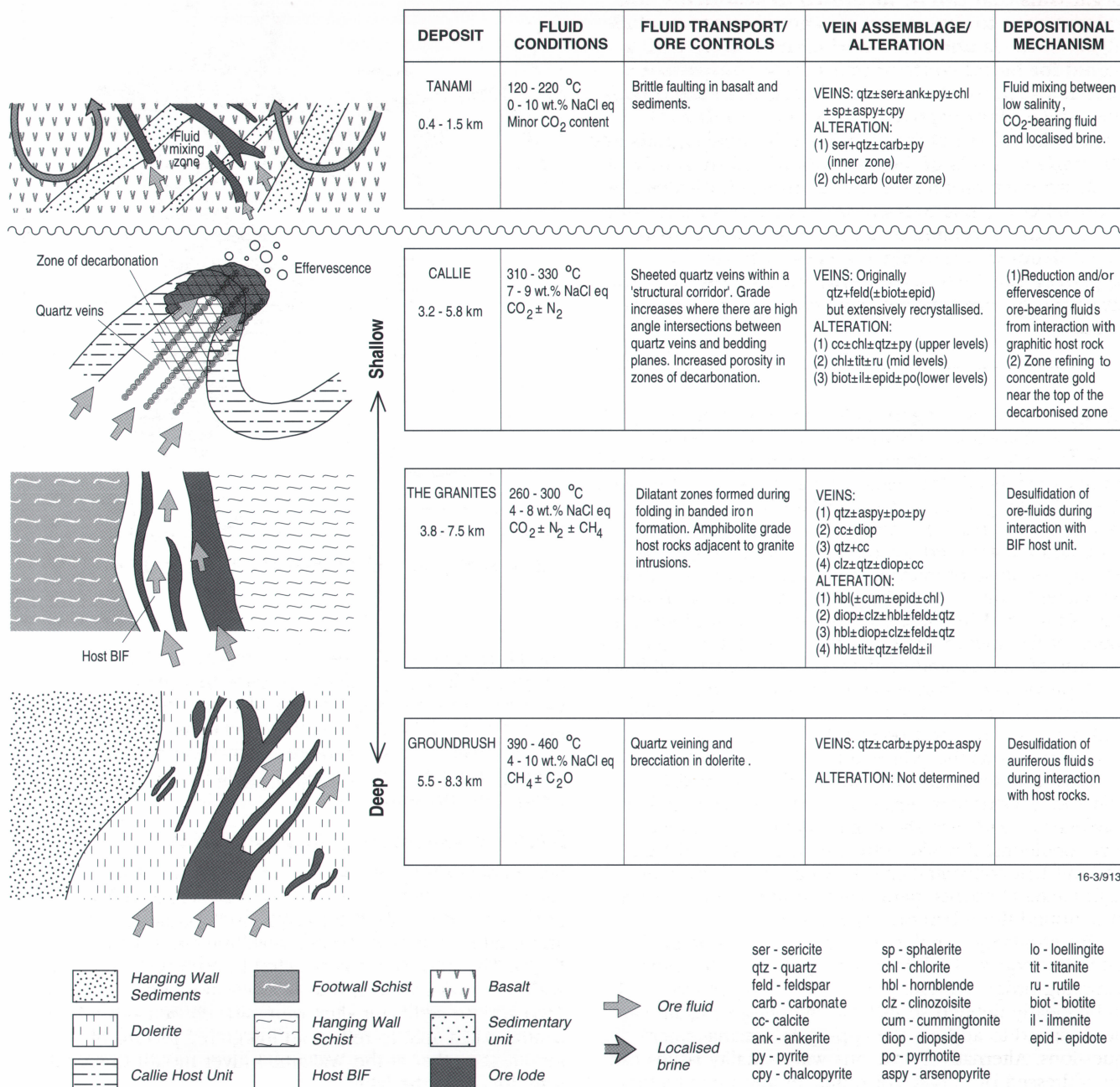
Acknowledgments: The authors thank Mike Huleatt, Greg Ewers, Bill McKay, Dave Huston and Yanis Mieizitis for comments and/or advice on this article.

The maps of recorded mineral occurrences, deposits and potential can be down loaded free from www.agso.gov.au/minerals/promotion/promote.html.

- Dr Lynton Jaques, Minerals Division, AGSO, phone +61 2 6249 9745 or e-mail lynton.jaques@agso.gov.au
- Neal Evans, Minerals Division, AGSO, phone +61 2 6249 9698 or e-mail neal.evans@agso.gov.au
- Subhash Jaireth, Minerals Division, AGSO, phone +61 2 6249 9419 or e-mail subhash.jaireth@agso.gov.au ☎

16. Mernagh TP. 2001. A fluid inclusion study of the Fosterville Mine: A turbidite-hosted goldfield in the Western Lachlan Fold Belt, Victoria, Australia. *Chemical Geology*; 173:91–106.

- Drs Andrew Wygralak, Andrew Crispe & Leon Vandenberg, Northern Territory Geological Survey, phone +61 8 8999 5441 or e-mail andrew.wygralak@nt.gov.au
- Drs Terry Mernagh, Geoff Fraser & David Huston, Minerals Division, AGSO, phone +61 2 6249 9640 or e-mail terry.mernagh@agso.gov.au
- Drs Geoff Denton & Brent McInnes, Exploration and Mining Division, CSIRO, phone +61 2 9490 8879 or e-mail g.denton@dem.csiro.au



16-3/913

Figure 8. Schematic diagram showing fluid-system model for the Tanami region

Sources of organic matter in Wallis Lake

GA Logan, DJ Fredericks, C Smith & DT Heggie

A study of lipid biomarkers at Wallis Lake has revealed sources of organic matter in sediment samples collected at five different sites. Lipid biomarkers are molecules derived from the cells of organisms that can be identified in sediments and related back to their sources. These sources include algae, bacteria and terrestrial plants, along with a signal for faecal contamination. Site comparisons reveal distinctive biomarker signals associated with terrestrial plant inputs at two river mouth sites. These sites also exhibit decreases in algal signals and the highest levels of faecal contamination. Analysis of down-core biomarker distributions indicates that biomarker signals become increasingly similar with depth. This is related to diagenesis and the more rapid degradation of algal tissues. A statistical approach has been used to interrogate the data and illustrate differences between and within sediment cores.

Wallis Lake (figure 1) is one of Australia's largest coastal lakes with an area of about 90 square kilometres. Sediment facies in the lake include a fluvial bay head delta near the entry points of the major rivers (Coolongolook and Wallamba Rivers), a shallow muddy central basin forming the southern part of the lake, and a marine tidal complex at the mouth of the estuary. Because of training walls, the estuary mouth is permanently open. The Wang Wauk/Coolongolook River and Wallamba Rivers are the main catchment tributaries. Much of the area traversed by these rivers and tributaries consists of cleared and partially cleared agricultural land.

A previous environmental study identified the presence of nutrient, animal and human faecal pollution, and other urban runoff pollutants from the Forster-Tuncurry area as the principal sources of pollution in the estuary.¹ But available data indicate that under dry conditions, estuary water quality complies with Australian guidelines.¹ Data also show that under low to moderate wet conditions, the lake waters contain high sediment and nutrient concentrations. As well, data show some high bacterial counts, particularly in the tributary rivers and around the urban drainage outlets.

Water-quality sampling of biological parameters in estuaries requires both intensive spatial and temporal sampling programs. The purpose of such surveys needs to be clearly defined so that the sampling program can be designed to address the appropriate management questions. Alternatively, various water-quality issues can be addressed by surveys of sediment and plant material. These surveys rely on the large spatial distribution of sediments and plant material, and the ability of sediments to integrate and record water-column characteristics.

This paper outlines an investigation of lipid biomarker compositions of sediment in Wallis Lake to determine the relative importance of urban and rural inputs. Lipid biomarkers were chosen because they can identify organic inputs to sediments and help trace the dispersal of these inputs through the estuary. Biomarkers are compounds of biological origin produced in cell walls

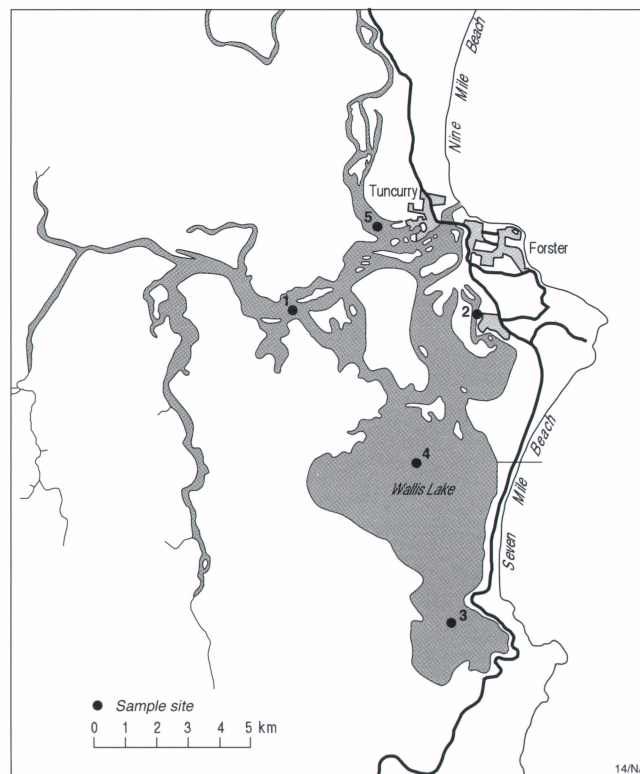


Figure 1. Map of Wallis Lake and sample locations

and fat storage areas. They can often be related to sources such as phytoplankton, terrestrial plants and bacteria. Certain biomarkers are also specific to particular groups of organisms; for example, diatoms, dinoflagellates or cyanobacteria. Furthermore, biomarkers may help identify forms of environmental contamination, such as petroleum and sewage.

Sample collection and analysis

Sediment cores were collected at three sites around Wallis Lake. Two of these core sites were chosen to reflect potential end members for rural (Coolongolook River) and urban catchments (canal development at Forster Keys). The third site was selected to represent deposition within the lake system, remote from these end members. Two surface sediment sites were also chosen—one in the central basin area to reflect an integrated picture of inputs; the other at the Wallamba River mouth to examine rural inputs to the lake.

The details of sample collection and analysis are covered elsewhere.² Briefly, cores were collected using a hand-operated piston corer and sediments were freeze dried before grinding. Biomarkers were extracted by repeated sonication in mixtures of organic solvents (dichloromethane and methanol). The combined total extract was then analysed by gas-chromatography mass-spectrometry (GC-MS). This procedure separates complex mixtures of molecules for identification and quantitation. By a process called Target Compound Analysis, the GC-

MS computer software was trained to recognise and look for 69 biomarkers of interest. Each compound was quantified against the internal standard and then its abundance related to the amount present in each gram of sediment. Compound abundances were then used in the statistical software package 'Statistica' to perform principal component, cluster and cononical variation analyses.

Identification of specific organic matter inputs

The different sources of organic matter are recognised both on the basis of individual biomarkers and the presence of diagnostic patterns of multiple biomarkers. Specific sources are identified and discussed below. The importance of certain inputs is assessed through several ratios developed to examine the variation of different biomarkers (table 1). The use of these ratios allows inter-site comparison and helps in the interpretation of the statistical data.

Algae

Dinoflagellates are single-celled algae that live in oceans, estuaries, lakes and ponds. They can cause 'red tides', which kill fish or poison humans who eat the fish or shellfish affected by such algal blooms. The presence of dinoflagellates is recorded chemically in sediments by dinosterol, a biomarker specific to dinoflagellates.³ It is present at all sites in Wallis Lake and throughout the sediment cores. This indicates that dinoflagellate production occurs across Wallis Lake and that dinoflagellates have been a component of the phytoplankton production over the entire depositional history of the cores (approximately 5000 years). Ratios of dinosterol to phytol can be used to estimate the comparative importance of dinoflagellates at each site. Phytol is derived from chlorophyll and is present in all photosynthetic plants. Dinosterol abundance ratios were lowest at sites 1 and 5 (1.8 and 0.5 respectively) compared with the other sites which ranged from 4.0 to 7.7. The percentage of dinosterol as part of the sum of all biomarkers quantified also indicates that abundances of dinosterol are highest away from the two river mouths (table 1). This suggests that dinoflagellate production was lower close to the river mouths.

The 'green algae' is the most diverse group of primarily aquatic algae, with more than 7000 species. The presence of green microalgae is indicated by C₃₀ 1,15 alkandiol.⁴ Again, this compound was found to be present at all sites and through each core. Generally speaking, this biomarker was most abundant and provided the highest ratios at sites 2, 3 and 4, away from the river influxes. For example, values for ratios of C₃₀ 1,15 alkandiol to phytol are 0.5 and 1.4 for sites 5 and 1, and range between 2.1 to 7.0 for the sites 2 to 4. The percentage abundance of C₃₀ 1,15 alkandiol is also higher away from the river mouths (table 1). As with the dinosterol data, this suggests that the algae group that produces C₃₀ 1,15 alkandiol is most commonly found away from the river mouths.

Diatoms are unicellular algae with cell walls that contain silica. They generally form an important component of photosynthetic production within estuaries, and often occur as a spring bloom. This happens when the concentration of silica and nutrients in combination with increased light and water temperatures allow for rapid growth. Different diatom species can produce a range of sterols, of these 24-methylcholesta-5,24(28)-dien-3 β -ol and 24-methylcholesta-5,22E-dien-3 β -ol are thought to be most diagnostic.⁵ However, certain sterols such as cholesterol, also known to be produced by this group, have other potential sources. Although cholesterol is abundant in animals, it may be predominantly derived from diatoms in Wallis Lake. This is

supported by the cluster analysis finding that cholesterol groups with compounds related to algal sources. Ratios of cholesterol to phytol and percentages of cholesterol as a function of total quantified lipids do not show marked variation with site (table 1). Except for site 1, cholesterol is the most abundant of all sterols in every sample. Most of the other diatom-related sterols⁵ have been identified at each site, indicating that diatoms are also an important component of the phytoplankton.

Bacteria

Cyanobacteria is the scientific name for blue-green algae—plant-like bacteria that can fix nitrogen and contain cyanobacterial toxins. Cyanobacteria commonly bloom in shallow, warm, slow-moving or still water and can cause a health risk in areas of human activity. They are more prevalent in fresh water than in brackish or marine conditions. Cyanobacteria, along with other bacterial groups, produce a group of compounds called hopanoids. The presence of 2-methyl-hopanoids is now thought to be diagnostic for cyanobacteria,⁶ although not all species in the group make this biomarker. C₃₂ hopanol is detected in the surface sediments at all sites, although in very low concentrations. However, no 2-methyl-hopanoids are detected at any of the sites. This suggests that if cyanobacteria are present, they are not significant contributors to the sedimentary organic matter. The analysis of these biomarkers is problematic so this conclusion is tentative. Further work using more specific chemical techniques would be required to assess the composition and distribution of the hopanoids to address the nature of the sources of these compounds.

Sulfate-reducing bacteria are also present in all samples. In particular, iso- and anteiso-branched fatty acids, as well as 10-methyl hexadecanoic acid are diagnostic of this group of

Site	Dinoflagellates		Green algae		Diatoms		Land plants		Herbivore faecal sterol ratio
	dinosterol/phytol	% dinosterol	alkandiol/phytol	% alkandiol	cholesterol/phytol	% cholesterol	triterpenoids/phytol	% triterpenoids	24ethylcoprostanol/24ethylcholestanol
1 river mouth	1.8	1.4	1.4	1.1	7.1	5.6	12.0	9.4	1.3
2 canal development	4.9	2.4	4.1	2.0	10.8	5.3	<0.1	<0.1	0.6
3 southern basin	7.7	2.6	7.0	2.3	14.1	4.7	<0.1	<0.1	0.4
4 central basin	4.0	2.3	2.1	1.2	7.8	4.4	1.9	1.1	0.5
5 river mouth	0.5	1.7	0.5	1.6	1.7	5.4	1.3	4.2	1.6

Table 1. Ratios of compounds to phytol based on quantified data from GC-MS analysis. The percentages are based on the abundance of each compound, as a function of the total of all lipids quantified. The triterpenoids are derived from a sum of β -amyrin, friedelin, oleanolic and ursolic acids.

bacteria. These fatty acids are a common feature of almost all sediments and reflect part of a community of bacteria involved in the decay of the organic matter.

Land plant

Terrestrial plant input is recognised by the presence of leaf waxes in all the sediments. Leaf waxes are composed of a series of *n*-alkanes, *n*-alcohols and *n*-acids with carbon chain lengths ranging between C₂₂ and C₃₂. The acid and alcohol series is dominated by even carbon numbered compounds, and the alkane series is dominated by odd carbon numbered compounds. Specific higher plant biomarkers called triterpenoids are also common in the sediments of each core. Sites 1 and 5 have a group of triterpenoid biomarkers (including friedelin, oleanoic and ursanolic acids) that are not present at any of the other sites. This suggests there is a specific terrestrial input in the sediments close to the river catchments, that is not present at other locations further from the river mouths.

Anthropogenic inputs

Urban sources of organic matter can include human sewage, outlined below, and also petroleum products. These can be from spillage, combustion of fossil fuels, and run-off from bitumen sealed roads. None of these sources could be identified in the sediments from site 2, chosen as the urban catchment end-member, nor were they found at any other sites. The impact of urban processes, therefore, is not significantly reflected in the biomarkers deposited at any of the chosen sites.

A group of sterols has been found to be diagnostic of faecal inputs.⁷ Human sewage contains a compound called 'coprostanol'—a biomarker that can trace sewage in the environment. None of the sites examined contains detectable concentrations of this biomarker. Even site 2, which was selected to represent an urban catchment, does not appear to be affected by human faecal contamination. In contrast, the biomarker for herbivore faecal inputs, 24-ethyl-coprostanol is detected at all sites. The presence of this marker is not in itself a direct indicator of faecal contamination, since it can form in sediments through natural processes. However, a ratio of this sterol to 24-ethyl-5 β -cholestan-3 β -ol with values greater than one is evidence for herbivore faecal inputs to an environment. Both site 1 and site 5 have sterol ratios greater than one (1.3 and 1.6 respectively), indicative of contamination by herbivores. In contrast, sites 2, 3 and 4 have values between 0.4 and 0.6 (table 1), which fall close to values expected naturally in anaerobic muds. These results suggest that contaminated run-off from rural catchments is affecting sites 1 and 5, but sites 2, 3 and 4 are probably not strongly affected by this form of contamination. Furthermore, the absence of 24-ethyl-*epi*-coprostanol (which is an important sterol in sheep faeces⁷) suggests that the herbivore faecal contamination at sites 1 and 5 is most likely from cattle.

Inter-site comparison

Inputs to surface sediments at sites 1 and 5 are clearly distinguished by a range of terrestrial biomarkers. These include several plant triterpenoids, such as oleanoic and ursolic acids, and the abundance of lipids derived from plant leaf waxes. Furthermore, these sites have lower abundances of biomarkers associated with green microalgae and dinoflagellates (table 1). Sites 2, 3 and 4 have similar biomarker compositions to one another and include terrestrial, planktonic and bacterial sources. Bacterial and phytoplankton sources can also be recognised at sites 1 and 5; however, these sites are dominated by biomarkers of land-plant origin. Significantly these sites also have strong signals derived from herbivore faecal contamination (table 1). This is an important finding, because it suggests that run-off from the rural catchment brings with it faecal material that may present a problem for water quality. The absence of coprostanol, the biomarker associated with human faecal contamination, indicates that sewage from urban sources is not significantly affecting Wallis Lake.

Multi-variate statistical analysis of biomarker data

Lipid biomarker analysis provides concentration data on some 69 separate compounds including fatty acids, alcohols, alkanes, sterols and triterpenoids. Multi-variate data sets of this size are often difficult to interpret because of the large number of permutations of variables that need to be considered. Principal Components Analysis (PCA) was used to investigate the basic structure of the data and compositional differences between cores at sites 1, 2 and 3. PCA is a method of reducing the number of variables in a data set to a minimum by creating principal components from the original, highly

correlated parameters. The principal components are selected so they are parallel to the major variation in the data. The first principal component or axis is parallel to the greatest variation in data (maximum variance), and the second axis is chosen to be parallel to the next greatest variation in the data.

PCA was carried out using the 'Statistica' software package produced by StaSoft. PCA within the Statistica package can only be performed where the number of analyses (cases) is less than the number of samples. Data were therefore broken down into two broad groups. The first group (group 1) contained sterol and triterpenoid compounds along with other compounds related to leaf waxes. It is most likely to differentiate variations in phytoplankton and terrestrial sources. The second group of compounds (group 2) contained short chain fatty acids, alcohols and *n*-alkanes, ranging between C₁₄ and C₂₀. These compounds are common to a greater number of sources (higher plant tissues, phytoplankton and bacteria), and therefore the group has a lower degree of specificity.

The PCA of the two groups shows that the data set is highly correlated, but in this paper only the first two axes for group one are considered. After PCA the biogeochemical reasons for the statistical variation must be assessed. This was partly done through examination of the PCA loadings (which for space reasons are not presented in this report). The variation in PC1 is related to depth but controlled by the concentration of compounds, which decreases down core. This is a normal feature of lipid biomarker analysis and reflects decay and early diagenesis of organic matter.^{8,9} PC2 is controlled by the different sources of organic matter, with negative PC loadings related to stronger terrestrial biomarker signals and positive loadings reflecting greater inputs of algal biomass. These PC loadings are used as axes in figures 2 and 3. The cross-plots of PC factors 1 and 2 show that sites 2 and 3 plot closely together and have similar trends. All sites converge to a common location on the graph. This can be explained by selective preservation of terrestrial material, leading to increasing similarity of all cores with depth.

When the first principal component of group 1 and group 2 are plotted against depth within each core (figure 2), all sites appear to exhibit similar trends. At the sediment-water interface, compound concentrations are generally high. But they decrease rapidly within a few

centimetres of the surface, primarily as a result of bacterial degradation within the surface sediment. Although there is a general loss of biomarkers, selective degradation of certain compounds occurs. This process leads to a biasing of the preserved organic matter. (These effects will be discussed below.) Biomarker compositions at sites 2 and 3 become more similar to site 1 with increasing depth in the cores. Generally, algal material is more easily recycled by bacteria and degrades faster than organic matter from higher plants. This leads to an apparent increase in the influence of higher plant sources with increasing depth in the core.

Group 1 (sterols, triterpenoids and waxes)

All sites show decreasing compound concentration with depth, except site 3. At 40-centimetres depth, site 3 had markedly higher biomarker concentrations. This difference is identified within the PCA, and illustrated

in the PC factors plotted against depth (figure 2). This particular sample has a high concentration of leaf-wax biomarkers and a total organic carbon content of 12 per cent. The high organic carbon content and high concentration of leaf-wax compounds suggest that this horizon received an unusually high input of terrestrial plant material.

Analysis of the fossil pollen record in the sediments at site 3 confirms the presence of a terrestrial wetland/swamp at this depth.^{2,10}

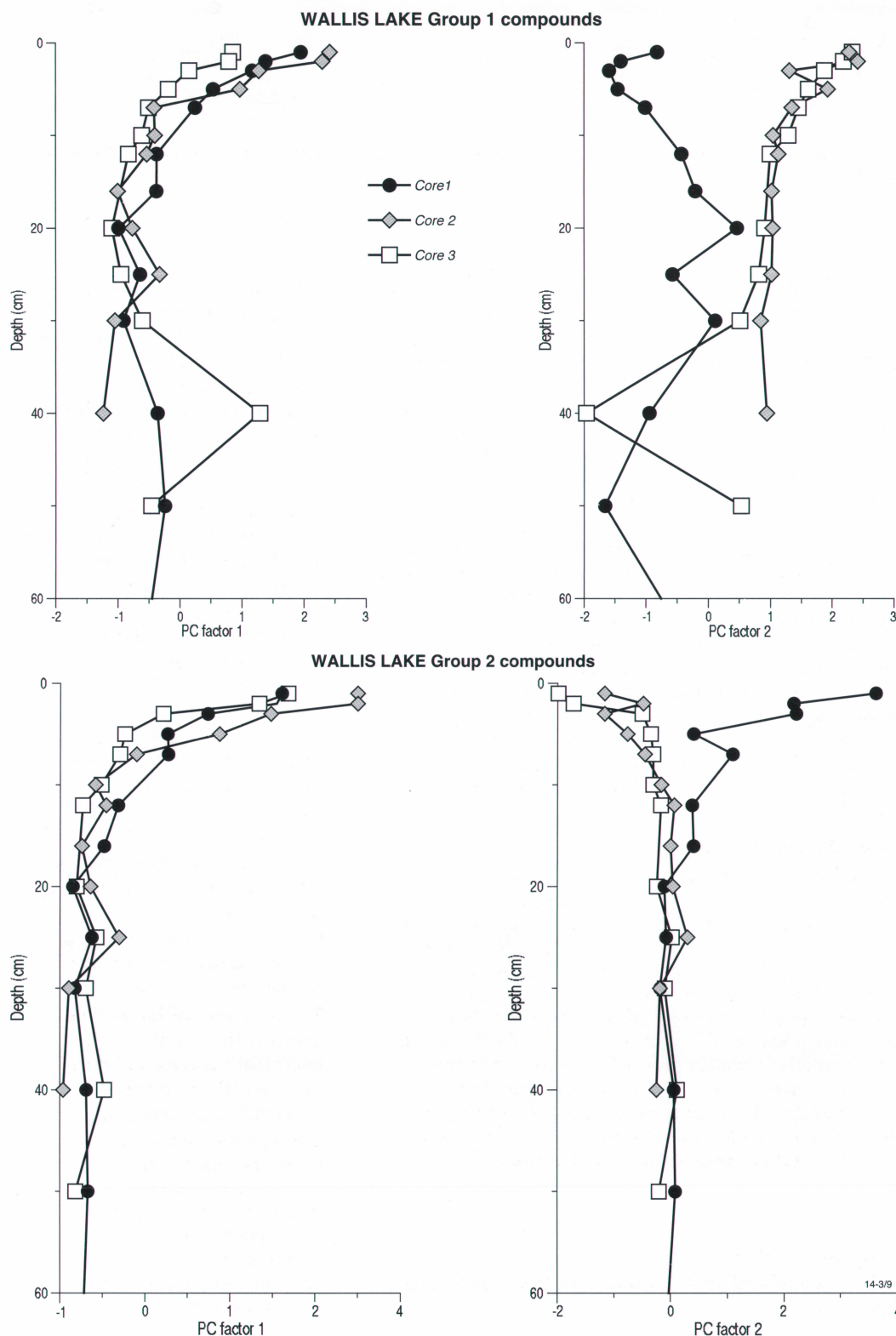


Figure 2. Principal components 1 and 2 plotted against depth. PC factor 1 for both compound groups is controlled by concentration/diagenesis. PC factor 2 contains greater source information.

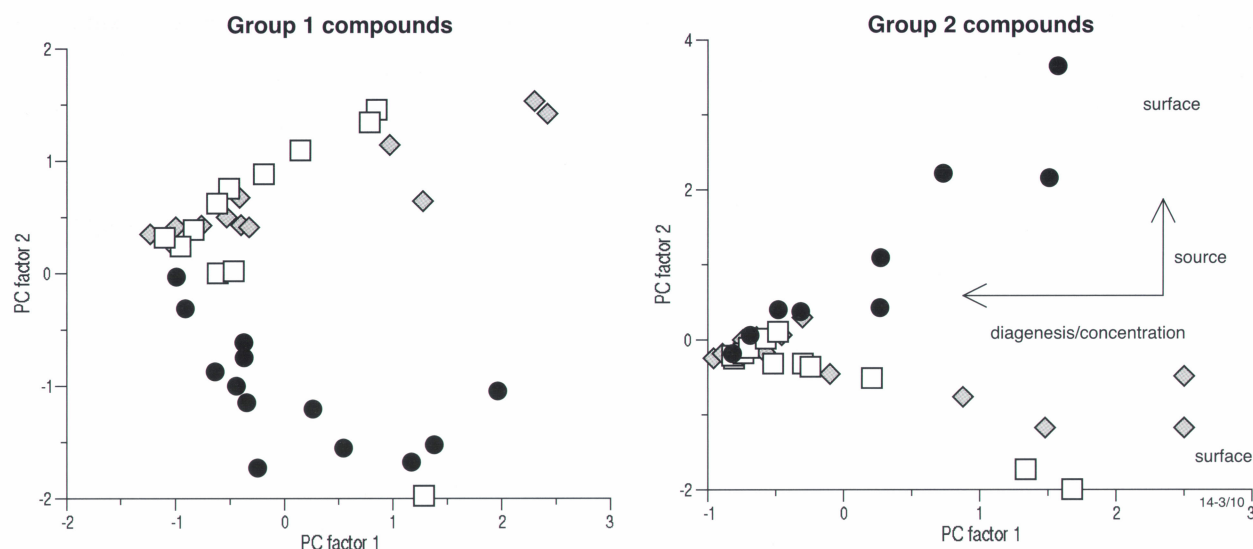


Figure 3. Cross-plots of principal components 1 and 2 for both compound groups illustrate that the two main controls on each grouping are the same.

This observation supports the data provided by biomarker analysis and helps explain the increased amount of organic carbon, as well as its unusually strong terrestrial plant signal.

Plotting the second principal component (PC2) of group 1 against depth shows that there is a clear difference between site 1 and sites 2 and 3, particularly from the surface to 20 centimetres (figure 2). These data suggest that organic matter deposited at sites 2 and 3 has not varied significantly during sedimentation of the cores. In contrast, the value of PC2 varies throughout the core collected at site 1, suggesting a variable input of a substantially different composition. Examination of the biomarker concentration data shows that samples from site 1 contain a group of terrestrial plant triterpenoids not present at either of the other sites, and that the components related to leaf waxes are more abundant in samples from this site. The data indicate that site 1 receives inputs from a particular group or species of terrestrial plants that is either not present in the catchment areas of sites 2 and 3 or not transported to these sites. Again this interpretation has been supported by pollen and spore analysis, which indicates that site 1 has received the greatest input of dry sclerophyll forest and woodland pollen, mainly *Eucalyptus gummifera* type.¹⁰ The similarity between sites 2 and 3 indicates that they are receiving similar algal and plant inputs. Since site 2 was chosen to study the effects of urban impact, the lack of variation compared with site 3 indicates that organic matter from the urban catchment is not significantly affecting the biomarker profiles at site 2.

Group 2 (fatty acids and compounds <C₂₀)

Group 2 compounds include biomarkers for phytoplankton, sediment bacteria and some higher plant material. PCA of group 2 compounds provides a similar interpretation to the group 1 data set. The value of PC1 is controlled primarily by concentration/diagenesis, and decreases with depth (figure 2). PC2 shows clear differences among sites, particularly in the upper 10–15 centimetres. Below this depth all sites are relatively similar. Although compounds of group 2 are less specific to terrestrial sources, the PCA cross-plot of factors 1 and 2 illustrates a similar divergence between site 1 and sites 2 and 3 (figure 3). As with biomarkers within group 1, differences in the upper sediment samples are due mainly to variation in terrestrial plant sources between site 1 and sites 2 and 3. The biomarker signal converges with depth. This similarity at depth, results from the presence of common microbial processes and the preferential preservation of terrestrial plant material at all sites.

Summary

The key points of this study are as follows:

1. Phytoplankton biomarkers (dinoflagellates, diatoms and green microalgae) are present in all cores.

2. Terrestrial inputs can be recognised at every site. Furthermore, specific land plant inputs from the Wallamba and Coolongolook Rivers are suggested by distinct biomarker abundances at sites 1 and 5.
3. No evidence of human faecal contamination, based on biomarker techniques, is identified in sediments at any site. Also, a specific urban biomarker signature could not be identified at any site.
4. Biomarkers have identified herbivore (cattle) faecal contamination at the mouths of the Wallamba and Coolongolook Rivers.
5. Freshwater from rivers at sites 1 and 5 may affect algal productivity or populations, based on decreases in the ratios of biomarkers related to certain algae.
6. Diagenesis and concentration affect biomarker distributions down each core.
7. Statistical methods can be used to assess changes in sources of biomarkers within a large data set.
8. The similarity of biomarkers at depth is the result of common microbial processes and the preferential preservation of terrestrial plant material at all sites.
9. The selective preservation of terrestrial plant material implies there is a relatively more rapid turnover of algal organic matter. This material will be an important source of nutrients and may support further algal productivity within the water column.

References

1. Webb, McKeown & Associates. 1999. Wallis Lake estuary processes study. Forster-Tuncurry: Great Lakes Council; unpublished consultants' report: 1–129.
 2. Logan GA, MacPhail M, Fredericks D, Smith C & Heggie D. 2001. Identification of urban and rural inputs to sediments in Lake Wallis. Canberra: AGSO professional opinion, 2001/2.
 3. Robinson N, Eglinton G, Brassell SC & Cranwell PA. 1984. Dinoflagellate origin for sedimentary 4 β -methyl steroids and 5 β (H)-stanols. *Nature*; 308:439–442.
 4. Volkman JK, Barrett SM & Blackburn SI. 1999. Eustigmatophyte microalgae are potential sources of C₂₉ sterols, C₂₂–C₂₈ *n*-alcohols and C₂₈–C₃₂ *n*-alkyl diols in freshwater environments. *Organic Geochemistry*; 30:307–318.
 5. Volkman JK. 1986. A review of sterol markers for marine and terrigenous organic matter. *Organic Geochemistry*; 9:83–99.
 6. Summons RE, Jahnke LL, Hope JM & Logan GA. 1999. 2-methylhopanoids as biomarkers for cyanobacterial oxygenic photosynthesis. *Nature*; 400: 544–557.
 7. Leeming R, Ball A, Ashbolt N & Nichols P. 1996. Using faecal sterols from humans and animals to distinguish faecal pollution in receiving waters. *Water Research*; 30(12):2893–2900.
 8. Meyers PA, Leenheer MJ, Eadie BJ & Maule SJ. 1984. Organic geochemistry of suspended and settling particulate matter in Lake Michigan. *Geochimica et Cosmochimica Acta*; 48(3):443–452.
 9. Volkman JK, Farrington JW, Gagosian RB & Wakeham SW. 1983. Lipid composition of coastal marine sediments from the Peru upwelling region. In: Bjoroy M, et al., eds. *Advances in organic geochemistry 1981*. Chichester: Wiley; 228–240.
 10. MacPhail MK. 2000. Wallis Lake, Great Lake Shire, NSW: Pollen evidence of urban impact on a coastal 'lagoon'. Forster-Tuncurry; unpublished consultants' report.
- Dr Graham Logan, Petroleum and Marine Division, AGSO, phone +61 2 6249 9460 or e-mail graham.logan@agso.gov.au
 - Dr David Fredericks, Petroleum and Marine Division, AGSO, phone +61 2 6249 9434 or e-mail david.fredericks@agso.gov.au
 - Craig Smith, Petroleum and Marine Division, AGSO, phone +61 2 6249 9560 or e-mail craig.smith@agso.gov.au
 - Dr David Heggie, Petroleum and Marine Division, AGSO, phone +61 2 6249 9589 or e-mail david.heggie@agso.gov.au

Publications

involving AGSO authors

December 2000 to April 2001

ABSTRACTS & PROCEEDINGS

Archibald NJ, Hill EJ, **Direen** NG, et al. 2001. AGCRC–Fractal Graphics north-eastern Lachlan Orogen project. In: Korsch RJ & Lyons P, eds. *Integrated geophysical and geological studies of the north-eastern Lachlan Orogen*, New South Wales. *Proceedings of the Eastern Lachlan Orogen Workshop*, Mar 7–9. Canberra: Australian Geological Survey Organisation, record 2001/9; 59.

Archibald NJ, Hill EJ, Holden D, **Direen** NG, et al. 2001. 3D models of the north-eastern Lachlan Orogen. In: Korsch RJ & Lyons P, eds. *Integrated geophysical and geological studies of the north-eastern Lachlan Orogen*, New South Wales. *Proceedings of the Eastern Lachlan Orogen Workshop*, Mar 7–9. Canberra: Australian Geological Survey Organisation, record 2001/9; 66–68.

Archibald NJ, Hill EJ, **Direen** NG, et al. 2001. Wavelet-based edge detection processing (worming) and interpretation of magnetic and gravity data sets, north-eastern Lachlan Orogen. In: Korsch RJ & Lyons P, eds. *Integrated geophysical and geological studies of the north-eastern Lachlan Orogen*, New South Wales. *Proceedings of the Eastern Lachlan Orogen Workshop*, Mar 7–9. Canberra: Australian Geological Survey Organisation, record 2001/9; 60–65.

Barton CE & Colhoun EA. 2000. [abstract]. Climate change and secular variation recorded in Tasmanian lakes. *Palaeomagnetism, Rock Magnetism & Environmental Magnetism Workshop*, Canberra, May 3–4. Canberra: Australian Geological Survey Organisation, record 2000/36; 2–3.

Bradshaw MT. 2001. [abstract]. Australia and eastern Indonesia at the cross-roads of Gondwana and Tethys—the implications for petroleum resources. *SEAPEX Exploration Conference 2001*, Singapore, Apr 4–6.

Budd AR, Bastrakova IV & Wyborn LA. 2001. [abstract]. Proterozoic S-type granites of Australia. In: Chappell BW & Fleming P, eds. *S-type granites and related rocks*. A symposium to mark the 70th birthday of Professor Allan White, Jan 11–12. Canberra: Australian Geological Survey Organisation, record 2001/2; 25–26.

Champion DC & Bultitude RJ. 2001. [abstract]. Palaeozoic S-type granites of the Hodgkinson Province, far north Queensland. In: Chappell BW & Fleming P, eds. *S-type granites and related rocks*. A symposium to mark the 70th birthday of Professor Allan White, Jan 11–12. Canberra: Australian Geological Survey Organisation, record 2001/2; 27–28.

Cross AJ, Korsch RJ, Raymond OL, Lyons P, Dabrowski R & Mills AW. 2001. The PREDICT geological information system and its application to the north-eastern Lachlan Orogen. In: Korsch RJ & Lyons P, eds. *Integrated geophysical and geological studies of the north-eastern Lachlan Orogen*, New South Wales. *Proceedings of the Eastern Lachlan Orogen Workshop*, Mar 7–9. Canberra: Australian Geological Survey Organisation, record 2001/9; 36–39.

de Caritat P, Gibson DL, Hill SM, et al. 2000. [abstract]. Regolith research in the Broken Hill region: An overview of CRC LEME activities. In: Peljo M, comp. *Abstracts of conference papers, Broken Hill Exploration Initiative*, May 2000. Canberra: Australian Geological Survey Organisation, record 2000/10; 12–15.

de Caritat P, Killick MF, Lavitt N, Tonui E, Dann R & Turner ML. 2000. [abstract]. Characterisation of regolith, sediment and groundwater in the Mundi Mundi–Curnamona region. In: Peljo M, comp. *Abstracts of conference papers, Broken Hill Exploration Initiative*, May 2000. Canberra: Australian Geological Survey Organisation, record 2000/10; 16–19.

- Direen** NG, Crawford AJ & Willcox JB. 2000. [abstract]. Structure and geological evolution of the Koonenberry Fold Belt, NSW: Implications for mineralisation. In: Peljo M, comp. Abstracts of conference papers, Broken Hill Exploration Initiative, May 2000. Canberra: Australian Geological Survey Organisation, record 2000/10; 33–34.
- Direen** NG, Lyons P, Korsch RJ & Glen RA. 2001. Three-dimensional integrated geophysical appraisal of major structures in the north-eastern Lachlan Orogen. In: Korsch RJ & Lyons P, eds. Integrated geophysical and geological studies of the north-eastern Lachlan Orogen, New South Wales. Proceedings of the Eastern Lachlan Orogen Workshop, Mar 7–9. Canberra: Australian Geological Survey Organisation, record 2001/9; 54–58.
- Finlayson** DM, Korsch RJ & Glen RA. 2001. Contrasts in crustal architecture north and south of the Lachlan Transverse Zone, north-eastern Lachlan Orogen. In: Korsch RJ & Lyons P, eds. Integrated geophysical and geological studies of the north-eastern Lachlan Orogen, New South Wales. Proceedings of the Eastern Lachlan Orogen Workshop, Mar 7–9. Canberra: Australian Geological Survey Organisation, record 2001/9; 40–44.
- Foster** KA, Shirliff G & Hill SM. 2000. [abstract]. Balaclava 1:25 000 regolith-landform map: Developing detailed mapping for regolith dominated terrains. In: Peljo M, comp. Abstracts of conference papers, Broken Hill Exploration Initiative, May 2000. Canberra: Australian Geological Survey Organisation, record 2000/10; 38–40.
- Gibson** DL. 2000. [abstract]. Regolith, landform history and sampling strategies in the Wonnaminta area, Koonenberry Belt. In: Peljo M, comp. Abstracts of conference papers, Broken Hill Exploration Initiative, May 2000. Canberra: Australian Geological Survey Organisation, record 2000/10; 41–44.
- Gibson** GM. 2000. [abstract]. Tectonic evolution of the Palaeoproterozoic Willyama Supergroup, Broken Hill: The early years. In: Peljo M, comp. Abstracts of conference papers, Broken Hill Exploration Initiative, May 2000. Canberra: Australian Geological Survey Organisation, record 2000/10; 45–47.
- Glen RA, **Korsch** RJ, Jones LEA, Lawrie KC, Shaw RD & Johnstone DW. 2001. Crustal structure of the Ordovician Macquarie Arc, Eastern Lachlan Orogen, NSW, based on deep seismic reflection profiling. In: Korsch RJ & Lyons P, eds. Integrated geophysical and geological studies of the north-eastern Lachlan Orogen, New South Wales. Proceedings of the Eastern Lachlan Orogen Workshop, Mar 7–9. Canberra: Australian Geological Survey Organisation, record 2001/9; 45–48.
- Glen RA, **Raymond** OL & Lyons P. 2001. Geological issues of the Eastern Belt of the north-eastern Lachlan Orogen. In: Korsch RJ & Lyons P, eds. Integrated geophysical and geological studies of the north-eastern Lachlan Orogen, New South Wales. Proceedings of the Eastern Lachlan Orogen Workshop, Mar 7–9. Canberra: Australian Geological Survey Organisation, record 2001/9; 7–11.
- Hill LJ, Eggleton RA, **de Caritat** P & Field JB. 2000. [abstract]. Biogeochemical and geochemical dispersion and residence in landscapes of western New South Wales. In: Peljo M, comp. Abstracts of conference papers, Broken Hill Exploration Initiative, May 2000. Canberra: Australian Geological Survey Organisation, record 2000/10; 51–52.
- Hill SM, Jones GL, **Foster** KA, et al. 2000. [abstract]. Mineralisation signatures in the regolith of the Broken Hill region. In: Peljo M, comp. Abstracts of conference papers, Broken Hill Exploration Initiative, May 2000. Canberra: Australian Geological Survey Organisation, record 2000/10; 53–56.
- Jones** LE, Drummond BJ & Goleby BR. 2001. Capabilities of the seismic reflection method in hard rock terranes. In: Korsch RJ & Lyons P, eds. Integrated geophysical and geological studies of the north-eastern Lachlan Orogen, New South Wales. Proceedings of the Eastern Lachlan Orogen Workshop, Mar 7–9. Canberra: Australian Geological Survey Organisation, record 2001/9; 12–25.
- Jones** LE & Johnstone DW. 2001. Acquisition and processing of the 1997 Eastern Lachlan (L146) and 1999 Lachlan (L151) seismic reflection surveys. In: Korsch RJ & Lyons P, eds. Integrated geophysical and geological studies of the north-eastern Lachlan Orogen, New South Wales. Proceedings of the Eastern Lachlan Orogen Workshop, Mar 7–9. Canberra: Australian Geological Survey Organisation, record 2001/9; 26–35.
- Klootwijk** C. 2000. [abstract]. Alternative Late Palaeozoic cratonic polepaths: The slip-path and the KG-path. Palaeomagnetism, Rock Magnetism & Environmental Magnetism Workshop, Canberra, May 3–4. Canberra: Australian Geological Survey Organisation, record 2000/36; 21.
- Klootwijk** C. 2000. [abstract]. Late Palaeozoic polepath for the New England Orogen: Constraints and implications from the Rocky Creek Block, Tamworth Belt. Palaeomagnetism, Rock Magnetism & Environmental Magnetism Workshop, Canberra, May 3–4. Canberra: Australian Geological Survey Organisation, record 2000/36; 19–20.
- Korsch** RJ. 2001. Integrated geophysical and geological studies of the north-eastern Lachlan Orogen, New South Wales: Outline and scope. In: Korsch RJ & Lyons P, eds. Integrated geophysical and geological studies of the north-eastern Lachlan Orogen, New South Wales. Proceedings of the Eastern Lachlan Orogen Workshop, Mar 7–9. Canberra: Australian Geological Survey Organisation, record 2001/9; 1–6.
- Lyons** P, Direen NG, Archibald NJ, Raymond OL & Korsch RJ. 2001. Mineral systems implications of multi-scale edge detection of crustal structures in the north-eastern Lachlan Orogen. In: Korsch RJ & Lyons P, eds. Integrated geophysical and geological studies of the north-eastern Lachlan Orogen, New South Wales. Proceedings of the Eastern Lachlan Orogen Workshop, Mar 7–9. Canberra: Australian Geological Survey Organisation, record 2001/9; 81–85.
- Mackey** TE. 2001. [CD-ROM]. Web-based mapping, GIS and image processing: The AGSO perspective. In: O'Donnell I, ed. Proceedings of the 5th National Forum on Information Management in the Geosciences: Geoscience Online, Canberra, Mar 28–29. Canberra: Australian Geological Survey Organisation, record 2001/13.

Maidment DW & Gibson GM. 2000. [abstract]. Regional lithological interpretation of the Broken Hill and Euriowie Blocks, NSW. In: Peljo M, comp. Abstracts of conference papers, Broken Hill Exploration Initiative, May 2000. Canberra: Australian Geological Survey Organisation, record 2000/10; 67–68.

O'Donnell I. 2001. [CD-ROM]. Report on GGIPAC. In: O'Donnell I, ed. Proceedings of the 5th National Forum on Information Management in the Geosciences: Geoscience Online, Canberra, Mar 28–29. Canberra: Australian Geological Survey Organisation, record 2001/13; 1.

Page RW, Stevens BP, **Gibson** GM & Connor CH. 2000. [abstract]. Geochronology of Willyama Supergroup rocks between Olary and Broken Hill, and comparison to northern Australia. In: Peljo M, comp. Abstracts of conference papers, Broken Hill Exploration Initiative, May 2000. Canberra: Australian Geological Survey Organisation, record 2000/10; 72–75.

Papp E, Foster KA, Shirliff G, Hill SM. 2000. [abstract]. Spectral characterisation of regolith units at Balaclava West, Broken Hill, NSW. In: Peljo M, comp. Abstracts of conference papers, Broken Hill Exploration Initiative, May 2000. Canberra: Australian Geological Survey Organisation, record 2000/10; 76–78.

Powell TG. 2001. [CD-ROM]. Information management in AGSO. In: O'Donnell I, ed. Proceedings of the 5th National Forum on Information Management in the Geosciences: Geoscience Online, Canberra, Mar 28–29. Canberra: Australian Geological Survey Organisation, record 2001/13.

Raymond OL & Scott M. 2001. AGCRC seismic lines 97AGSL2 and 97AGSL3 excursion notes. In: Korsch RJ & Lyons P, eds. Integrated geophysical and geological studies of the north-eastern Lachlan Orogen, New South Wales. Proceedings of the Eastern Lachlan Orogen Workshop, Mar 7–9. Canberra: Australian Geological Survey Organisation, record 2001/9; 86–96.

Raymond OL, Sherwin L, Lyons P & Scott M. 2001. The Jemalong Trough: Further evidence of Silurian–Devonian rifting in the Eastern Lachlan Orogen. In: Korsch RJ & Lyons P, eds. Integrated geophysical

and geological studies of the north-eastern Lachlan Orogen, New South Wales. Proceedings of the Eastern Lachlan Orogen Workshop, Mar 7–9. Canberra: Australian Geological Survey Organisation, record 2001/9; 69–76.

Roberts J, Opdyke ND, **Claoue-Long** J, Irving E & Jones PJ. 2000. [abstract]. Stratigraphic evidence for redefinition of the base of the Kiaman reversed superchron. Palaeomagnetism, Rock Magnetism & Environmental Magnetism Workshop, Canberra, May 3–4. Canberra: Australian Geological Survey Organisation, record 2000/36; 43.

Root J. 2001. [CD-ROM]. Online geoscience information: Where to next? In: O'Donnell I, ed. Proceedings of the 5th National Forum on Information Management in the Geosciences: Geoscience Online, Canberra, Mar 28–29. Canberra: Australian Geological Survey Organisation, record 2001/13.

Skirrow RG. 2000. Gold-copper-bismuth deposits of the Tennant Creek district, Australia: A reappraisal of diverse high-grade systems. In: Porter TM, ed. Proceedings of the Hydrothermal Iron Oxide Copper-Gold and Related Deposits: A Global Perspective conference, Perth, Dec 4–5. Glenside (SA): Australian Mineral Foundation; 149–160.

Skirrow RG, Ashley PM, McNaughton NJ & Suzuki K. 2000. [abstract]. Time–space framework of Cu–Au–(Mo) and regional alteration systems in the Curnamona province. In: Peljo M, comp. Abstracts of conference papers, Broken Hill Exploration Initiative, May 2000. Canberra: Australian Geological Survey Organisation, record 2000/10; 83–86.

Tan KP, Eggleton RA & **de Caritat** P. 2000. [abstract]. Geochemical mapping of element distribution in the regolith at Portia and North Portia prospects, Benagerie Ridge Magnetic Complex, Curnamona, South Australia. In: Peljo M, comp. Abstracts of conference papers, Broken Hill Exploration Initiative, May 2000. Canberra: Australian Geological Survey Organisation, record 2000/10; 92–93.

Williams PJ & **Skirrow** RG. 2000. Overview of iron oxide-copper-gold deposits in the Curnamona Province and Cloncurry district (eastern Mount Isa Block), Australia. In: Porter TM, ed. Proceedings of the Hydrothermal

Iron Oxide Copper-Gold and Related Deposits: A Global Perspective conference, Perth, Dec 4–5. Glenside (SA): Australian Mineral Foundation; 105–122.

ARTICLES

Auzende JM, van de Beuque S, Regnier M, Lafoy Y & **Symonds** PA. 2000. Origin of the New Caledonian ophiolites based on a French–Australian seismic transect. *Marine Geology*; 162(2–4):225–236.

Boreham CJ, Hope JM, Hartung-Kagi B & van Aarsen BJ. 2000. More sources for gas and oil in Perth Basin: Study highlights potential for multiple petroleum systems. *AGSO Research Newsletter*, Dec; 33:5–9.

Boreham CJ, Hope JM & Hartung-Kagi B. 2001. Understanding source, distribution and preservation of Australian natural gas: A geochemical perspective. *APPEA Journal*; 41(1):523–547.

Brauhart CW, **Huston** DL & Andrew AS. 2000. Oxygen isotope mapping in the Panorama VMS district, Pilbara Craton, Western Australia: Applications to estimating temperatures of alteration and to exploration. *Mineralium Deposita*; 35(8):727–740.

Brincat MP, **O'Brien** GW, Lisk M, de Ruig M & George SC. 2001. Hydrocarbon charge history of the northern Londonderry High: Implications for trap integrity and future prospectivity. *APPEA Journal*; 41(1):483–495.

de Caritat P, Killick MF, Lavitt N, Tan KP & Tonui E. 2000. 3D conceptual modelling to aid mineral exploration in the southern Callabonna Sub-basin. *MESA Journal*; 19:46–47.

de Caritat P, Reimann C, Bogatyrev I, et al. 2001. Regional distribution of Al, B, Ba, Ca, K, La, Mg, Mn, Na, P, Rb, Si, Sr, Th, U and Y in terrestrial moss within a 188 000 km² area of the central Barents region: Influence of geology, seaspray and human activity. *Applied Geochemistry*; 16(2):137–159.

Dentith MC, Dent VF & **Drummond** BJ. 2000. Deep crustal structure in the south-western Yilgarn Craton, Western Australia. *Tectonophysics*; 325(3–4):227–255.

- Drummond** BJ, Barton TJ, Korsch RJ, et al. 2000. Evidence for crustal extension and inversion in eastern Tasmania, Australia, during the Neoproterozoic and early Palaeozoic. *Tectonophysics*; 329(1-4):1-21.
- Drummond** BJ, Goleby BR, Owen AJ, et al. 2000. Seismic reflection imaging of mineral systems: Three case histories. *Geophysics*; 65(6):1852-1861.
- Drummond** BJ, Goleby BR & Swager CP. 2000. Crustal signature of late Archaean tectonic episodes in the Yilgarn Craton, Western Australia: Evidence from deep seismic sounding. *Tectonophysics*; 329(1-4):193-221.
- Edwards** DS, Kennard JM, Preston JC, Summons RE, Boreham CJ & Zumberge JE. 2000. Bonaparte Basin: Geochemical characteristics of hydrocarbon families and petroleum systems. *AGSO Research Newsletter*, Dec; 33:14-19.
- Fraser** G, McDougall I, Ellis DJ & Williams IS. 2000. Timing and rate of isothermal decompression in Pan-African granulites from Rundvagshetta, East Antarctica. *Journal of Metamorphic Geology*; 18(4):441-454.
- Fraser** G, Worley B & Sandiford M. 2000. High-precision geothermobarometry across the High Himalayan metamorphic sequence, Langtang Valley, Nepal. *Journal of Metamorphic Geology*; 18(6):665-681.
- Goleby** BR, Drummond BJ & Mifsud J. 2000. An approach to using seismic reflection imaging in mineral provinces—an example at a province scale. *Preview*; 88:17-19.
- Hallam A, Wignall PB, Yin J & **Riding** JB. 2000. An investigation into possible facies changes across the Triassic-Jurassic boundary in southern Tibet. *Sedimentary Geology*; 137(3-4):101-106.
- Hallsworth CR, Morton AC, **Claoue-Long** J & Fanning CM. 2000. Carboniferous sand provenance in the Pennine Basin, UK: Constraints from heavy mineral and detrital zircon age data. *Sedimentary Geology*; 137(3-4):147-185.
- Harris** PT. 2000. Ripple cross-laminated sediments on the East Antarctic shelf: Evidence for episodic bottom water production during the Holocene?. *Marine Geology*; 170(3-4):317-330.
- Hinrichs KU, **Summons** RE, Orphan V, Sylva SP & Hayes JM. 2000. Molecular and isotopic analysis of anaerobic methane-oxidizing communities in marine sediments. *Organic Geochemistry*; 31(12):1685-1701.
- Huston** DL. 2001. Geochemical dispersion about the Western Tharsis Cu-Au deposit, Mt Lyell, Tasmania. *Journal of Geochemical Exploration*; 72(1):23-46.
- Jackson** MJ, Southgate PN & Page RW. 2000. Gamma-ray logs and U-Pb zircon geochronology; essential tools to constrain lithofacies interpretation of Paleoproterozoic depositional systems. In: Grotzinger JP & James NP, eds. Carbonate sedimentation and diagenesis in the evolving Precambrian world. Society for Sedimentary Geology, special publication 67; 23-41.
- Kamenetsky VS, Binns RA, Gemmell JB, **Mernagh** TP, et al. 2001. Parental basaltic melts and fluids in eastern Manus backarc basin: Implications for hydrothermal mineralisation. *Earth & Planetary Science Letters*; 184(3-4):685-702.
- Kenig F, Popp BN & **Summons** RE. 2000. Preparative HPLC with ultrastable-Y zeolite for compound-specific carbon isotopic analyses. *Organic Geochemistry*; 31(11):1087-1094.
- Labrenz M, Druschel GK, Thomsen ET, **Logan** GA, et al. 2000. Formation of sphalerite (ZnS) deposits in natural biofilms of sulfate-reducing bacteria. *Science*; 290(5497):1744-1747.
- Lavering** I. 2000. The use of palaeoecology in petroleum exploration, production and environment protection. *PESA News*, Jun-Jul; 18.
- Mackey** TE, Gunn PJ, Meixner AJ & Blake DH. 2000. Mapping Australian geology under cover: A case study applied to the Boulia and Springvale 1:250 000 map sheets, Queensland. *Preview*; 87:28-32.
- Mackness BS, Whitehead PW & **McNamara** GC. 2000. New potassium-argon basalt date in relation to the Pliocene Bluff Downs Local Fauna, northern Australia. *Australian Journal of Earth Sciences*; 47(4):807-811.
- Messent B, **Edwards** DS, Baron HS & Witham B. 2000. Variations in fluorescent response of oil slicks using an airborne laser fluorosensor system. *AAPG Bulletin*; 84(9):1465.
- Page RW, Stevens B, **Gibson** GM & Conor CH. 2000. Geochronology of Willyama Supergroup rocks near Broken Hill. *Minfo: New South Wales Mining and Exploration Quarterly*; 68:28-30.
- Palmer** D, Fredericks DJ, Smith C & Heggie. 2000. Nutrients from sediments: Implications for algal blooms in Myall Lakes. *AGSO Research Newsletter*, Dec; 33:2-4.
- Petkovic** P, Collins CD & Finlayson DM. 2000. A crustal transect between Precambrian Australia and the Timor Trough across the Vulcan Sub-basin. *Tectonophysics*; 329(1-4):23-38.
- Pike** J. 2000. Minerals laboratory staff develops new ICP-MS preparation method. *AGSO Research Newsletter*, Dec; 33:12-14.
- Planke S, **Symonds** PA, Alvestad E & Skogseid J. 2000. Seismic volcano-stratigraphy of large-volume basaltic extrusive complexes on rifted margins. *Journal of Geophysical Research*, B: Solid Earth & Planets; 105(8):19 335-19 351.
- Powell** TG. 2001. Understanding Australia's petroleum resources, future production trends and the role of the frontiers. *APPEA Journal*; 41(1):273-286.
- Reimann C, Banks D & **de Caritat** P. 2000. Impacts of airborne contamination on regional soil and water quality: The Kola Peninsula, Russia. *Environmental Science & Technology*; 34(13):2727-2732.
- Rigg AJ, Allinson G, **Bradshaw** J, et al. 2001. The search for sites for geological sequestration of CO₂ in Australia: A progress report on GEODISC. *APPEA Journal*; 41(1):711-723.
- Rigg AJ & **Bradshaw** J. 2000. The GEODISC program: Research into geological sequestration of CO₂ in Australia. *AAPG Bulletin*; 84(9):1482.
- Ryburn** R. 2000. China plans to re-map by computer. *Australian Geologist*; 114:23-24.
- Ryburn** R. 2000. The importance of the 'backend' to online delivery of geoscience information. *AGSO Research Newsletter*, Dec; 33:10-11,20.

Sami TT, James NP, Kyser TK, **Southgate** PN, Jackson MJ & Page RW. 2000. Evolution of late Paleoproterozoic ramp systems, lower McNamara Group, north-eastern Australia. In: Grotzinger, JP & James NP, eds. Carbonate sedimentation and diagenesis in the evolving Precambrian world. Society for Sedimentary Geology, special publication 67; 243–274.

Sikes EL, Samson CR, Guilderson TP & Howard WR. 2000. Old radiocarbon ages in the south-west Pacific Ocean during the last glacial period and deglaciation. *Nature*; 405(6786):555–559.

Skirrow RG & Ashley PM. 2000. Proterozoic Cu-Au systems of the Curnamona Province—members of a global family? *MESA Journal*; 19:48–50.

Skirrow RG, Camacho A, Lyons P, et al. 2000. Metallogeny of the southern Sierras Pampeanas, Argentina: Geological, $^{40}\text{Ar}/^{39}\text{Ar}$ dating and stable isotope evidence for Devonian Au, Ag-Pb-Zn and W ore formation. *Ore Geology Reviews*; 17(1–2):39–81.

Smithies RH & **Champion** DC. 2000. The Archaean high-Mg diorite suite: Links to tonalite-trondhjemite-granodiorite magmatism and implications for Early Archaean crustal growth. *Journal of Petrology*; 41(12):1653–1671.

Stewart LK, **Heap** AD & Woolfe KJ. 2000. Evaluating the influence of tidal currents on the distribution of silt in Nara Inlet, central Great Barrier Reef, Australia. *Sedimentary Geology*; 136(1–2):59–69.

Tandon K, Lorenzo JM & **O'Brien** GW. 2000. Effective elastic thickness of the northern Australian continental lithosphere subducting beneath the Banda Orogen (Indonesia): Inelastic failure at the start of continental subduction. *Tectonophysics*; 329(1–4):39–60.

Taylor G, O'Sullivan PB, Pillans B, **Gibson** DL, Kohn BP & Pain CF. 2000. Long-term landscape evolution of the Northparkes region of the Lachlan Fold Belt, Australia:

Constraints from fission track and paleomagnetic data—discussion and reply. *Journal of Geology*; 108(6):749–752.

Wilford JR & Butrovski. 2000. Customised regolith maps incorporate hydrologic modelled attributes for geochemical exploration. *AGSO Research Newsletter*, Dec; 33:21–24.

Williams ND & **Holdway** DA. 2000. The effects of pulse-exposed cadmium and zinc on embryo hatchability, larval development, and survival of Australian crimson spotted rainbow fish (*Melanotaenia fluviatilis*). *Environmental Toxicology*; 15(3):165–173.

Winchester ST, **Foster** C & O'Leary T. 2000. The environmental response of Middle Ordovician large organic walled microfossils from the Goldwyer and Nita formations, Canning Basin, Western Australia. *Review of Palaeobotany & Palynology*; 113(1–3):197–212.

BOOKS & REPORTS

Blewett RS. 2000. [CD-ROM]. Facsimile copy of the Aerial Geological and Geophysical Survey of Northern Australia (AGGSNA) reports 1–26, 28, 46 and 51–59 for Western Australia on the Pilbara goldfield. Canberra: Australian Geological Survey Organisation, record 2000/5.

Blewett RS. 2000. [CD-ROM]. A 'virtual' structural field trip of the North Pilbara. Canberra: Australian Geological Survey Organisation, record 2000/45.

Blewett RS, Wellman P, Ratajkoski M & Huston DL. 2000. Atlas of north Pilbara geology and geophysics, 1:1.5 million scale. Canberra: Australian Geological Survey Organisation, record 2000/4.

Finlayson DM, Gudmundsson O, Itikarai I, et al. 2001. The Rabaul Earthquake Location and Caldera Structure (RELACS) program: Operations report. Canberra: Australian Geological Survey Organisation, record 2001/1.

Giddings JW, **Gibson** GM & Maidment DW. 2000. Rock property–structural geology synergy at work in Broken Hill: A case for structural control of linear magnetic anomalies. Canberra: Australian Geological Survey Organisation, record 2000/36.

Heap A, Bryce S, Ryan D, et al. 2001. Australian estuaries and coastal waterways—a geoscience perspective for improved and integrated resource management. A report to the National Land & Water Resources Audit, theme 7: Ecosystem health. Canberra: Australian Geological Survey Organisation, record 2001/7.

Jackson MJ, Southgate PN, Winefield PR, Barnett K & Zeilinger I. 2000. [CD-ROM]. Revised sub-division and regional correlations of the McArthur Basin succession based on NABRE's 1995–8 sequence stratigraphic studies. Canberra: Australian Geological Survey Organisation, record 2000/3.

Langford RL, Wyche S & **Liu** S-F. 2000. Geology of the Wiluna 1:100 000 sheet. Perth: Western Australia Geological Survey, explanatory notes.

Owen AJ, Bateman R, **Barton** TJ, Drummond BJ, Goleby BR & Sauter PC. 2001. Kalgoorlie seismic profiling 1997: Operations, processing and interpretation report. Canberra: Australian Geological Survey Organisation, record 2001/6.

Soames CL, Gudmundsson O & **Finlayson** DM. 2000. The Rabaul Earthquake Location and Caldera Structure (RELACS) Program: Post-survey data processing. Canberra: Australian Geological Survey Organisation, record 2000/40.

Wilson DJ. 2000. [CD-ROM]. AGSO marine survey 176: Direct hydrocarbon detection north-west Australia—Yampi Shelf, southern Vulcan Sub-basin and Sahul Platform (July/September 1996): Operational report & data compendium. Canberra: Australian Geological Survey Organisation, record 2000/42.

AGSO reference librarian Bev Allen compiled this list of papers and reports. For information about their availability phone Bev on +61 2 6249 9200 or e-mail bev.allen@agso.gov.au. For information about article or report contents contact the AGSO author (name in bold) by e-mailing ...@agso.gov.au or phoning reception on +61 2 6249 9111.

North Pilbara National Geoscience Mapping Accord project (1995–2000)

Scientific highlights

RS Blewett, DL Huston & DC Champion

AGSO and the Geological Survey of Western Australia (GSWA) conducted a multidisciplinary project in the North Pilbara region under the National Geoscience Mapping Accord (NGMA) between 1995 and 2000. The research was driven by a need to ascertain whether exploration- and mineral-deposit models based upon late Archaean examples were suitable for older Archaean terranes. The goal was to document differences between late Archaean and the early to mid-Archaean mineral systems, and then develop regional thematic synthesis datasets to construct more robust models for the entire Archaean era.

This paper highlights the diversity of the Pilbara's mineral systems, discusses exploration tools used to map alteration haloes, considers geochemistry and crustal provenance, explores the 3D geometry of the granitoid–greenstone terrane, and promotes the regional synthesis and GIS, which assist exploration in the Pilbara and other Precambrian terranes.

The Archaean Pilbara Craton is an ovoid entity 600 kilometres by 550 kilometres located in the north-west part of Western Australia. The North Pilbara region represents the mostly exposed northern 25 per cent of this craton. The rest is concealed by late Archaean and 'younger' cover rocks. The Pilbara Craton is a granitoid–greenstone terrane characterised by a distinctive, and relatively intact, ovoid pattern of granitoid batholiths (50–120 km diameter) and enveloping greenstones. Crustal-scale shear zones are limited to the central and western part of the North Pilbara region. The craton's tectonic history spans 800 million years (3.65 to 2.85 Ga). Much of the crustal growth occurred in a series of tectono-thermal events made up of repeated cycles of granitoid magmatism and greenstone volcanism, followed by deformation and metamorphism. The Pilbara Craton has a great diversity of mineral deposits. It hosts some of the world's oldest mineral systems of their type, many of which were active more than once. The oldest systems include: syngenetic barite (3490 Ma), VHMS base metals (3460 Ma, 3240 Ma, 3125 Ma, 2950 Ma), lode Au±Sb (3400–3300 Ma, 2900 Ma), porphyry Cu–Mo (3320 Ma), komatiite-hosted Ni–Cu (>3270 Ma), layered mafic-ultramafic complex-hosted V or Ni–Cu–PGE (2925 Ma), pegmatite Sn–Ta (2850 Ma) and epithermal Au (3450 Ma?, 2760 Ma).

Archaean mineral systems

Table 1 lists a number of fundamental tectonic and metallogenic differences between the granitoid–greenstone terranes of the Pilbara Craton (3.65–2.8 Ga) and highly mineralised Neoarchaeal provinces such as the Eastern Goldfields in Western Australia or the Abitibi in Canada. Several major differences are apparent, the most significant of which is possibly the duration of crustal growth. Both the Abitibi and the Eastern Goldfields grew over relatively short periods of less than 200 million years, compared with the Pilbara Craton's development over more than 800 million years. There is extensive crustal recycling in the Pilbara Craton because of this long history of crustal growth. Other important differences between the North Pilbara and Neoarchaeal terranes are the shape and depth extent of the granite complexes and greenstone belts (table 1). More importantly though, in terms of mineral systems, is the extent of shear zones. The Pilbara Craton has few province-scale shear zones, whereas major shear zones in the Eastern Goldfields and Abitibi provinces commonly extend more than 200 kilometres.

These differences in tectonic development may have had a direct bearing on the mineral endowment of the North Pilbara region. For instance, protracted crustal growth may have been a two-edged sword. It probably is responsible in part for the diversity of mineral systems, but slow growth may have hampered the development of large ones. Rapid growth from magmatic and volcanic events in the Abitibi and Eastern Goldfields provinces produced a lot of heat over a short time, facilitating the development of large mineral systems. In contrast, slow growth in the Pilbara may have facilitated a large variety of different mineral systems, but the rate of heat production was probably too low to drive enough fluid to form large mineral systems. The major metallogenic epoch in the North Pilbara Craton was the development of the Central Pilbara Tectonic Zone, an event that introduced a relatively large amount of heat into the crust in a short time (<100 Ma).

A second factor that may have hampered development of large mineral systems is the lack of large-scale shear zones. The longest shear system in the North Pilbara, the Sholl Shear Zone, is exposed over only 200 kilometres. Major shear zones in the Eastern Goldfields and Abitibi provinces are typically longer than 200 kilometres, and some exceed 500 kilometres. Long shear systems may facilitate large mineral systems by allowing fluid circulation in an extended part of the Earth's crust.

New potential, old province

The perception that the Pilbara is well exposed and therefore all mineral deposits have been discovered is ill-founded. Less than 25 per cent of the craton is exposed and, even in areas of exposure, new mineral systems have been recently found (e.g., the well-preserved, high-level Archaean epithermal gold systems¹), which has resulted in new ground uptake and investment in the Pilbara.

Table 1. Comparison of the Pilbara Craton with highly mineralised Neoarchaeon provinces

	Pilbara Craton	Eastern Goldfields, Superior provinces	Comments
Crustal growth	Extensive recycling of crust by many events over a long period	Major crustal growth event in a short period	
Granite geometry	Domal and ovoid geometry	Elongate geometry	
Greenstone geometry	Greenstones (and granitoids) extend to 14-km depth.	Greenstones extend to 5–7 km where they are underlain by low-angle detachments and deep tapping shear zones.	
Shear zones	Craton-scale shear zones are not common. With few exceptions (e.g., Sholl and Mallina Shear Zones), shear zones are local features.	Craton-scale shear zones are common. These shear zones are first-order controls on lode gold deposits.	
Crustal level exposed	Mostly greenschist facies metamorphism. Local amphibolite facies (LP-HT) in greenstones near granitoids, local kyanite-bearing suggests some higher pressure.	Mostly greenschist facies metamorphism in greenstones. Local amphibolite facies in greenstones near granitoids. In the Eastern Goldfields there are extensive gneiss belts in 'external' granites.	Extensive gneisses in the Eastern Goldfields may imply deeper crustal levels and therefore larger throws on greenstone-bounding faults and shear zones.
Diversity of mineral systems	Atypical Archaean deposits such as Sn-Ta pegmatites, porphyry Mo-Cu deposits and epithermal Au are common in the Pilbara. More 'typical' deposit types are also present.	Characterised by 'typical' Archaean deposits like lode Au, VHMS (Abitibi) and komatiite-hosted Ni-Cu. VHMS not common in EGP.	Many deposit types present in the North Pilbara Terrane are more typical of Proterozoic or Phanerozoic terranes.
Size of mineral systems	Many different mineral systems operated, but the associated mineral deposits tend to be small, and total endowment is apparently small.	Relatively few mineral systems operated, but they produced much larger deposits (e.g., lode Au and VHMS) and a very high endowment.	
Temporal distribution of mineralising events	Episodic mineralising events over a period of 800 Ma (e.g., 4 VHMS events and 2 orogenic gold events)	Single, global(?) events (e.g., 2710±20 Ma for VHMS and 2630±10 Ma for orogenic gold)	
VHMS deposits	Significant Pb and baryte; some deposits in calc-alkaline settings.	Generally lack Pb; always lack baryte; mainly in tholeiitic settings.	Pilbara characteristics are more like Phanerozoic systems.

Extensive areas of the North Pilbara are presently exposed close to the (ca. 2775 Ma) Hamersley Province unconformity surface.² This exceptional preservation significantly improves younger mineralising events of gold and possibly diamonds in the mostly older mid-Archaean Pilbara granite–greenstone terrane. Areas of high-level (epithermal) systems preserved in the west and far east Pilbara have been documented by the NGMA project. The systems are interpreted as being related to NNW-trending dextral faults and associated relay movements during the early stages of the Hamersley Province extensional event. Epithermal veins cut the (ca. 2765 Ma) Opaline Well Granite, and similarly aged Gregory Range Granite.

Application of exploration tools

The North Pilbara project has had significant success in developing and applying exploration tools for the Pilbara and other provinces. Most of the project's effort focused on mapping alteration systems in both well-exposed and poorly exposed

regions. Successful techniques include the HYMAP multispectral scanner, airborne gamma-ray spectrometrics, oxygen isotopes, and whole-rock geochemical depletion patterns.

HYMAP, an airborne 128 channel multispectral scanner, was flown over two 20-kilometre-long by five-kilometre-wide strips in the Mallina–Indee area of the Pilbara.³ The HYMAP data successfully mapped alteration minerals such as pyrophyllite and sericite, distinguished Fe-chlorite from Mg-chlorite, and separated dolomite from calcite in calcrete. Resultant images are presented as image abundance maps with a 10-metre pixel cell size. Several sericite-pyrophyllite targets generated from the HYMAP images produced anomalous gold on subsequent analysis,³ demonstrating the predictive value of this tool. This work has featured widely as an excellent example of the application of remote sensing as a mapping tool in regolith-dominated areas.

Work in the Panorama volcanic-hosted massive sulphide (VHMS) district generated reliable vectors to ore by using oxygen isotopes, converting these to palaeotemperatures, and locating circulation and discharge cells in subvolcanic intrusions.⁴ The calculated temperatures not only define fluid pathways, but may predict Zn/Cu ratios in VHMS deposits.

In the same VHMS mineralising system, whole-rock geochemistry was also used as a mapping tool. District-scale depletion of Zn and Cu has been mapped, and these depletion zones define fluid pathways.⁵ These data, with mass balance calculations, indicate that Zn, Cu, Pb, Mo, Ba and S could have been entirely derived from the volcanic pile, and that a magmatic-hydrothermal source is not required.^{5,6}

To date, most users of gamma-ray spectrometric data have generated standard red-green-blue images for their interpretation. But AGSO applied a number of data processing techniques. The enormous dynamic range of the data involved large areas of over-saturation (white) from K-U-Th-rich granites, and equally large areas of undersaturation (black) from mafic and ultramafic rocks.⁷ Dose counts were converted to ppm U and Th and % K, and used to generate ‘chemical’ maps that closely matched traditional lithological maps. These images highlighted areas of mapping discrepancy—a result of error or changed rock chemistry (alteration). Images of the K, Th, U principal components were developed, and used to define evolutionary paths for the granitoid complexes.⁷

Simple K/Th ratios were used to map K-depletion anomalies associated with the Panorama alteration system.⁸ These anomalies map the same interpreted fluid pathways in the VHMS system determined from whole-rock chemistry^{5,6} and oxygen isotopes⁴.

Geochemistry and crustal provenance

AGSO and GSWA have compiled a comprehensive whole-rock geochemical database. One of the exciting findings from this has been the recognition of high-Mg diorite (sanukitoid) in the Central Pilbara Tectonic Zone.⁹ These rocks, previously only described from Canada, indicate a mantle source that had been modified by subduction. They provide evidence for a setting where, at least in the Central Pilbara Tectonic Zone, the entire thickness of the crust was available for fluid movement at around 2950 Ma. This has implications for fluid movement and tapping into deep crustal and mantle sources at this time. The association of gold at the Towerana porphyry, and an intrusion of the mineralised Mallina Shear Zone, may indicate a link between mineralisation and high-Mg diorite. The recognition of voluminous 2950 million-year-old and younger magmatism along the margin of the Central Pilbara Tectonic Zone and east Pilbara granite–greenstone terrane, in the Yule, Carlindi and Pippingarra granitoid complexes and within the Mallina basin,^{9,10} provide further strong evidence for a major thermal event at this time and a favourable environment for mineralisation.

AGSO’s contribution to the geochronological database was in dating crustal provenance and inheritance using the Sm–Nd isotopic technique. Nd model ages, when combined with U–Pb zircon ages, provide estimates of crustal residence times. When the ages from the two methods are close (<100 Ma), these data can indicate a juvenile or mantle derivation. If the Sm–Nd age is much older (>100 Ma), it suggests some degree of crustal recycling. A major finding of this work has been the recognition of relatively juvenile crust in the Central Pilbara Tectonic Zone, sandwiched between older crust on the west and east.¹¹ In the Central Pilbara, Nd isotope model ages of granitic rocks and felsic and mafic volcanic rocks are only 30–130 million years older than their U–Pb emplacement/depositional age. This is consistent with the high-Mg diorite occurrences, all of which suggest that the Central Pilbara Tectonic Zone ‘saw’ the mantle at various times through its evolution.

Regional synthesis and GIS

Most stakeholders require regional synthesis datasets in order to provide an overarching framework to their targeted areas. AGSO created a comprehensive set of digital themes for the entire Pilbara Craton. Data collection began with acquiring new 400-metre flight-line spaced geophysics (released as map sheet images and digital data), and compiling these surveys into a craton-wide data set. The complete set of geophysical and geological data were released as a two-CD GIS set,¹² a 1:1.5 million scale colour atlas,¹³ and a thematic series of 1:500 000 scale maps and images—print-on-demand or postscript files). A ‘teaching’ GIS of the Marble Bar area was also produced.¹⁴

The project documented the variety of mineral deposits—especially gold¹⁵, VHMS^{4–6,8}, Sn–Ta¹⁶—and high-level deposits², and produced databases (GIS) and maps. Results of Pilbara gold are presented as an online record that draws on a guide written for an industry field excursion (June–July 1999) examining the key deposits and relationships.¹⁵ Historical records and information were also captured as part of the synthesis, including the 1930s Aerial Geological and Geophysical Survey of Northern Australia (AGGSNA) reports that are now on CD.¹⁷ They contain much valuable information about deposit location, mine plans, assays, geology and geological maps.

A regional structural synthesis involving a new deformation chronology and kinematics of some of the major shear zones has been documented. These results are presented in a novel CD,¹⁸ with hotlinked images and field photos, which can be read either in a spatial or temporal sense, or in a traditional way. Advances in knowledge of the structural geology include:

1. a better understanding of shear zone timing and movement senses;
2. an improved understanding of the complexity of the polyphase deformation; and
3. recognition of the importance of horizontal compression as a tectonic driving force.

These results provide a clearer link between regional tectonics and mineral deposits, especially in the understanding of the lode gold deposits.

3D geometry of the Pilbara

To understand a mineral system, the three-dimensional architecture of a province needs to be constrained. AGSO developed the first 3D model of the entire North Pilbara region.^{7,19} This was achieved by integrating the regional synthesis datasets such as gravity, aeromagnetism and seismic refraction data. Applications of the 3D knowledge include constraints on tectonic models, identification of the important shear zones that transect the crust, and estimates of depth and volumes of metal reservoirs and fluid pathways. Analysis of the geophysical data and 3D model has resulted in the following new observations:

- the Pilbara Craton is ovoid, has a 600 by 550 kilometre diameter, and is only 25 per cent exposed;
- the average crustal depth is 30–32 kilometres (thickening to the south), with the mid-crust at 14 kilometres;
- the greenstones are highly magnetic. Best-fit geophysical modelling shows that the greenstones extend to the base of the mid-crust (14 km), and that most granitoids have steep (vertical) contacts also to the base of the mid-crust (14 km);
- the north-east has on average a more dense and less magnetic crust than the north-west;
- major shear zones are present in the north-west and the far east (Proterozoic reworking); and
- circular patterns of granitoids are everywhere except for the north-west.

Conclusions

The North Pilbara project has made significant advances towards an understanding of the geology and metallogeny, and these results will assist exploration in the Pilbara and other terranes. The geology and metallogeny of the Pilbara Craton, however, differ significantly from the late Archaean provinces such as the Eastern Goldfields and the Superior provinces, so exploration models from these provinces need to be modified for use in the Pilbara Craton. Exploration difficulties will be made easier by the project's work, which includes improved knowledge on the timing and controls of some of the significant mineral systems, new exploration tools and digital datasets, and a new appreciation of the three-dimensional geometry of the granite–greenstone belts.

References

1. Huston DL, Keiller B, Standing J, Blewett RS & Mernagh TP. 2000. Epithermal deposits of the Central Pilbara Tectonic Zone, Pilbara Craton: Description and exploration significance. AGSO Research Newsletter; 32:34–39.
2. Marshall AE. 2000. Low-temperature–low-pressure ('epithermal') vein deposits of the North Pilbara granite–greenstone terrane, Western Australia. Canberra: Australian Geological Survey Organisation, record 2000/1.
3. Bierwirth P, Blewett RS & Huston DL. 1999. Finding new mineral prospects with HYMAP: Early results from a hyperspectral remote sensing case study in the West Pilbara. AGSO Research Newsletter; 31:1–3.
4. Brauhart CW, Huston DL & Andrew AS. 2000. Definition of regional alteration in the Panorama VMS district using oxygen isotope mapping: Implications for the origin of the hydrothermal system and applications to exploration. *Mineralium Deposita*; 35:727–740.
5. Brauhart CW, Huston DL, Grove DI, Mikucki EJ & Gardoll SJ. 2001. Geochemical mass transfer patterns as indicators of the architecture of a complete volcanic-hosted massive sulfide hydrothermal alteration system in the Panorama District, Pilbara, Western Australia. *Economic Geology*; in press.
6. Huston DL, Brauhart CW, Driberg SL, Davidson GJ & Groves DI. 2001. Metal leaching and inorganic sulfate reduction in volcanic-hosted massive sulfide mineral systems: Evidence from the Paleoproterozoic Panorama district. *Geology*; in press.
7. Wellman P. 1999. Interpretation of regional geophysics of the Pilbara Craton, north-west Australia. Canberra: Australian Geological Survey Organisation, record 1999/4.
8. Huston DL, Brauhart CW, Wellman P & Andrew AS. 1998. Gamma-ray spectrometric and oxygen-isotope mapping of regional alteration haloes in massive sulphide deposits: An example from Panorama, Central Pilbara Craton. AGSO Research Newsletter; 29:14.
9. Smithies RH & Champion DC. 1999. High-Mg diorite from the Archaean Pilbara Craton—anorogenic magmas derived from a subduction-modified mantle. *Perth: Geological Survey of Western Australia, annual review 1998–99*; 45–50.
10. Champion DC & Smithies RH. 2000. The geochemistry of the Yule Granitoid Complex, East Pilbara granite–greenstone terrane: Evidence for early felsic crust. *Perth: Geological Survey of Western Australia, annual review 1999–2000*; 42–48.
11. Sun S-s & Hickman AH. 1998. New Nd-isotopic and geochemical data for the Pilbara: Implications for Archaean crustal evolution and shear zone movement. AGSO Research Newsletter; 28:25–28.
12. Ratajkoski M, Blewett RS, Wellman P & Huston DL. 2000. [CD]. The North Pilbara project synthesis GIS, v1.0. Canberra: Australian Geological Survey Organisation.
13. Blewett RS, Wellman P, Ratajkoski M & Huston DL. 2000. Atlas of North Pilbara geology and geophysics (1:1.5 million scale). Canberra: Australian Geological Survey Organisation, record 2000/4.
14. Ratajkoski M, Blewett RS & Wellman P. 1999. The North Pilbara GIS teaching package, v1.0. Canberra: Australian Geological Survey Organisation.
15. Huston DL, Blewett RS, Mernagh T, Sun S-s & Kamprad J. 2001. Gold deposits of the Pilbara Craton: Results of AGSO Research, 1998–2000. Canberra: Australian Geological Survey Organisation, record 2001/4.
16. Sweetapple MT. 2001. Characteristics of Sn-Ta-Be-Li-industrial mineral deposits of the Archaean Pilbara Craton, Western Australia. Canberra: Australian Geological Survey Organisation, record 2000/44.
17. Blewett RS, comp. 2000. [CD]. Facsimile copy of the aerial geological and geophysical survey of northern Australia (AGGSNA): Reports (1 to 26, 28, 46, 48, 51 to 59) for Western Australia (Pilbara goldfield). Canberra: Australian Geological Survey Organisation, record 2000/5.
18. Blewett RS. 2000. [CD]. North Pilbara 'virtual' structural field trip. Canberra: Australian Geological Survey Organisation, record 2000/45.
19. Wellman P. 2000. Upper crust of the Pilbara Craton, Australia: 3D geometry of a granite–greenstone terrane. *Precambrian Research*; 104:175–186.

Acknowledgments: The authors thank Resolute Ltd, Lynas NL, Sons of Gwalia and Welcome Stranger for ground access, field support, and access to data and samples. They also thank GSWA for field support, cooperation, and data/information sharing in running a successful joint project in the Pilbara. This work would not have been done without the excellent scientific input from Peter Wellman and Shen-su Sun (ex-AGSO), Phil Bierwirth (ANU), Carl Brauhart (UWA), and Marcus Sweetapple (Curtin). Reviews from Dean Hoatson, Subhash Jaireth, Arthur Hickman and Ian Lambert focused the paper considerably.

- Dr Richard Blewett, Minerals Division, AGSO, phone +61 2 6249 9713 or e-mail richard.blewett@agso.gov.au
- Dr David Huston, Minerals Division, AGSO, phone +61 2 6249 9577 or e-mail david.huston@agso.gov.au
- Dr David Champion, Minerals Division, AGSO, phone +61 2 6249 9215 or e-mail david.champion@agso.gov.au

Metallogenic potential of mafic-ultramafic intrusions in the Arunta Province, central Australia

Some new insights

DM Hoatson

Recent field investigations by AGSO, as part of the National Geoscience Agreement with the Northern Territory Geological Survey, evaluated the geological setting and economic potential of Proterozoic mafic-ultramafic intrusions in the Arunta Province of central Australia. Historically, the Arunta Province was generally thought to have low potential for mineralising systems associated with mafic-ultramafic rocks, because of its high-grade metamorphic character and protracted tectonothermal history spanning more than 1500 million years.¹ Field observations and new preliminary geochemical data, however, indicate that intrusions from the western and central Arunta have some potential for Ni-Cu-Co sulphide deposits, and the eastern Arunta could be prospective for platinum-group element (PGE) mineralisation. These results highlight, for the first time, geographical differences in mineral prospectivity, and the PGE potential of the eastern Arunta.

facilitated by aeromagnetic and gamma-ray spectrometric data and Landsat 5 Thematic Imagery. In addition to the mafic-ultramafic intrusions themselves, co-mingled felsic rocks, cross-cutting intrusions, and country rocks have been sampled for detailed U-Pb zircon and baddeleyite geochronology. This will be used to place the various mafic-ultramafic magmatic systems within the event chronology of the Arunta. Mineral separates from the first 12 high Zr-bearing (80 to 220 ppm) mafic samples crushed have yielded zircon of variable abundance and morphology. The geochronological data will be incorporated with whole-rock geochemical and Sm-Nd isotopic studies for information on the timing of magmatic/metamorphic events, tectonic environments, and economic potential.

A regional geochemical study undertaken in late 2000 involved sampling 16 mafic-ultramafic bodies from a 90 000 square kilometre area encompassing most of the central and northern parts of the Arunta (figure 1). The Arunta is a geologist's Mecca for examining the intrusions, for they are generally well exposed, and differential movements along province-scale fault systems have allowed their exposure from different levels in the crust. The collection of samples along type traverses across each body was

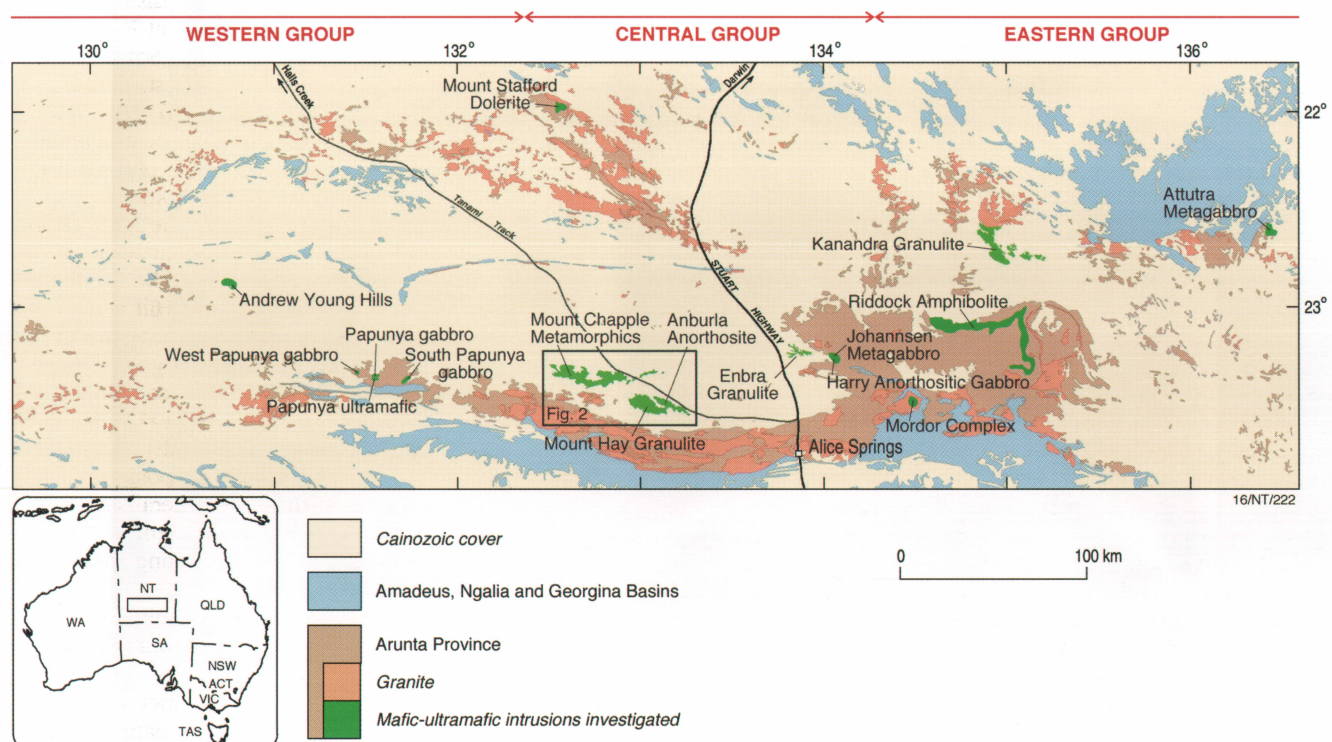


Figure 1. Mafic-ultramafic intrusions investigated in the Arunta Province

Geological setting and classification

The mafic-ultramafic intrusions have been provisionally subdivided into three broad geographical groups (western, central and eastern) on the basis of lithologies, metamorphic-structural histories, degree of fractionation, and limited geochronology. This classification will be refined when further geochemical-isotopic data become available. The intrusions form large homogeneous metagabbroic bodies, folded high-level mafic sills, steeply dipping amphibolite sheets, and relatively undeformed ultramafic plugs with alkaline and tholeiitic affinities. Metamorphic grades range from granulite to sub-amphibolite facies. Chilled and contaminated margins and net-vein complexes—the results of comingling mafic and felsic magmas—indicate that most intrusions crystallised *in situ* and were not tectonically emplaced. In contrast to intrusions from other nearby Proterozoic provinces (East Kimberleys, Musgrave Block), the Arunta bodies are generally more homogeneous in composition and are poorly layered. Moreover, primitive ultramafic rocks are rare and chromitites have not been documented.

Intrusions of the western group (Andrew Young Hills, Papunya gabbro, Papunya ultramafic, South Papunya gabbro, West Papunya gabbro) are generally small, evolved mafic bodies that display variable amounts of crustal contamination. Andrew Young Hills is a high-level gabbro-norite-tonalite body strongly contaminated with felsic crustal material and enriched in sulphur. Papunya ultramafic is a rare ultramafic ovoid body of plagioclase pyroxenite. Recent mapping by the NTGS suggest that the intrusions of the western group are related to the $\sim 1635 \pm 9$ Ma Andrew Young Igneous Complex.^{2,3} Intrusions of the central group (Enbra Granulite, Johannsen Metagabbro, Mount Chapple Metamorphics, Mount Hay Granulite; figure 2) are typically medium to large homogeneous mafic-felsic bodies emplaced prior to the main granulite events that affected the Mount Hay and Strangways regions at ~ 1780 – 1760 Ma and ~ 1730 – 1720 Ma.⁴ The mafic granulites locally contain well-preserved, medium-grained ‘intergranular’ textures, rare compositional layering, and mafic pillows associated with hybrid felsic rocks that indicate the protoliths were probably homogeneous sequences of gabbros that comingled with felsic

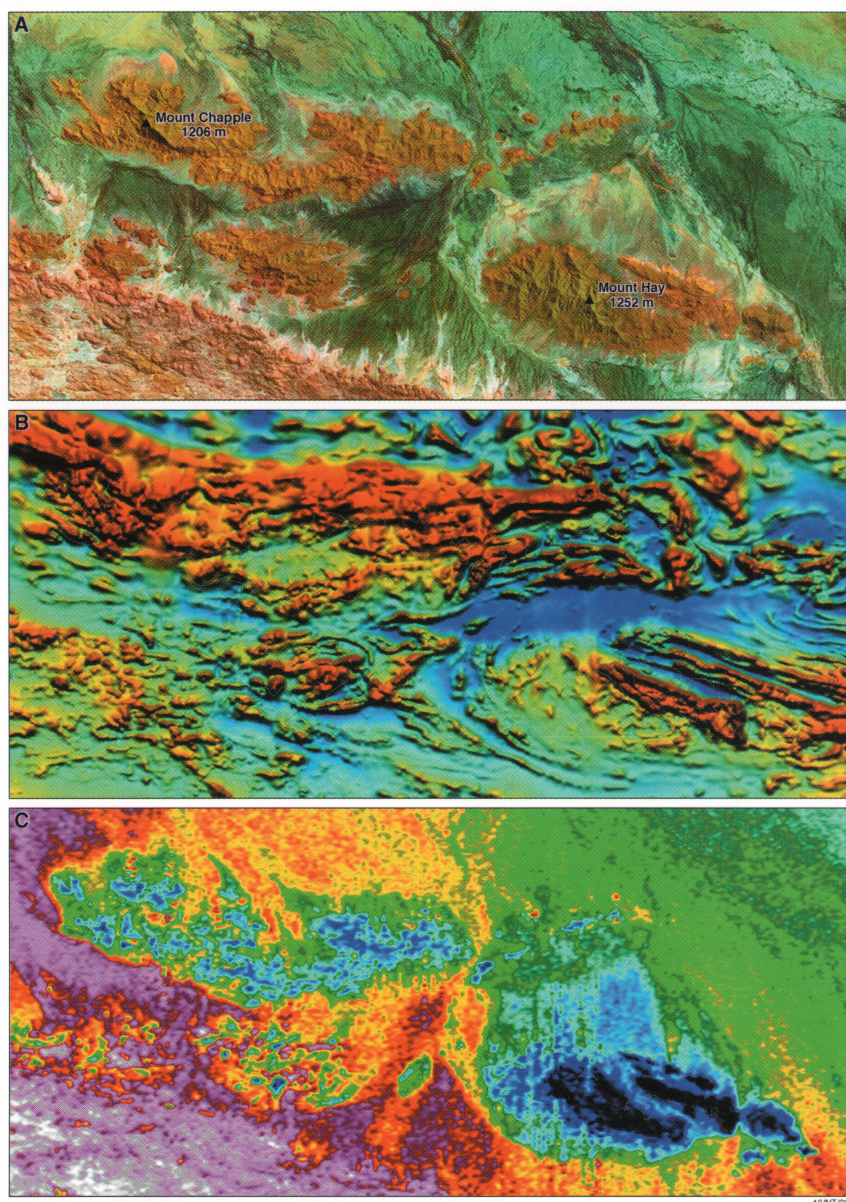


Figure 2. Remote sensing and geophysical images that highlight the uniform compositions of the Mount Hay and Mount Chapple granulite bodies.

A: Landsat 5 Thematic Mapper (using bands 1, 4 and 7 displayed as red, green and blue, respectively). **B:** Total Magnetic Intensity (reduced to pole, northerly illumination). **C:** Gamma-ray spectrometrics (potassium band)

magmas (figure 3). Relatively thin anorthositic sequences (Anburla Anorthosite, Harry Anorthositic Gabbro) are in places spatially associated with the mafic granulites. The eastern group comprises both pre-orogenic (Attutra Metagabbro, Kanandra Granulite, Riddock Amphibolite) and relatively undeformed (Mordor Complex) intrusions of variable form and composition. Weakly recrystallised gabbro and pyroxenite host thin magnetite-ilmenite lenses in the Attutra Metagabbro; moderately dipping concordant sheets of amphibolite and metasediments up to 70 kilometres long characterise the Riddock Amphibolite; and the Mordor Complex consists of a cluster of small differentiated alkaline plugs emplaced at ~ 1150 Ma.⁵

Regional mineral prospectivity

The timing of S saturation in evolving mafic-ultramafic magmas in part determines the type of mineralisation in layered intrusions. PGE-bearing stratabound layers (e.g., Merensky Reef, Bushveld Complex; Great Dyke of Zimbabwe) are generally favoured by PGE-enriched primitive magmas that were S undersaturated prior to emplacement in the magma chamber. If these magmas attain S saturation too early in their evolution (i.e., in the mantle or during their ascent through the crust), the PGEs will be rapidly depleted in

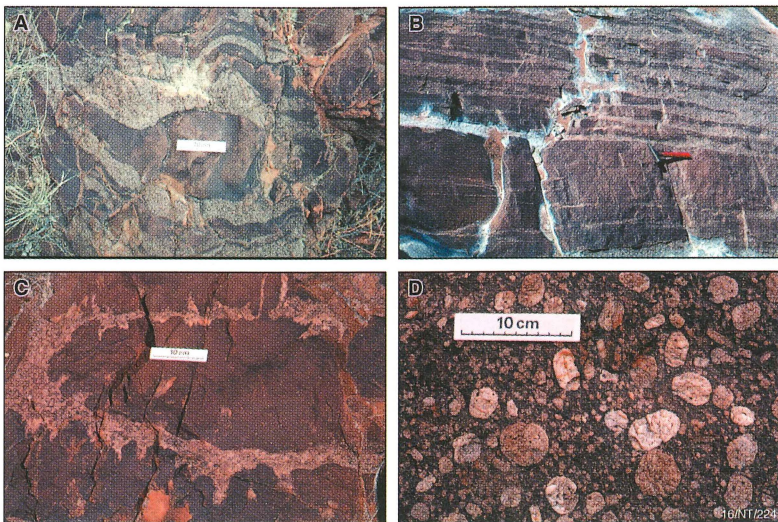
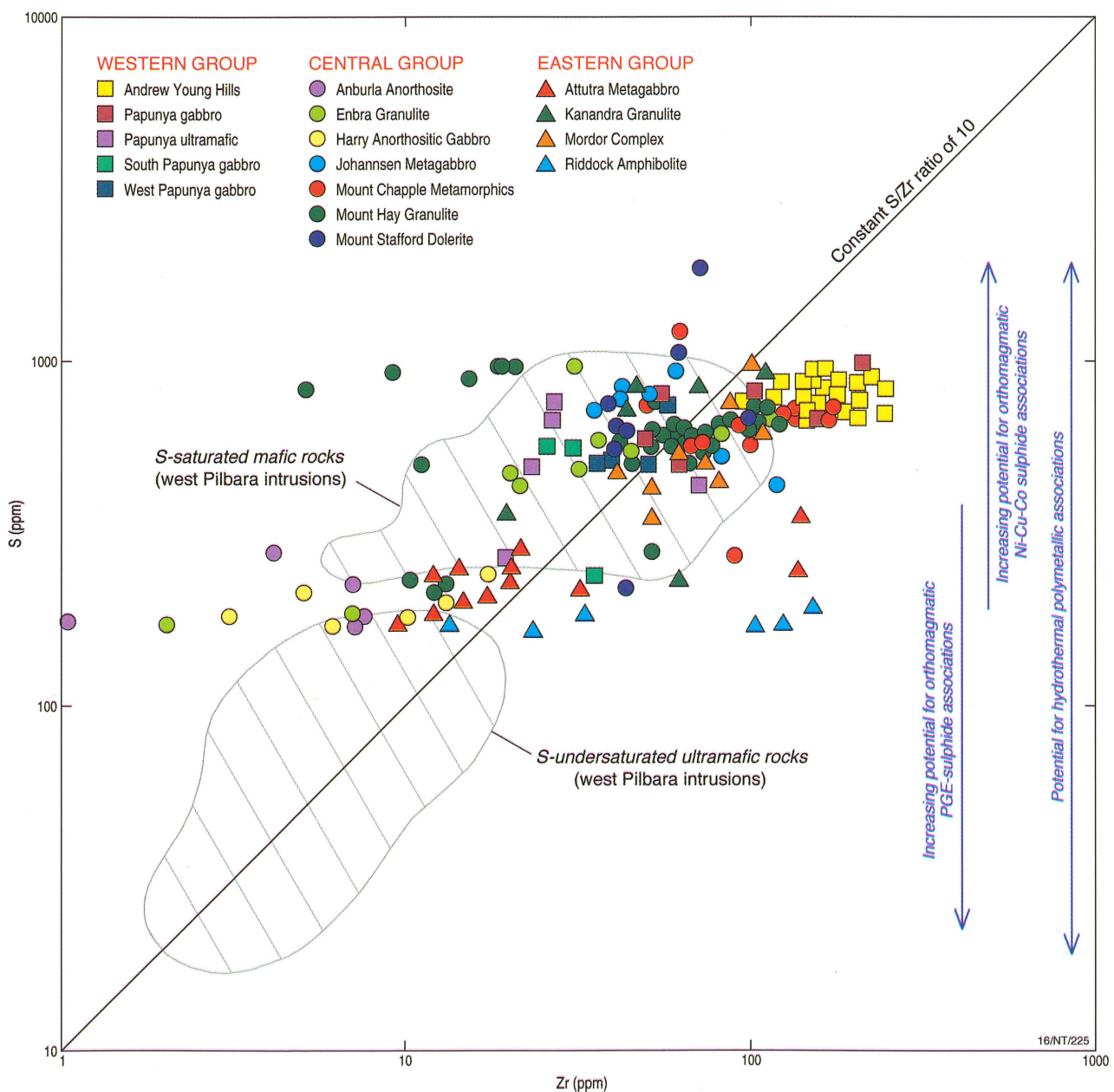


Figure 3. Contact relationships of mafic and felsic magmas. **A:** Irregular mafic granulite pillow and layers, Enbra Granulite (scale bar = 10 cm). **B:** Stacked sequence of mafic granulite (dark) and charnockite (light) layers, Mount Hay Granulite. **C:** Mafic pillow with cusped and contaminated margins, Andrew Young Hills (scale bar = 10 cm). **D:** Resorbed alkali feldspar xenocrysts in tonalite, Andrew Young Hills

Figure 4. Logarithmic plot of whole-rock S and Zr concentrations in mafic and ultramafic rocks from the Arunta Province. The fields for S-saturated and S-undersaturated rocks from mineralised intrusions in the west Pilbara Craton¹⁶ are also shown.



the magmas owing to their extremely high sulphide melt/silicate melt partition coefficients (about 10^3 – 10^5)⁶, and fail to form PGE-enriched layers in the chamber. In contrast, massive concentrations of Ni-Cu-Co sulphides in embayments along basal contacts or in feeder conduits (e.g., Voisey's Bay,

Canada) are generally associated with magmas that attained early S saturation through such processes as crustal contamination. These

deposits are favoured by dynamic feeder systems, S-bearing country rocks, and a structural framework that facilitates the rapid emplacement of voluminous amounts of hot primitive magmas not depleted in Ni by early protracted olivine crystallisation.⁷

The economic implications of the Arunta intrusions can be broadly assessed by comparing concentrations of S with an incompatible element that provides an index of fractionation, such as Zr. Figure 4 shows that the Arunta intrusions fall into two major geochemical groups:

1. a S-rich group (~300 to 1200 ppm S) from the western and central Arunta that has some potential for orthomagmatic Ni-Cu-Co sulphide associations; and
2. a relatively S-poor (<300 ppm S), slightly more primitive group from the eastern Arunta that has greater potential for orthomagmatic PGE-sulphide associations. Of this group, the Riddock Amphibolite and Attutra Metagabbro appear to have the most favourable low S concentrations for PGE mineralisation.

Both groups have potential for hydrothermal polymetallic deposits of PGEs-Cu-Au±Ag±Pb spatially associated with the intrusions. However, the absence of thick sequences of primitive rocks (peridotite, orthopyroxenite) throughout the Arunta downgrades the potential for PGE-chromite associations.

The recent emerging evidence that the eastern Arunta is prospective for PGE mineralisation is supported by company investigations at two locations. Tanami Gold NL noted that hydrothermal quartz-carbonate-tourmaline veins associated with chlorite-hematite altered amphibolite near Mount Riddoch contained up to 0.6 ppm Pt, 1.4 ppm Pd, 5.8 ppm Au, 6.8 per cent Cu, and 12 ppm Ag.⁸ Hunter Resources reported anomalous Pd (up to 215 ppb), Au (up to 104 ppb), and Cu (up to 2400 ppm) concentrations in massive magnetite hosted by gabbro of the Attutra Metagabbro.⁹ Interestingly, Western Mining have also documented elevated concentrations of PGEs and Au (up to 1 ppm) in magnetite-ilmenite horizons near their recently discovered Ni-Cu-Co sulphide deposit in the west Musgrave Block (WMC website: June 30, 2000).

Exploration challenges

The occurrence of hydrothermal and orthomagmatic PGEs in the eastern Arunta takes on considerable significance in view of the radical revision being recently proposed for the tectonothermal history of the Harts Range region. U-Pb and Sm-Nd geochronological studies suggest that sediments and igneous rocks of the Harts Range Group (Irindina Supracrustal Assemblage) represent a rift sequence that was 'deposited' during the late Neoproterozoic to Cambrian and was metamorphosed to granulite facies in an extensional setting during the early Ordovician (480–460 Ma).^{10,11} The igneous rocks include basalt, volcanoclastics, anorthosite, and ultramafic intrusives.¹² The Harts Range region therefore appears to be a new sub-province characterised by relatively young rifting, extensional, metamorphic (and therefore mineralisation) processes quite distinct from those documented elsewhere in the Arunta. The variety and abundance of mafic-ultramafic rocks in a tectonically dynamic part of the Arunta and the known mineralisation near Mount Riddoch and Attutra enhances the prospectivity of this region for PGEs.

A major challenge in exploring for Ni-Cu-Co sulphide deposits in the Arunta is to locate feeder conduits or depressions within the basal contact that may be covered by shallow alluvial cover. The identification of these favourable environments in large prospective bodies such as Andrew Young Hills, Mount Chapple and Mount Hay will be most likely achieved through sophisticated geophysical (airborne electromagnetic) and remote-sensing techniques in association with diamond drilling, petrological information, and possibly an element of luck. For example, the Discovery Hill gossan at Voisey's Bay was found fortuitously during a regional stream-sampling program for diamond indicator minerals. A follow-up horizontal-loop electromagnetic survey of the gossan indicated a 1200-metre-long continuous conductor at depth. Airborne magnetics indicate that the more prospective primitive parts of Andrew Young Hills and Mount Chapple appear to be under alluvium several kilometres distant from the main outcropping parts of the bodies.

The granulite metamorphic overprint in the central group of Arunta intrusions should not be regarded as a major impediment for exploration, since Ni-Cu-Co sulphide deposits at similar high metamorphic grades are preserved in the East Kimberley (Bow River, Corkwood, Keller Creek, Norton¹³) and overseas.^{14,15} In some of these deposits, metal grades have been

enhanced by the remobilisation and recrystallisation of sulphides into low-stress areas.

References


1. Collins WJ. 2000. Introduction to Arunta Inlier. In: Collins WJ, ed. Granite magma segregation and transfer during compressional deformation in the deep crust? Proterozoic Arunta Inlier, central Australia. Sydney: Geological Society of Australia, field guide F4:1–7.
2. Edgoose C, Scrimgeour I, Close D & Meixner T. 2001. The SW Arunta—a terrain getting younger by the minute. Abstracts: Annual Geoscience Exploration Seminar, Alice Springs, Mar 20. Darwin: Northern Territory Geological Survey, record GS 2001–0006.
3. Young DN, Edgoose CJ, Blake DH & Shaw RD. 1995. 1:250 000 geological map series: Mount Doreen, Northern Territory. Darwin: Northern Territory Department of Mines and Energy & Australian Geological Survey Organisation, explanatory notes SF 52–12.
4. Pietsch B. 2001. Towards an Arunta framework. Abstracts: Annual Geoscience Exploration Seminar, Alice Springs, Mar 20. Darwin: Northern Territory Geological Survey, record GS 2001–0006.
5. Nelson DR, Black LP & McCulloch MT. 1989. Nd-Pb isotopic characteristics of the Mordor Complex, Northern Territory: Mid-Proterozoic potassic magmatism from an enriched mantle source. Australian Journal of Earth Sciences; 36:541–551.
6. Fleet ME, Crocket JH, Liu M & Stone WE. 1999. Laboratory partitioning of platinum-group elements (PGE) and gold with application to magmatic sulfide-PGE deposits. Lithos; 47:127–142.
7. Scoates JS & Mitchell JN. 2000. The evolution of troctolite and high Al basaltic magmas in Proterozoic anorthosite plutonic suites and implications for the Voisey's Bay massive Ni-Cu sulfide deposit. Economic Geology; 95:677–701.
8. Tanami Gold NL. 2000. Quarterly report, Dec 31.
9. Hunter Resources Ltd. 1988. Attutra NT, EL 5171. Darwin: Martyn & Associates, open file report CR 88/279.
10. Hand M, Mawby J, Kinny P & Foden J. 1999. U-Pb ages from the Harts Range, central Australia: Evidence for early Ordovician extension and constraints on Carboniferous metamorphism. Journal of the Geological Society, London; 156:715–730.
11. Mawby J, Hand M & Foden J. 1999. Sm-Nd evidence for high-grade Ordovician metamorphism in the Arunta Block, central Australia. Journal of Metamorphic Geology; 17:653–668.

12. Buick IS, Miller JA, Williams IS, Hand M & Mawby J. 2001. Deep holes in the Centralian Superbasin—SHRIMP zircon constraints on the depositional age of granulites in the eastern Arunta Block. Geological Society of Australia abstracts; 64:13–14.
13. Hoatson DM & Blake DH, eds. 2000. Geology and economic potential of the Palaeoproterozoic layered mafic-ultramafic intrusions in the East Kimberley, Western Australia. Canberra: Australian Geological Survey Organisation, bulletin 246.
14. Cawthorn RG & Meyer FM. 1993. Petrochemistry of the Okiep copper district basic intrusive bodies, northwestern Cape Province, South Africa. Economic Geology; 88:590–605.
15. Maier WD & Barnes S-J. 1999. The origin of Cu sulfide deposits in the Curaçá Valley, Bahia, Brazil: Evidence from Cu, Ni, Se and platinum-group element concentrations. Economic Geology; 94:165–183.
16. Hoatson DM, Wallace DA, Sun S-s, Macias LF, Simpson CJ & Keays RR. 1992. Petrology and platinum-group-element geochemistry of Archaean layered mafic-ultramafic intrusions, west Pilbara Block, Western Australia. Canberra: Australian Geological Survey Organisation, bulletin 242.

Acknowledgments: This manuscript draws on many fruitful discussions with colleagues from the Northern Territory Geological Survey, including Kelvin Hussey, Ian Scrimgeour, David Young, Dorothy Close and Christine Edgoose. The NTGS identified the western group of mafic intrusions and provided geological information that formed a basis for this sampling program.

David Huston, Jonathan Claoue-Long and Alastair Stewart are thanked for their constructive reviews of the manuscript. Alastair Stewart is acknowledged for his contributions in the field. David Maidment and John Creasey provided the geophysical and remote sensing images, and Lana Murray and Angie Jaensch drew the figures.

The traditional owners of the Papunya area are thanked for permitting access to the western Arunta.

► Dr Dean Hoatson, Minerals Division, AGSO, phone +61 2 6249 9593 or e-mail dean.hoatson@agso.gov.au 

Rapid mapping of soils and salt stores

Using airborne radiometrics and digital elevation models

JR Wilford, DL Dent, T Dowling & R Braaten

Salinisation of land and rivers is a major problem throughout Australia's agricultural regions. There is a pressing need to map or predict where the salt is, and to understand the nature of salt stores and the conduits through which salt and water are delivered to streams and the land surface.

This article describes a new method (an integrated, catchment-based approach) of modelling natural gamma-ray emissions from the Earth's surface for soil/regolith mapping, and combining the results with topographic indices to delineate salt stores and salt outbreaks in the landscape. Modelled thematic maps produced using this approach allow catchments to be ranked according to their salinity risk, or potential risk, for prioritising remedial management.

Large areas of land in Australia are affected by dryland salinity with more than 240 000 hectares affected in New South Wales and Victoria alone.^{1,2} In the next 50 years this area is likely to increase substantially. In Australia, annual damage and loss in production caused by dryland salinity has been estimated at 270 million dollars.³

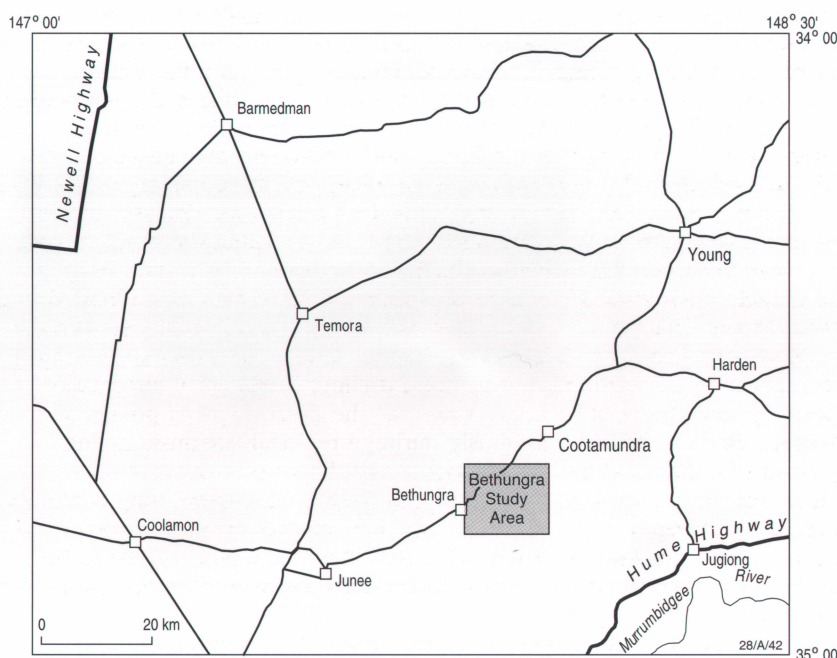


Figure 1. Location of study area within the Cootamundra 1:250 000 map sheet

The salts causing the problem are a common constituent of the regolith and are widespread in Australia. There is consensus that the replacement of natural vegetation by shallow-rooted crops and pastures that use less water has led to increased ground-water recharge and rising ground-water tables. Rising water tables that bring salt to the surface not only affect crops and water quality, but also cause infrastructure damage to towns and transport networks (e.g., roads and railways).

There is an urgent requirement to know where the highest concentrations of salt are, how they are stored in the regolith, and the pathways along which salt is delivered to streams and the land surface.

Study area

The study area (15 by 12 km) is part of the Lachlan Fold Belt of southern Australia, located immediately east of the township of Bethungra, New South Wales (figure 1). Rocks in the area (figure 2) consist of leucocratic granites, rhyolites, rhyodacites and minor siltstones and sandstones.⁴ Colluvial and residual clays, sands and minor gravels occur along broad valley floors, footslopes and on rises (9–30 metres relief). The terrain has moderate to high relief (figure 3) with bedrock exposed on steeper

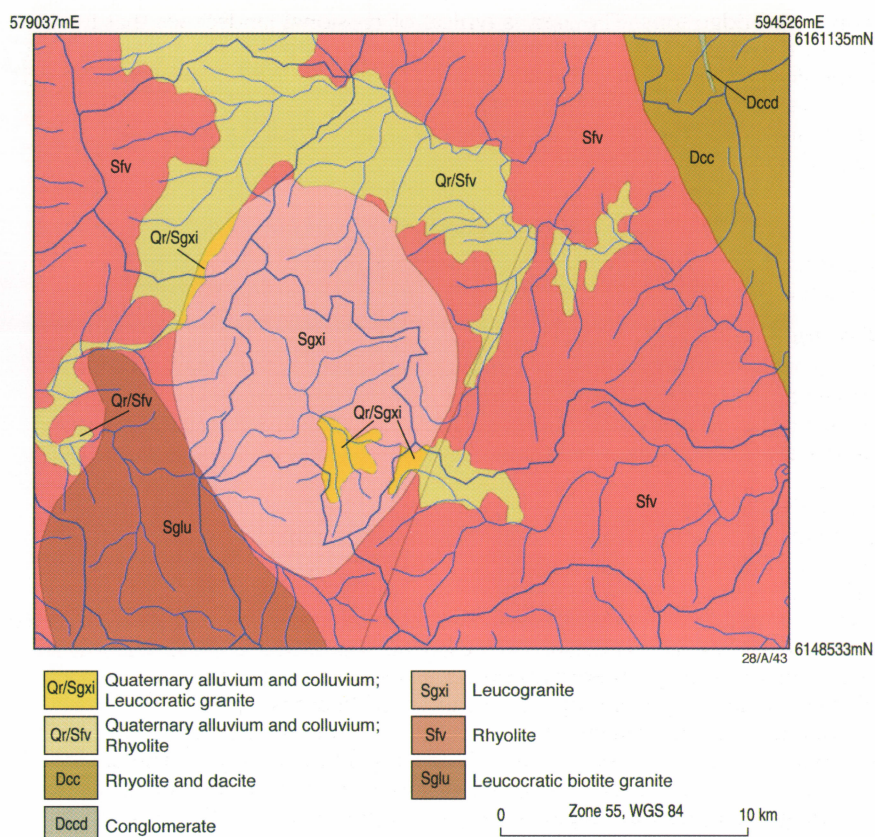


Figure 2. Bedrock lithologies with catchment boundaries and streams overlaid

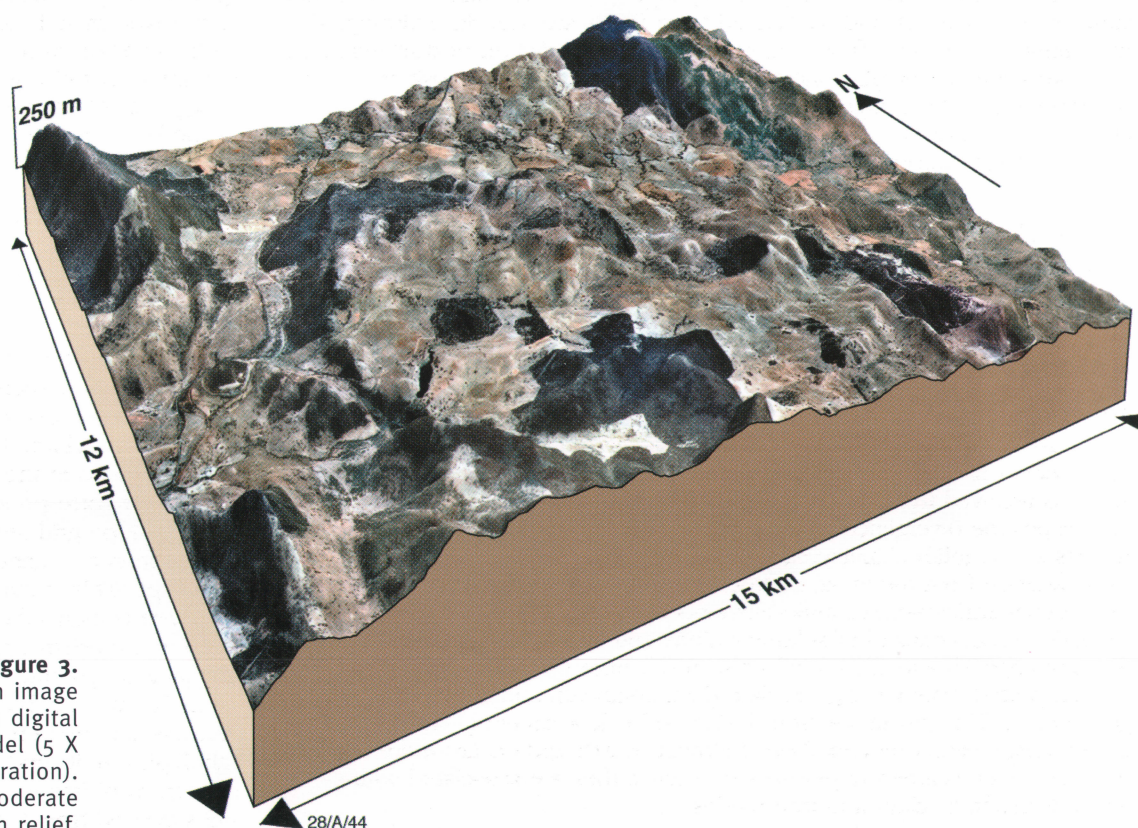


Figure 3. Orthophotograph image draped over a digital elevation model (5 X vertical exaggeration). The area has moderate to high relief.

slopes and ridge tops. The area is typical of erosional landscapes that form part of the south-west slopes of New South Wales. The study complements a geological systems approach to understanding the processes involved in land and water salinisation, that focuses mainly on the interpretation of airborne electromagnetic (EM) data over depositional landforms with a complex regolith cover.⁵

Datasets

Datasets used in the study include airborne gamma-ray spectrometry imagery, a digital elevation model, and catchment and geological polygons.

Gamma-ray spectrometry

Gamma-ray data were clipped from the Cootamundra 1:250 000 map sheet survey flown by AGSO, with 250-metre flight-line spacing and a final grid resolution of 80 metres. Airborne gamma spectrometry measures the natural radiation from potassium (K), thorium (Th) and uranium (U) in the upper 30 centimetres of the Earth's surface. Potassium is measured directly from the radio-element decay of ⁴⁰K. Thorium and U are inferred from daughter elements associated with distinctive isotopic emissions from ²⁰⁸Tl and ²¹⁴Bi in their respective decay chains. Since the concentrations of Th and U are inferred from daughter elements, they are usually expressed in equivalent parts per million eU and eTh. Potassium has a much higher crustal abundance than eTh and eU and is usually expressed as a percentage (K%). Gamma-ray spectrometric surveys, therefore, measure the abundance of these radio-elements emanating from topsoil and exposed bedrock.

Gamma-ray spectrometry surveys have been widely used in geophysical exploration, and more recently in soil and regolith mapping.⁶⁻¹⁰ The ability of gamma-rays to pass through vegetation to the receiver on the aircraft is an advantage in agricultural regions. Crops and pastures mask the underlying soils, making data from other remote sensors such as Landsat TM difficult to interpret.

Digital elevation model

A digital elevation model of the study area was generated using 1:90 000 aerial photography. Soft photogrammetric techniques were used to create a 50-metre resolution elevation model with one- to five-metre vertical accuracy. Orthophotographic images with a two-metre resolution were also generated (figure 3). The orthophotographs and the DEM were geometrically corrected and warped using differential GPS control points.

Digital elevation models are used widely in terrain classification and modelling. Primary surfaces (e.g., slope, aspect) and secondary or compound surfaces (e.g., wetness index) derived from DEMs are used in hydrological modelling (e.g., surface flow, soil saturation and prediction of discharge and recharge sites) and geomorphological (e.g., erosional and depositional processes) modelling. Dymond et al. demonstrated the use of DEMs in automated land-resource mapping.¹¹ Broader applications of DEMs for hydrological, geomorphological and botanical studies are described by Moore et al.¹²

Vector datasets

Geology polygons were derived from the digital 1:250 000 geological map⁴ and catchments were generated from the DEM based on third-order streams.

Modelling gamma-ray spectrometry data

Separating bedrock from regolith responses

Gamma-ray radiation emitted from the ground reflects the chemical composition of the bedrock and overlying soil. Although the gamma-ray signal is received from only the topsoil, the authors reason that in erosional landscapes the divergence of the gamma signal from the bedrock 'signature' reflects soil/regolith characteristics to much greater depths (several metres). This variation from the initial bedrock response is due largely to dilution or preferential enrichment of radio-elements by bedrock weathering and soil formation (e.g., removal of soluble cations and accumulation of sesquioxides that scavenge Th and U). It could also result from the bedrock being buried by transported material (e.g., aeolian dust, colluvium and alluvium). As a general rule, K is lost in solution during bedrock weathering. (K is soluble under most weathering conditions.) However, eTh and eU are more likely to be retained as weathering progresses because they are associated with resistant minerals, clays and iron oxides.

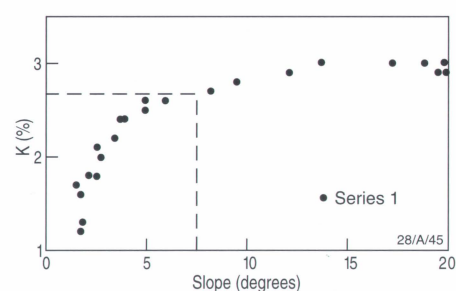


Figure 4. Slope in degrees against potassium (%). Inflection in the curve at around seven degrees separates erosional and depositional processes.

Geomorphic thresholds

GIS techniques have been developed to calculate the gamma-ray bedrock response from different rock-types using a slope grid derived from the DEM. The geology map is used to identify major bedrock units or major lithological/geochemical groups, since the soil response is likely to vary from one bedrock type to another. The bedrock response is differentiated from that of the regolith by plotting the gamma-ray responses against slope (figure 4). Inflection points in the scatter plot correlate with landform thresholds that are used to separate erosional sites from depositional sites. Higher erosion rates on steeper slopes are associated with bedrock materials and thin soils. Here the corresponding gamma-ray response largely reflects the geochemistry of the bedrock. Gentler slopes gain material from above (colluvium) or preserve thicker accumulations of regolith due to lesser rates of erosion. In these parts of the landscape, the corresponding gamma-ray response reflects weathered materials. The relationships between erosion and accumulation and the corresponding gamma-ray response can be used to establish the denudation balance in landscapes.⁷

Once the slope threshold value that partitions erosional landscape facets has been determined, it is used to generate a clipped slope threshold grid. All pixels in the gamma-ray image that correspond with the clipped slope grid are averaged to give a bedrock signature for each rock type. This mean bedrock response is then subtracted from each pixel in the original geophysical channels to generate residual grids for Total Count, K, eTh and eU. The analysis may be performed using lithological units and/or catchments, as regions of interest. However, the units derived from the geology map

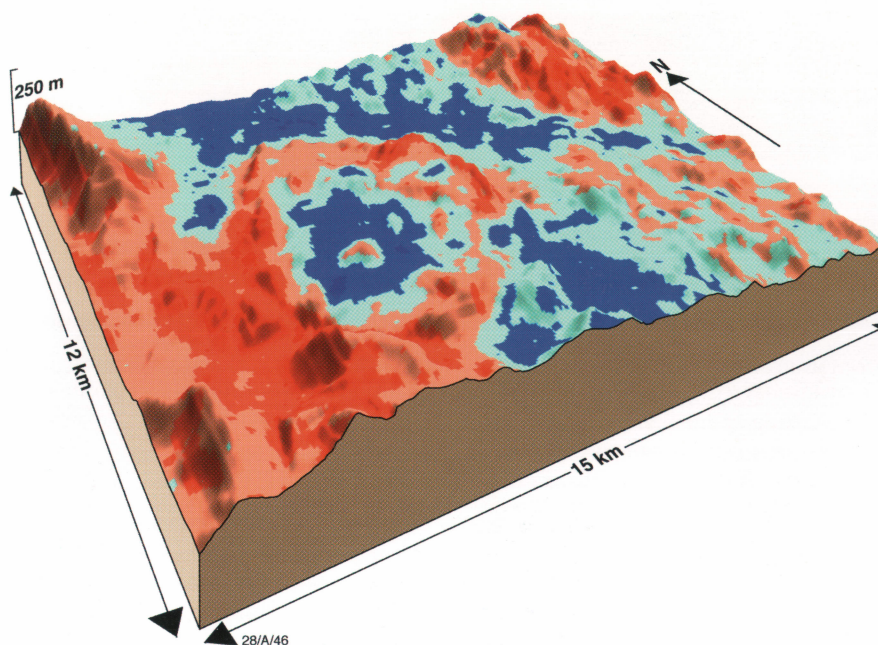


Figure 5. Residual K modelled on geology and catchments. Areas of low divergence from the bedrock mean are shown in reddish hues. These values correspond to exposed bedrock and thin soils. Increasing negative divergence from the bedrock means (shown in green to blue hues) corresponds to clay soils and weathered colluvial sediments. The residual K grid has been draped over a digital elevation model. (5 X vertical exaggeration)

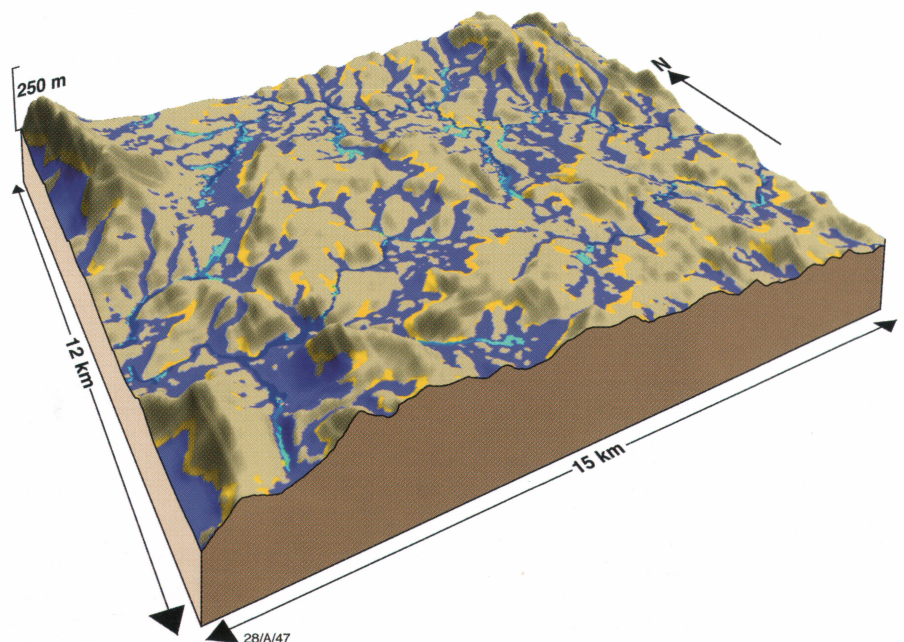


Figure 6. Wetness index derived from FLAG draped over a digital elevation model. Areas in purple and blue show likely surface discharge and local wetness. (5 X vertical exaggeration)

may be inaccurate or have variations due to alteration that is not shown on the map. These effects should be considered when interpreting the image response. Radio-element values centred around the mean bedrock response generally relate to thin soils over bedrock or exposed bedrock. They may also correspond to actively eroded and recently deposited alluvium that still retains the radio-element signature of the bedrock. In erosional landscapes, these sediments tend to be restricted to narrow corridors along streams. Deviation either above or below the mean will largely reflect weathering of bedrock or sediments (figure 5). Where detailed lithology is not known, lithological signatures can still be derived and extrapolated within catchments.

Terrain analysis

Fuzzy Landscape Analysis GIS (FLAG) software was used to derive terrain indices including a landscape position index that can be interpreted as topographic wetness or recharge/discharge zones.¹³ FLAG derives and combines a number of topographic indices (scaled from 0–1) from elevation data using the principles of fuzzy set theory. The overall landscape position or wetness index predicts those areas that are both low in their local vicinity (valleys) and low relative to the whole study area. These are sites most likely to exhibit surface wetness and discharge (figure 6). FLAG has been used effectively in salinity studies, identifying waterlogged soils and soil landscape mapping.^{14–17}

Results

Mapping residual and transported regolith

Residual modelling of the potassium channel using a greater than seven degree slope geomorphic cut-off value (figure 4) was performed for each catchment and geology unit. The modelled bedrock response was then subtracted from the original K grid to derive a residual K grid (figure 5) with values ranging from -1.8 to 2.4. The bedrock mean has a value of zero. Negative values delineate weathered colluvium and thick clay soils overlying highly weathered mottled saprolite. These soils and saprolite are thickest along broad valley floors and in gently undulating landforms with less than 35 metres local relief. Soil and highly weathered saprolite on undulating

landforms are typically between two to five metres thick, as determined by field observations. Under the broad valley floors, the saprolite is likely to be considerably thicker. Positive values correspond with thin, stony soils (typically less than one metre thick). Because the K signal alone was effective in separating regolith from bedrock materials, the other three channels (Total Count, eTh and eU) were not used in the analysis. The highly weathered mottled saprolite is usually several metres thick. Most of the primary minerals in the saprolite have been weathered, leaving clay and quartz. The saprolite grades into saprock with lower porosity at depth.

Comparing modelled soils with stream salinities

An electrical conductivity (EC) survey of streams, springs and seeps was carried out to test any relationship between salt concentration and the modelled residual K image. Field assessment consisted of 59 stream EC measurements and 31 seep and spring EC measurements.

Measurements were made during April–June 2000 and March 2001. Sample sites included a range of landforms and gamma-ray responses. Some ‘noise’ would have been introduced to the data because of short-term variation in rainfall amount and intensity over the period of measurement (e.g., variable amounts of base flow and surface flow). Recorded EC measurements are therefore better considered within broad classes than as precise values.

Stream, seep and spring EC values were plotted and overlain on the residual K image (figure 7). Visual inspection showed a good relationship between soils and the EC of streams, springs and seeps. To statistically quantify this relationship, catchment areas for each stream sample point are defined, based on the DEM. The residual K grid value was then computed for each catchment and plotted against EC (figure 8). A relationship between stream EC and the residual K grid was found, with higher stream EC values corresponding to negative residual values.

The EC values ranged from 110 to greater than 3000 μScm . Scatter across the EC values was higher for the more negative residual values. For streams with more positive residual values, the EC values were consistently low (figure 8). The linear relationship between stream EC and the K residual was not exceptionally strong (Pearson's $r = -0.58$, $p < .05$).

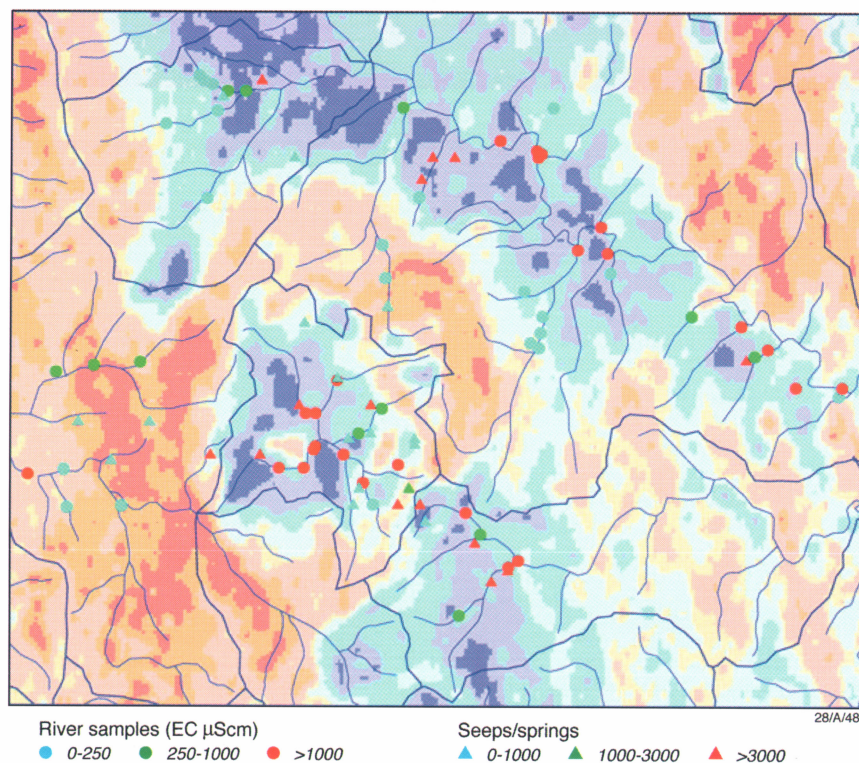


Figure 7. Modelled residual K, with stream EC values superimposed. The soil and bedrock are in red hues, and deeper clay soils and highly weathered saprolite in blue hues.

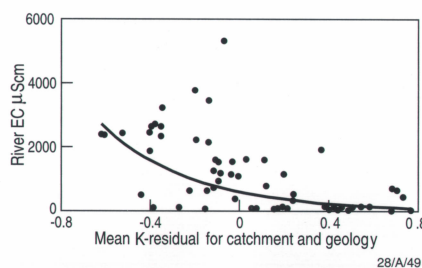


Figure 8. Chart showing residual K with EC measurements from streams and seeps

The relationship was clearer when the streams were grouped into two classes: those draining from areas with highly negative residual values, and those from areas with more positive residual values. There appears to be a natural break at a residual of about 0.37 for these two populations (figure 8). For the 15 stream samples with mean catchment residuals greater than 0.37, the mean EC was 189, the median was 124 and the standard deviation was 218. For the 44 stream samples with residuals less than 0.37, the mean stream EC was 1499, the median 1394 and the standard deviation 1187. A t-test showed a highly significant difference between the two means ($p < 0.00001$).

Combining modelled soils with terrain indices

The wetness grid derived from FLAG was scaled from 0 to 1 and identified areas of high potential surface-water saturation. Values from 0 to 1 showed an increasing wetness trend. The wetness grid was re-scaled from 0 to -1 values and then combined with the K residual grid in which values from 0 to -1 showed increasing negative divergence from the bedrock response (e.g., related to colluvium and thick clay soils). The two grids were combined to produce a final grid with values between -1 and 1 (figure 9). This final grid showed salt stores and the potential discharge or waterlogged sites where one would expect to find saline seeps. A good correlation between independently derived photographic mapped salt scalds¹⁸ and the predicted saline seeps supported the interpretation.

Discussion

Rapid soil mapping

This approach provides a rapid method for mapping and separating deeper regolith and soils from thin soils over bedrock. Colluvial and residual clay soils were delineated using the K residual grid. The method worked best where there was a strong contrast between the radio-element chemistry of the bedrock and the weathered constituents that overlie the bedrock. The K grid was effective over the whole Bethungra area because of the relatively high potassium content of the acid rocks in the area. In areas of contrasting bedrock geochemistry, more complex modelling using all gamma-ray channels is required to effectively map regolith from bedrock materials.¹⁹

The technique has several advantages when compared with more conventional discrete data classification approaches of interpreting and combining gamma-ray spectrometry and DEM datasets. Firstly the modelled datasets are fuzzy or gradational. This better describes the continuous nature and transitional boundaries of regolith and soil materials and hydrological attributes in landscapes. Secondly, the technique not only identifies soil and regolith materials, but also their associated geomorphic relationships. It is a knowledge-driven approach. This contrasts with a standard classification procedure where it is often difficult to 'unmix' the attributes in the final discrete classes.

Salt stores and EC measurements

In the Bethungra area there was a good correlation between high stream EC and clay distribution in the catchment. This suggests that the clays, and the highly weathered saprolite typically associated with them, are a major source or store of salts. These soils are largely confined to smooth hills with low relief (typically less than 35 metres) and on lower concave slopes and broad valley floors. Catchments with steep rocky hills and relatively higher relief shed predominantly fresh water. Combining these gamma-ray predicted salt stores with a wetness index grid derived from the DEM shows where salt outbreaks might occur, or where the highest salt loads are discharging into the streams. Hence these datasets have the potential to enhance existing GIS-based modelling approaches that use a variety of land attributes and environmental features for salt hazard mapping.²⁰ Structural controls within saprolite-dominated landscapes that can have an important control on salt

movement and surface concentration were not assessed in this study.²¹ Future work will incorporate structural analysis (DEM and airborne magnetics) to improve the predictive power of the technique.

Although there was a clear match between EC measurements and predicted salt stores, the overall correlation coefficient was relatively low. This is likely to reflect variable rainfall conditions when field measurements were recorded. Where there is no salt source, there is less opportunity for a stream to acquire a high salt load, resulting in consistently low EC values for streams draining areas with few predicted salt stores. Where streams drain through salt stores, the salt concentration of the stream will depend on the proportion of water derived from surface run-off as opposed to ground water (base flow).

Surface flows have less opportunity to intersect regolith salt stores. As a result, they are fresher and dilute more saline base flow. The partitioning of flow between surface and ground water varies with antecedent soil moisture, rainfall amount and intensity—all of which would have varied between field visits and between streams on the same visit. The variability in surface versus ground water influence on streams is likely to be the reason for the scatter in EC values for streams draining low-residual (high salt-source) areas.

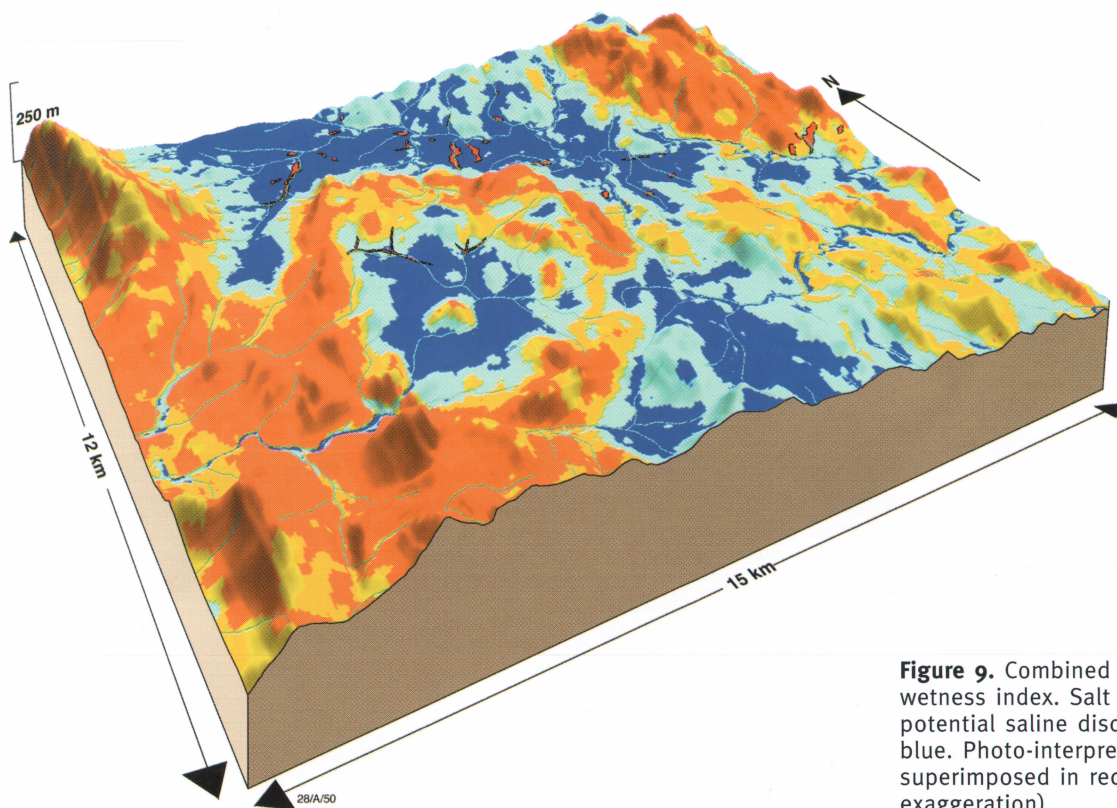


Figure 9. Combined K residual with wetness index. Salt stores and high potential saline discharge sites in blue. Photo-interpreted salt scalds superimposed in red. (5 X vertical exaggeration)

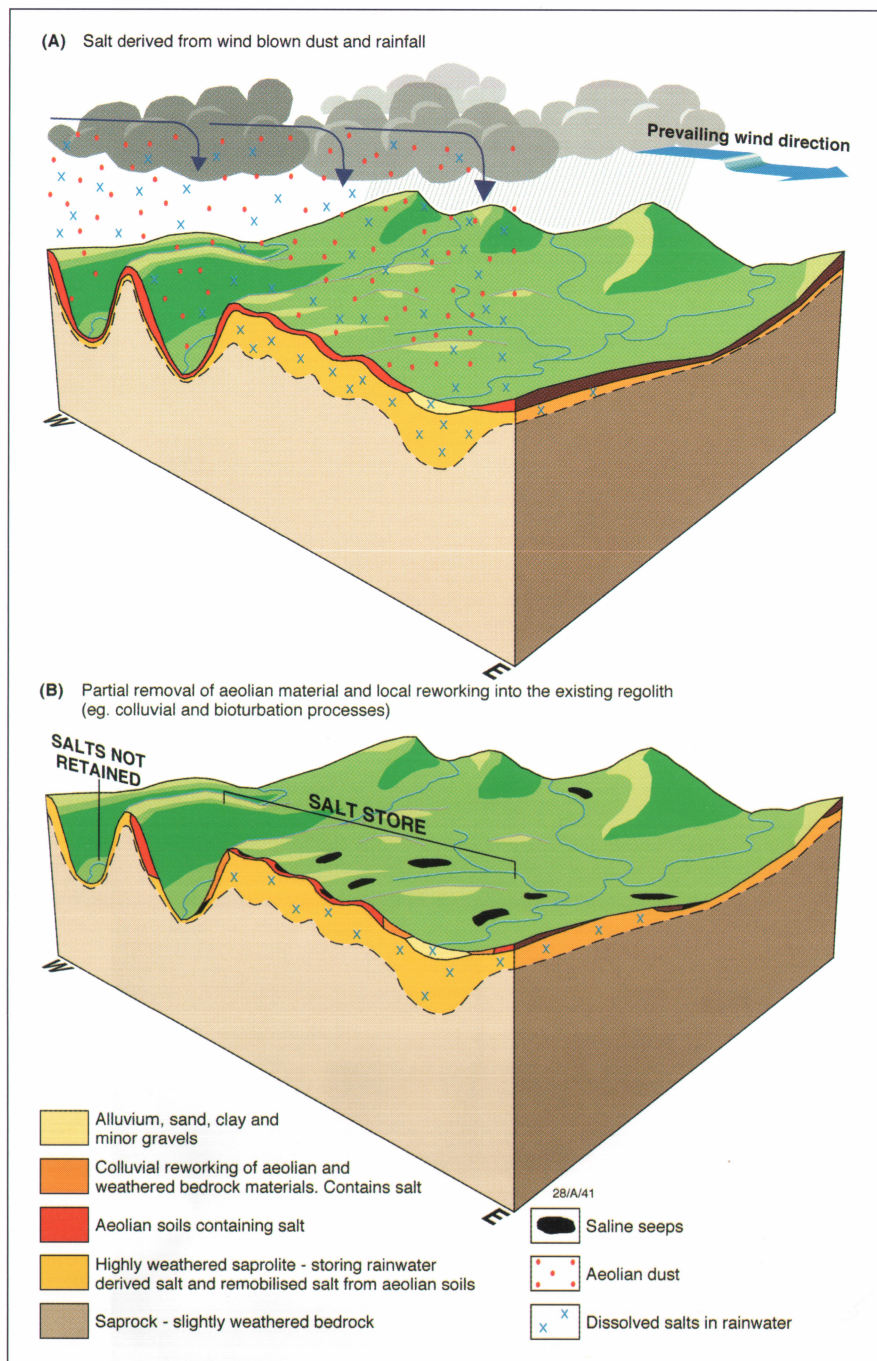


Figure 10. Conceptual model of salt stores and dispersion pathways. **A:** Aeolian dust bringing in salt, probably during arid climatic phases. Salts also derived from rainfall. **B:** Salts stored in the regolith and aeolian deposits. These materials are preserved in geomorphically stable parts of the landscape. Natural water-table fluctuations, and rising water tables caused by tree clearing in areas of high salt storage, result in saline seeps and leakage into streams.

Salt origin and location

Salts are likely to be mainly derived from rainfall and wind-blown dust. Bedrock weathering contributes little to the salts found in the regolith.²² Highly weathered and porous saprolite probably soaks up atmospheric salts. Work in the Boorowa River catchment showed that streams draining catchments containing thick regolith had consistently higher salt loads than streams incised into fresher bedrock.²²

Aeolian dust is widely distributed over much of south-eastern Australia.²³⁻²⁵ These aeolian materials also carried with them considerable amounts of salt, which are now being remobilised.^{26,27}

Clay soils in the Bethungra area fit with descriptions of known aeolian sites in south-eastern Australia.^{10,28,29} Some components of these clay soils are probably aeolian derived. It is no coincidence that these clay soils and underlying highly weathered saprolite are found in geomorphically stable parts of the landscape where aeolian materials are most likely to be preserved.

The highest salt stores tend to be associated with both aeolian soils and highly weathered regolith, and the lowest associated with thin residual regolith (figure 10). Preliminary 1:5 EC measurements through these more deeply weathered profiles indicate that the salt is in the lower two-thirds of the clay layer and mottled saprolite zone. This suggests that base flow rather than surface flow is the main pathway for salts discharging into streams.

It is debatable whether saline seeps and high stream salinities in the Bethungra area are solely a result of rising ground-water tables caused by post-European native tree clearing. Historical evidence from gold mining records show that ground water in the Temora and Wyalong areas (north-west of the Bethungra study) were highly saline.³⁰ Studies on the south-eastern Dundas Tablelands in Victoria indicate pre-European salinity based on historical records, past stream flow and bore hydrograph records, and pedological studies (suggesting prolonged seasonal waterlogging).³¹ In the Bethungra area it is possible that tree clearing and associated rising ground water has accelerated a natural, near-surface mobilisation of salt in the landscape.

Conclusion

Modelled gamma-ray spectrometry data combined with DEM-derived terrain indices is an effective technique for predicting salt stores and salt outbreaks in erosional landscapes in the Bethungra area. Thematic maps quickly generated by this approach can be used directly in developing farm management plans and in prioritising areas for remedial action. In addition, salt store maps produced by this technique have potential in developing more robust hydrological models for dryland salinity.

More detailed field validation and studies in other areas with contrasting bedrock types, alteration styles and landforms are currently under way to test this application in a wider landscape context. Further work will involve refining the technique, incorporating structural lineament

analysis and applications for depositional areas, and combining the result with other datasets (e.g., climatic grids, land use) using Regolith Expert—a system currently under development in the Cooperative Research Centre for Landscape, Environment and Mineral Exploration.

References

- Allan MJ. 1993. Victorian dryland salinity database. Melbourne: Centre for Land Protection Research, Department of Conservation & Natural Resources, Victoria.
- Bradd JM & Gates G. 1996. Dryland salinity in New South Wales: A state perspective. Sydney: Department of Land & Water Conservation, technical report TS95.113.
- Conacher A & Conacher J. 2000. Environmental planning and management in Australia. Melbourne: Oxford University Press.
- Warren AY, Gilligan LB & Raphael NM. 1996. Cootamundra 1:250 000 geological sheet SI/55-11. Edn 2. Sydney: Geological Survey of New South Wales.
- Lawrie KC, Munday TJ, Dent DL, et al. 2000. A geological systems approach to understanding the processes involved in land and water salinisation: The Gilmore project area, central-west New South Wales. AGSO Research Newsletter, May; 32:13-15,26-32.
- Wilford JR, Pain CF & Dohrenwend JC. 1992. Enhancement and integration of airborne gamma-ray spectrometric and Landsat imagery for regolith mapping—Cape York Peninsula. 9th ASEG Geophysical Conference & Exhibition, Gold Coast, Oct 5-8.
- Wilford JR, Bierwirth PN & Craig MA. 1997. Application of airborne gamma-ray spectrometry in soil/regolith mapping and applied geomorphology. AGSO Journal of Australian Geology & Geophysics; 17(2):201-216.
- Dauth C. 1997. Airborne magnetic, radiometric and satellite imagery for regolith mapping in the Yilgarn Craton of Western Australia. Exploration Geophysics; 28:199-203.
- Cook SE, Corner RJ, Groves RJ & Grealish G. 1996. Application of airborne gamma radiometric data for soil mapping. Australian Journal of Soil Research; 43(1):183-194.
- Dickson BL & Scott KM. 1998. Recognition of aeolian soils of the Blayney district, NSW: Implications for exploration. Journal of Geochemical Exploration; 63:237-251.
- Dymond JR & Harmsworth GR. 1994. Towards automated land resource mapping using digital terrain models. ITC Journal; 129-138.
- Moore ID, Lewis A & Ladson AR. 1991. Digital terrain modelling: A review of hydrological, geomorphological and biological applications. Hydrologic Processes; 5(1):3-30.
- Roberts DW, Dowling TI & Walker J. 1997. FLAG: A fuzzy landscape analysis GIS method for dryland salinity assessment. Canberra: CSIRO Land & Water, technical report 8/97.
- Laffan SW. 1996. Rapid appraisal of ground-water discharge using fuzzy logic and topography. In: Proceedings of 3rd International Conference on Integrating GIS and Environmental Modelling, Santa Fe, Jan 21-25.
- Dowling TI. 2000. Consulting report: FLAG analysis of catchments in the Wellington region of NSW. Canberra: CSIRO Land & Water, consulting report 12/00.
- Dowling TI, Summerell G & Walker J. 2001. Soil wetness as an indicator of dryland salinity: A fuzzy landscape analysis GIS. In: Proceedings of the International Symposium on Environmental Software Systems, Banff, May 22-25.
- Summerell GK, Dowling TI, Wild JA & Beale G. 2001. Fuzzy landscape analysis GIS and its application for determining seasonally wet and waterlogged soils. Australian Journal of Soil Research; in prep.
- Department of Land & Water Conservation. 1999. Salinity outbreak mapping from aerial photographs. Described in: Littleboy M, Piscopo G, Beecham R, Barnett P, Newman L & Alwood N. 2001. Dryland salinity extent and its impacts. Canberra: National Land & Water Resources Audit, technical report.
- Wilford JR, Dent D & Dowling T. 2001. Smart interpretation of airborne radiometrics and digital elevation models for salinity mapping. The Land; in prep.
- Bradd JM, Milne-Home WA & Gates G. 1997. Overview of factors leading to dryland salinity and its potential hazard in New South Wales, Australia. Hydrogeology Journal; 5(1):51-67.
- George RJ, McFarlane D & Nulsen B. 1997. Salinity threatens the viability of agriculture and ecosystems in Western Australia. Hydrogeology Journal; 5(1):6-21.
- Evans WR. 1998. What does Boorowa tell us? Salt stores and ground-water dynamics in a dryland salinity environment. In: Groundwater sustainable solutions. Melbourne: IAH conference proceedings; 267-274.
- Butler BE. 1956. Parna and aeolian clay. Australian Journal of Science; 18:145-151.
- Walker PH & Costin AB. 1971. Atmospheric dust accession in south-eastern Australia. Australian Journal of Soil Research; 9:1-5.
- Chartres CJ, Chivas AR & Walker PH. 1988. The effect of aeolian accessions on soil development on granitic rocks in south-eastern Australia, II: Oxygen-isotope, mineralogical and geochemical evidence for aeolian deposition. Australian Journal of Soil Research; 26:17-31.
- Keifert L. 1977. Characteristics of wind transported dust in eastern Australia. Brisbane: Griffith University, Faculty of Environmental Sciences, PhD thesis.
- Melis MI & Acworth RI. 2001. An aeolian component in Pleistocene and Holocene valley aggradation: Evidence from Dicks Creek catchment, Yass, New South Wales. Australian Journal of Soil Research; 39(1):13-38.
- Chen XY. 2001. The red clay mantle in the Wagga Wagga region, New South Wales: Evaluation of an aeolian dust deposit (Yarabee Parna) using methods of soil landscape mapping. Australian Journal of Soil Research; 39(1):61-80.
- Gatehouse RD, Williams IS & Pillans BJ. 2001. Fingerprinting wind-blown dust in south-eastern Australian soils by uranium-lead dating of detrital zircon. Journal of Soil Research; 39(1):7-12.
- Andrews EC. 1910. The Forbes-Parkes goldfield. Sydney: Geological Survey of New South Wales, mineral resources 13. In: Wilson & McNally. 1996. Symposium on the Geological Evolution of Eastern Australia. Sydney: Sydney University Consortium of Geology & Geophysics; 71-73.
- Dahlhaus PG, MacEwan RJ, Nathan EL & Morand VJ. 2000. Salinity on the south-eastern Dundas Tableland, Victoria. Australian Journal of Earth Sciences; 47:3-11.

Acknowledgments: The authors thank reviewers Colin Pain, Ian Lambert, Ross Brodie and Richard Blewett for their constructive comments. They also thank Vivien Dent for assistance with the stream salinity measurements and the NSW Department of Land & Water Conservation for use of its salt outbreak dataset. Jacklyn Brachmanis and Simon Debenham are thanked for their comments on an earlier draft of the paper.

- John Wilford, CRC for Landscape Environment & Mineral Exploration, AGSO, phone +61 2 6249 9455 or e-mail john.wilford@agso.gov.au
- Dr David Dent & Robert Braaten, Bureau of Rural Sciences, phone +61 2 6272 5690 or e-mail david.dent@brs.gov.au
- Trevor Dowling, Land & Water Division, CSIRO, phone +61 2 6272 4883 or e-mail trevor.dowling@cbr.clw.csiro.au